ROLES FOR EXTRA-HYPOTHALAMIC OSCILLATORS IN THE AVIAN CLOCK

A Dissertation

by

STEPHEN PAUL KARAGANIS

Submitted to the Office of Graduate Studies of
Texas A&M University
in partial fulfillment of the requirements for the degree of

DOCTOR OF PHILOSOPHY

May 2008

Major Subject: Biology

ROLES FOR EXTRA-HYPOTHALAMIC OSCILLATORS

IN THE AVIAN CLOCK

A Dissertation

by

STEPHEN PAUL KARAGANIS

Submitted to the Office of Graduate Studies of
Texas A&M University
in partial fulfillment of the requirements for the degree of

DOCTOR OF PHILOSOPHY

Approved by:

Chair of Committee,	Vincent M. Cassone
Committee Members,	Deborah Bell-Pedersen
	David J. Earnest
	Terry L. Thomas
	Mark J. Zoran
Head of Department,	Vincent M. Cassone

May 2008

Major Subject: Biology

ABSTRACT

Roles for Extra-Hypothalamic Oscillators in the Avian Clock.

(May 2008)

Stephen Paul Karaganis, A.B., Wabash College

Chair of Advisory Committee: Dr. Vincent M. Cassone

Avian circadian clocks are composed of a distributed network of neural and peripheral oscillators. Three neural pacemakers, located in the pineal, the eyes, and the hypothalamus, control circadian rhythms of many biological processes through complex interactions with slave oscillators located throughout the body. This system, an astonishing reflection of the life history of this diverse class of vertebrates, allows birds to coordinate biochemical and physiological processes and harmonize them with a dynamic environment. Much work has been done to understand what roles these pacemakers have in avian biology, how they function, and how they interact to generate overt circadian rhythms. The experimental work presented in this dissertation uses the domestic chicken, *Gallus domesticus*, as a model to address these questions and carry forward current understanding about circadian biology in this species. To do so, we utilized a custom DNA microarray to investigate rhythmic transcription in cultured chick pineal cells. We then sought to identify genes which might be a component of the pineal clock by screening for rhythmic transcripts that are sensitive to a phase-shifting light stimulus. Finally, we surgically removed the eyes or pineal from chickens to examine

the roles of these extra-SCN pacemakers in regulating central and peripheral rhythms in metabolism and clock gene expression.

Using these methods, we show that the oscillating transcriptome is diminished in the chick pineal *ex vivo*, while the functional clustering of clock controlled genes is similar. This distribution reveals multiple conserved circadian regulated pathways, and supports an endogenous role for the pineal as an immune organ. Moreover, the robustness of rhythmic melatonin biosysnthesis is maintained *in vitro*, demonstrating that a functional circadian clock is preserved in the reduced subset of the rhythmic pineal transcriptome. In addition, our genomic screen has yielded a list of 28 genes that are candidates for functional screening. These should be evaluated to determine any potential role they may have as a component of the pineal circadian clock. Finally, we report that the eyes and pineal similarly function to reinforce rhythms in brain and peripheral tissue, but that metabolism and clock gene expression are differentially regulated in chick.

DEDICATION

I dedicate this work to my family, my friends, and to Monica. They have many times illuminated my path, where it was too dark to see.

ACKNOWLEDGEMENTS

I heartily thank my committee, Dr. Bell-Pedersen, Dr. Earnest, Dr. Thomas, and Dr. Zoran, and especially my advisor, Vinnie, for their tireless encouragement, support, and guidance. I also thank past members of the Cassone lab, particularly Drs. Aki Adachi, Mike Bailey, Paul Bartell, Beth Cantwell, Arjun Natesan, and Jen Peters, as well as current members Barb Earnest, Jiffin Paulose, and Vikram Shende. Their contributions to my life as a graduate student, both scientifically and otherwise, are too many to enumerate. Special thanks also goes to Dr. Philip Beremand, for his ever-available technical expertise and scholarly advice, and to the the faculty, staff, and students of the Biology Department as a whole, to which I have always felt bonded in camaraderie and shared purpose.

Finally, I thank my family, my fiancé, and all my friends for their unwavering support. No doubt I have won some cosmic lottery that entitles me to such good company.

NOMENCLATURE

LD	Light:Dark Cycle
DD	Constant Darkness
ZT	Zeitgeber Time
CT	Circadian Time

TABLE OF CONTENTS

Page

ABSTRACT iii

DEDICATION v

ACKNOWLEDGEMENTS vi

NOMENCLATURE vii

TABLE OF CONTENTS viii

LIST OF FIGURES x

LIST OF TABLES xii

CHAPTER

I INTRODUCTION 1

Formal and Classical Properties of Circadian Biology 1
Central Circadian Organization in Avian Species 6
Evolution of Avian Molecular Clocks 15
Peripheral Clocks 19
Objectives 21

II CIRCADIAN GENOMICS OF THE CHICK PINEAL GLAND *IN VITRO* 23

Introduction 23
Materials and Methods 26
Results 31
Discussion 40

III A FUNCTIONAL SCREEN OF THE RHYTHMIC PINEAL TRANSCRIPTOME: REGULATION BY LIGHT AND NOREPINEPHRINE 45

Introduction 45
Materials and Methods 47

CHAPTER Page

Results 51
Discussion 59

IV MODULATION OF CIRCADIAN METABOLIC AND CLOCK GENE mRNA RHYTHMS BY EXTRA-SCN OSCILLATORS 66

Introduction 66
Materials and Methods 69
Results 72
Discussion 97

V SUMMARY AND SIGNIFICANCE 104

Genomic Properties of the Pineal Pacemaker *In Vitro* 104
The Pineal and Eyes as System Pacemakers 113
Future Directions 116
Final Conclusions 119

REFERENCES 120

APPENDIX A 139

APPENDIX B 149

APPENDIX C 166

VITA 195

LIST OF FIGURES

FIGURE		Page
1	Pineal melatonin rhythms	33
2	Rhythmic transcripts *in vivo* and *in vitro*	36
3	Rhythmic gene functions	37
4	Microarray validation	39
5	Inhibition of melatonin production by light and norepinephrine	52
6	Light regulated, NE-insensitive gene transcripts	56
7	Phase inversions of candidate gene mRNA rhythms in DD	58
8	Microarray validation of selected genes	60
9	2DG uptake in brain	73
10	2DG uptake in peripheral tissues	77
11	Clock gene expression in telencephalon	81
12	Clock gene expression in diencephalon	84
13	Clock gene expression in optic tectum	86
14	Clock gene expression in liver	89
15	Clock gene expression in heart	92
16	Circadian phase plots for brain	95
17	Circadian phase plots for peripheral tissues	98
18	Mel_{1C} receptor protein in diencephalon	143
19	Mel_{1C} receptor protein in retina	145

FIGURE Page

20 Visual assay for transfection efficiency using GFP fluorescence 151

21 shRNA target sequences..... 153

22 shRNA probe sequences..... 155

23 Transient transfection of astrocytes with cry1^{shRNA} 157

24 Transient transfection of pinealocytes with per3^{shRNA} 160

25 Titering VSV-G lentivirus..... 161

26 Lentiviral transduction of astrocyte and pineal cultures with cry1^{shRNA} 164

LIST OF TABLES

TABLE		Page
1	Comparative gene list	54
2	Candidate gene list	55
3	Cosinor analysis (2DG uptake)	76
4	Cosinor analysis (clock gene mRNA expression)	78
5	Lentiviral titers	163

CHAPTER I

INTRODUCTION

Formal and Classical Properties of Circadian Biology

General Overview

All organisms on earth have evolved adaptations which allow them to occupy a distinct niche in order to compete for limited resources within the environment. The environment continuously changes over time, resulting in a shifting landscape of niche dynamics and forcing organisms to adapt in order to survive. Many such changes occur in a manner or timescale to which organisms may not anticipate; other variations, such as the day/night cycle, the lunar cycle, or the annual seasonal cycle, occur at specific periodicities that can be sensed and processed by biological lifeforms. These alterations in the external milieu often provide new temporal niches and environmental challenges to which organisms may anticipate and adapt.

Perhaps the most influential of all such periodic events is the day/night cycle which occurs as the earth spins about its axis, completing one rotation every twenty four hours. The resulting daily rhythm of exposure to solar radiation has occurred with unbroken consistency for billions of years, pre-dating the emergence of life on earth. It is not surprising, therefore, that eons of exposure to day/night cycles have exerted enormous selective pressure on organisms to evolve some form of biological

---

This dissertation follows the style of the Journal of Neuroscience.

timekeeping mechanisms that allow them to anticipate, exploit, and ultimately thrive under these twenty-four hour environmental rhythms.

Indeed, current understanding of biological systems is that such timekeeping mechanisms are a fundamental and ubiquitous property of living organisms on earth. The first documented characterization of circadian rhythms (from Latin *circa*, meaning "about" and *diem*, meaning "day") was made by French astronomer Jacques de Mairan in 1729, through his careful observations of leaf movements in the *Mimosa pudica* plant (Sweeney, 1987). Since this initial discovery, the science of chronobiology has expanded into a diverse and fast moving field of research. Modern biological science has uncovered twenty four hour rhythms in every manner of organism from unicellular bacteria and protozoa to multicellular fungi, plants, and animals (Dunlap, 1999; Bell-Pedersen et al., 2005). This body of research explores circadian properties within a wide variety of species and attempts to unify them at all levels of organization, from the molecular to the organismal level.

The ancestral origins and complete evolutionary history of circadian clocks is not known. While there is little similarity in the molecular composition of circadian oscillators among distantly related taxa (Dunlap, 1999; Bell-Pedersen et al., 2005), there are three fundamental properties common to all such biological clocks, which define a formal understanding of circadian rhythms. The first defining characteristic of circadian rhythms is that they occur endogenously with a period (τ) of approximately twenty four hours in constant environmental conditions (Pittendrigh, 1960). As true circadian rhythms are intrinsic to an organism, they must persist in constant conditions, and are

thereby distinguished from other rhythms that are driven by rhythmic exposure to external stimuli. Under such conditions a circadian oscillator will "free run", exhibiting a periodicity close to twenty four hours (Bünning, 1977; Pittendrigh, 1981a), the exact value of which is dependent upon the molecular properties of the clock driving the rhythm, and is species dependent.

Entrainment

A second fundamental property of circadian rhythms is that they can be "entrained", or synchronized, to an exogenous rhythmic stimulus of a certain period (T) range, conferring a more precisely controlled phase (ϕ) on the organism's rhythm. Many such environmental stimuli, referred to as a "zeitgebers", have been identified, including light, temperature, food availability, social interaction, and others (Pittendrigh and Minis, 1964; Aschoff et al., 1971; Stephan 2002). Among these, light appears to be the most ubiquitous as well as efficacious zeitgeber overall (Pittendrigh, 1981b); as a result, photic entrainment pathways have been the most extensively studied circadian clock inputs.

There is a clear adaptive benefit for an organism to have the ability to entrain its circadian rhythms. Entrainment affords a necessary level of plasticity, allowing an individual to "tune" its internal rhythms to those of a shifting environment. This ability to shift the phasing of internal rhythms would be important, for instance, in order to accommodate variations in photoperiod (day length) due to seasonal change and geographical location.

While it is not difficult to understand the important survival benefits of possessing an "entrainable" circadian oscillator, current understanding of biological mechanisms of entrainment is limited. There are two classical models of entrainment in chronobiology, known as *parametric* and *non-parametric* entrainment (Pittendrigh, 1981b). The two theories propose different mechanisms by which a zeitgeber perturbs the internal oscillator to achieve rhythm synchronization. Under the parametric model, the zeitgeber (classically light) acts to modulate the oscillator in continuous fashion, by constantly changing its angular velocity, thus resulting in a new phase trajectory. Such a model predicts a light stimulus will indirectly elicit a phase shift by altering τ. According to the non-parametric model, it is the timing of exposure to a photic stimulus which directly shifts the angular position, or phase, of the oscillator, without effecting its velocity. In reality, it appears that both mechanisms play a role (Pittendrigh, 1981b), although non-parametric paradigms are sufficient to entrain animals, as is evidenced in studies utilizing skeleton photoperiods (Pittendrigh and Minis, 1964).

Non-parametric entrainment studies have yielded copious quantitative data that reveal the relationship between the timing of a light stimulus and the magnitude and directionality of a resulting phase shift. This relationship can be illustrated in the form of a graph known as a phase response curve (PRC) (DeCoursey PJ, 1960), where the magnitude of a phase shift is plotted as a function of the timing of a light stimulus under free-running conditions (circadian time or CT). PRC's carried out on a number of animal systems reveal there is a differential effect of light when applied at different phases of a circadian cycle (Daan and Pittendrigh, 1976). Typically, a light stimulus has

little or no effect when applied during the subjective day, a portion of the cycle in constant darkness (DD cycle) which corresponds to the illuminated portion, or photophase, of a light:dark cycle (LD cycle). On the other hand, a light stimulus applied during the *early* subjective night (corresponding to the dark portion, or scotophase, of an LD cycle) elicits a phase delay, while the same stimulus applied during *late* subjective night elicits a phase advance. The magnitude of the phase shift is also dependent on time.

Numerous studies reveal that different animal species exhibit specific PRC signatures. These are generally divided into one of two classes of PRCs: Type 1 and Type 0 curves. Type 1 and Type 0 PRCs have distinct shapes, which likely reflect the evolution of specialized adaptations by which organisms meet specific environmental challenges. They may also reflect sensory limitations in some species (Daan and Pittendrigh, 1976).

Temperature Compensation

A third universal feature of circadian clocks is that they maintain a near constant period of oscillation over a relatively broad range of temperatures. The rate at which most biochemical, and hence physiological processes occur is highly temperature dependent, exhibiting a Q_{10} of 2-3. As a consequence, a significant shortening or lengthening of circadian period would be predicted for molecular oscillators abiding by this rule when exposed to higher or lower temperatures, respectively. However, the average Q_{10} measured for circadian rhythms (~1.1) is significantly less than what is

observed for most other processes within a normal range of temperatures (Kalmus, 1940; Pittendrigh, 1954; Pittendrigh, 1961). Since truly temperature "independent" biochemical processes are not thermodynamically feasible, it is understood that circadian rhythms must exhibit "temperature compensation". This terminology reflects the hypothesis that temperature compensation is an active process whereby circadian clocks are buffered against extreme variations in period as the temperature changes. The mechanism(s) by which this phenomenon occurs, however, is poorly understood.

Central Circadian Organization in Avian Species

Evolution of a Distributed Centralized Clock

Analyses of these formal properties have led to the synthesis of an established model for studying the biological basis of circadian clocks. In this model, the biological clock is dissected into three discrete components: 1) a central pacemaker; 2) input pathways which modulate pacemaker function; and 3) output pathways that connect the oscillator to biological processes. The central pacemaker is the core of this endogenous timekeeping system in that it functions autonomously, and dictates the rhythmic output of the circadian system. At its most reduced level, it must consist of a molecular feedback loop which persists via its own autoregulation (Dunlap, 1999). Input pathways, on the other hand, must contain the machinery necessary to transduce information from sensory structures to mediate entrainment of the pacemaker. Finally, output pathways must exist to produce biological rhythms that exhibit a phase dictated by the central pacemaker. Most experiments in circadian biology are designed to

explore the workings of one of these three components, although the separation between them may prove to be subtle, given their complex relationship.

These fundamental clock components are realized by all organisms possessing a circadian timekeeping mechanism. Yet the evolution of biological clocks in diverse species has given rise to multitudinous variations in the organization of circadian systems at the cellular and organismal levels. In some species, all three components of a circadian clock are localized to a single cell, which as a unit comprises a complete "clock". This is observed in both unicellular (e.g. cyanobacteria) and multicellular (e.g. fungi) organisms. In higher animal taxa, circadian clocks have evolved into distributed, yet physiologically specialized systems. These system-level clocks derive from an interaction between spatially segregated, but centralized clock components. This dichotomy can be seen in many animal species, from *Drosophila* to humans.

Birds in particular have evolved some of the most highly specialized and complex circadian systems of all life forms. In birds, three separate neural pacemakers interact to form a complex circadian network. These are the pineal gland, the ocular retina, and the avian homolog of the mammalian hypothalamic suprachiasmatic nucleus (SCN) (Gwinner and Brandstätter, 2001; Underwood et al., 2001). Furthermore, in addition to transmitting photic information by way of the retina, as in mammals, birds are capable of sensing and processing light via extraocular photoreceptors located in the pineal as well as in deep encephalic structures (Menaker, 1972; Menaker et al., 1997). To further complicate matters, there is a great deal of variation in how each component contributes to the circadian system as a whole between different species of birds, and

possibly even within an individual bird when subjected to certain environmental conditions (Gwinner and Brandstätter, 2001; Underwood et al., 2001). The retention of this distributed and variable system in birds, as compared to the more "streamlined" mammalian system, perhaps reflects some important selective advantage for avian species to compete within their highly specialized niches.

The Pineal

The pineal gland is a photoreceptive pacemaker in all species of birds studied, and is able to act at a distance through the nightly synthesis and humoral secretion of the indoleamine hormone melatonin. In this way, the pineal exerts control over various physiological processes including other components of the circadian system (Underwood, 1990; Cassone, 1998). Its hierarchical dominance varies from species to species, however. In passerine birds such as the house sparrow, pinealectomy abolishes locomotor activity rhythms when animals are placed in constant conditions (Ebihara and Kawamura, 1981; Fuchs, 1983; Gaston and Menaker, 1968; Gwinner, 1978; McMillan, 1972; Pant and Chandola-Saklani, 1992), demonstrating that the pineal plays a dominant role in the circadian system of this species. In contrast, pinealectomy disrupts, but does not abolish locomotor rhythms in columbiform birds such as pigeon (Ebihara et al., 1984), and has little or no effect on activity rhythms in galliform birds such as quail or chick (Simpson and Follett, 1981; McGoogan and Cassone, 1999).

The rhythmic properties of the pineal organ persist *in vitro* (Deguchi, 1979; Kasal et al., 1979), as well as its ability to be entrained (Menaker et al., 1997; Oishi et

al., 2001; Natesan et al., 2002). In fact, intact clock function can be reduced to the level of the individual pinealocyte (Nakahara et al., 1997). Because all of the functional clock components are preserved in culture, and because melatonin is an important and easily measured primary output, the pineal is an attractive general model for studying circadian clock properties, as well as in understanding the specific role the pineal plays in animals.

Retinal Clocks

The retinae of the eyes also contain circadian clocks in birds, and they drive local rhythms of ocular physiology, as well as influence distant components of the circadian system in some species. Local processes regulated within the eyes include rhythmic turnover of photoreceptor outer segments (Pierce et al. 1993), electrophysiological properties (McGoogan and Cassone, 1999; Ko et al., 2001; Ko et al., 2003), and melatonin biosynthesis (Adachi et al., 1995; Binkley et al., 1979; Hamm and Meneaker, 1980; Reppert and Sagar, 1983). Furthermore, molecular rhythms in clock genes and melatonin biosynthesis persist *in vitro* (Toller et al., 2006).

In some species of bird, such as quail and pigeons, the retinae contribute significantly to blood plasma levels of melatonin (Underwood et al., 1984; Oshima et al., 1989). Surgical removal of the eyes abolishes or disrupts free-running rhythms in these birds, although pigeons do not become completely arrhythmic unless pinealectomized as well (Underwood, 1994; Ebihara et al., 1984; Oshima et al., 1989). It is likely that the retinae influence the circadian system in these species through rhythmic melatonin release, since exogenous melatonin administration can entrain, disrupt, or rescue

physiological rhythms in birds (Underwood et al., 2001). In chicken, enucleation also abolishes locomotor activity rhythms (Nyce and Binkley, 1977). However, little or no retinal melatonin is released into the blood of these animals (Cogburn et al., 1987; Reppert and Sagar, 1983), suggesting that in chick, the retina can regulate distant circadian tissues through a neural pathway. Similarly, systemic ocular regulation of circadian rhythms appears to involve a neural component in quail, but not in pigeons (Underwood et al., 2001).

At least one neural pathway, the retinohypothalamic tract (RHT), physically and functionally connects the retina to the circadian system. This tract, consisting of glutamatergic processes from retinal ganglion cells, directly innervates the avian SCN, and appears to contribute to entrainment of the clock by light in some species (McMillan et al., 1975; Barrett and Underwood, 1991). Light-mediated entrainment may originate in the retinal ganglion cells themselves through the action of one or more opsin based photopigments (Provencio et al., 2000; Bailey and Cassone, 2004). Therefore the retina, in addition to acting as a local and systemic pacemaker, can also act as an entrainment pathway by humoral and neurological connectivity to the SCN.

The Suprachiasmatic Nucleus

Unlike birds, mammals possess a single central nervous system pacemaker located in the suprachiasmatic nucleus (SCN) of the hypothalamus. Alhough circadian pacemakers are distributed in the CNS of birds, the avian hypothalamus contains a homolog to the mammalian SCN, which acts as a third and major component of avian

circadian systems. Again, this role is complex and probably species specific. For instance, lesioning the SCN abolishes locomotor activity rhythms in species of sparrow, quail, and pigeon (Ebihara and Kawamura, 1981; Simpson and Follett, 1981; Takahashi and Menaker, 1982; Yoshimura et al., 2001). However, in contrast to mammals, an intact SCN is not sufficient to sustain rhythmicity indefinitely under constant conditions, though pinealectomy and/or enucleation often abolishes rhythms only after a gradual rhythm dampening (Underwood et al., 2001).

While the presence of a hypothalamic clock in birds is clear, the precise anatomical location of the functionally equivalent avian SCN has been a subject of some controversy. In bird hypothalamus, there are two candidate sites for the homologous avian SCN, each of which has similarities to the mammalian structure. The first is the medial hypothalamic nucleus (MHN), or medial SCN (mSCN) which occupies a similar position in the brain as the mammalian counterpart. The other structure, located lateral to this site, is termed the visual SCN (vSCN) because it is innervated by the retina. Studies have shown that in fact both avian structures, like the mammalian SCN, are retinorecipient by way of the retinohypothalmic tract (RHT) (Cassone and Moore, 1987; Norgren and Silver, 1989; Shimizu et al., 1994; Cantwell and Cassone, 2006a).

Rhythmic binding of radiolabeled melatonin (2-[^{125}I]iodomelatonin, or IMEL) is specific to the vSCN, however, as is melatonin receptor expression (Lu and Cassone, 1993b; Reppert et al., 1995). Also, the vSCN exhibits rhythmic metabolic activity, which in house sparrow, along with IMEL binding, is abolished by pinealectomy and

restored by rhythmic administration of melatonin, (Lu and Cassone, 1993a; Lu and Cassone, 1993b; Cantwell and Cassone, 2002). These studies provide powerful evidence that the vSCN contains a melatonin responsive pacemaker. On the other hand, numerous studies demonstrate a direct role for the mSCN as a pacemaker as well. Though precise electrolytic lesion of specific nuclei is technically difficult, targeted ablation of the mSCN has been shown to abolish rhythmicity in pigeons, where histological examination verified the vSCN were left intact (Yoshimura et al., 2001). In contrast, lesions targeting the vSCN in pigeons did not abolish rhythmicity in these animals (Ebihara et al., 1987). Moreover, *in situ* hybridization shows multiple clock genes are rhythmically expressed in the mSCN, but not the vSCN, of several species of bird (Yoshimura et al., 2001). In house sparrow, however, expression of at least one clock gene, *per2*, is rhythmic in both structures (Brandstätter, 2001).

Histological characterizations of the avian nuclei demonstrate that both structures have neurochemical profiles common to the mammalian SCN, but that neither the mSCN nor the vSCN is a direct correlate (Norgren and Silver, 1990; Shimizu et al., 1994). A recent study corroborates this observation, and reports that a hybrid cytoarchitectural morphology is shared by these structures as well (Cantwell and Cassone, 2006b). Therefore, it is likely that the complex avian SCN, like other components of the circadian system, has evolved to take on a more distributed and specialized form in birds.

Extraocular Photoreceptors

Circadian inputs, like the oscillators themselves, are distributed in the avian nervous system. As a consequence, birds possess multiple functioning entrainment pathways which are individually sufficient to entrain the animal. For instance, birds can still entrain to a LD cycle following enucleation (Underwood et al., 2001). As stated, one extraocular site possessing photoreceptors is the pineal gland. Here, secretory pinealocytes can respond to light and subsequently mediate entrainment of the whole system by secretion of melatonin. The photopigment(s) mediating this response is unknown, but likely candidates are melanopsin and pineal-specific pinopsin (Natesan et al., 2002).

Some birds, however, can still entrain to light cues after the removal of the pineal gland as well as the eyes, demonstrating that a third location for circadian photoreceptors must exist. There is evidence that structures capable of mediating photoperiodic responses to light are contained in the ventral hypothalamus and that rhodopsin may be involved in this response (Underwood et al., 2001). It is not known whether these photoreceptors contribute to circadian entrainment.

The Neuroendocrine Loop

The complex circadian system of birds is governed by a species dependent interaction between three spatially distributed neural pacemakers. Each of these pacemakers exhibits at least a partial degree of autonomy, enabling independent regulation of local processes. At the same time, neural and humoral coupling allow the

pacemakers to cooperate in order to produce an emergent organismal clock. One mechanism which has been hypothesized to explain this interaction is the "neuroendocrine loop" model (Cassone and Menaker, 1984). To understand this model, it is necessary to explain how each of the components of the loop are physiologically connected.

As has been discussed, the pineal, and in some species the retina, influence the SCN by secreting melatonin into the blood. This effect, mediated by G_i protein coupled melatonin receptors, results in a general inhibition of SCN neuronal activity (Cassone et al., 1987). The SCN is in turn connected to the pineal via a polysynaptic neural pathway. In this pathway, neurons from the SCN synapse with cells in the hypothalamic paraventricular nucleus (PVN), where descending projections innervate the intermediolateral cell column (IML) in the thoracic spinal cord. In turn, these neurons synapse with the superior cervical ganglia (SCG), and sympathetic nerve fibers innervate the pineal gland (Moore, 1996). Norepinephrine released from the terminals bind α_2 adrenergic receptors, inhibiting melatonin biosynthesis. These connections thus link the pineal and SCN in a neuroendocrine circuit, or loop.

According to the neuroendocrine loop model, the pineal and SCN oscillators damp out unless reinforced through their mutual coupling. During the day, the SCN inhibits the pineal from producing melatonin, while during the night, melatonin inhibits the SCN. In this way, the damped oscillators sustain themselves through a mutual inhibition carried out by each arm of the loop (Cassone and Menaker, 1984). Additional

complexity is added to this model when the species specific contribution of retinal input is taken into account.

Evolution of Avian Molecular Clocks

The Drosophila Molecular Model

The first molecular circadian clock component, the *Drosophila period* gene, was a seminal discovery made in the laboratory of Seymour Benzer in 1971 (Konopka and Benzer, 1971). Since that time, various so-called "clock genes" have been discovered in numerous species. Useful molecular and genetic models such as *Synechococcus*, *Neurospora*, *Drosophila*, and *Mus musculus* have led to an explosion in molecular clocks research that has revealed a great deal about the molecular underpinnings of circadian systems. Perhaps most striking is the considerable conservation in the fundamental processes (if not sequences) which drive circadian rhythms, over great genetic distances and millions of years of evolution. (Dunlap, 1999).

The most well understood molecular animal model is *Drosophila*, the organism which begat molecular clocks research in all other models. The core of this system is composed of a primary molecular feedback loop, which includes both positive and negative elements. Positive elements consist of two genes, *clock* (*clk*) and *cycle* (*cyc*), encoding transcription factors containing a basic helix-loop-helix and *Per-ARNT-Sim* (bHLH/PAS) domain. These proteins dimerize in the cytoplasm and are then translocated into the nucleus, where they activate expression of multiple genes by binding E-box *cis* regulatory sequences in their promoters. Among the activated genes

are *period* (*per*) and *timeless* (*tim*), which are transcribed, translated, and then also dimerize to enter the nucleus. There they inhibit activation of their own transcription by interfering with the CLOCK-CYC complex. Other important accessory proteins, including several kinases, regulate protein stability and timing of nuclear entry. This adds another layer of control that is necessary to ensure precision of circadian periodicity (Gallego and Virshup, 2007). Entrainment is effected by activation of a photoreceptor, which promotes *tim* phosphorylation and subsequent ubiquitin mediated proteosomal degradation, resulting in a phase shift of the clock. The most well characterized photoreceptive molecule involved in entrainment is *cryptochrome* (*cry*) (Hardin, 2005).

The Mammalian Molecular Model

Many aspects of the *Drosophila* molecular clock are conserved in vertebrates, though regulation is somewhat more complex. The most well understood vertebrate molecular clocks are those of mammals, where the mouse model has proven to be a powerful and fruitful molecular tool. Multiple clock gene homologues have been cloned in mammals, including *clock*, three *period* genes (*per1*, *per2*, and *per3*), and two *cryptochrome* genes (*cry1* and *cry2*). There seems to be considerable similarity in the function of these multiple isoforms, and their purpose is not completely understood. However, as individual mutations in these genes produce significant phenotypic differences, the functions of these genes cannot be entirely redundant (Ko and Takahashi, 2006).

In mouse (and other mammals), the transcriptional regulatory loop is preserved, though considerably modified. The positive arm of the loop is similar, such that the dimerization partner for *clock* protein is the gene product of *bmal1*, the mammalian ortholog of *cycle*. However, mammalian *cryptochromes* do not act as photoreceptors and therefore do not mediate entrainment as in fruit flies. Rather, the *cryptochromes* have become part of the negative transcriptional complex by dimerizing with PER proteins and repressing the BMAL1-CLK activation complex (Reppert and Weaver, 2002). Entrainment by light, though less well understood in mammals, involves induction of *per1* transcription, rather than TIM protein degradation (Reppert and Weaver, 2002; Yu and Hardin, 2006). There is no known clock function for the mammalian *tim* gene.

A second conserved transcriptional loop has been identified in mammals as well. In this pathway, which serves as a stabilizing loop, BMAL1-CLK complexes activate transcription of two retinoic acid related orphan nuclear receptors, *rev-erbα* and *rorα*, which are then translated and enter the nucleus. Once in the nucleus, REV-ERBα and RORα proteins competitively bind to retinoic acid related orphan response elements (RORE's) located in the promoter of *bmal1*. The two proteins have opposing effects, as REV-ERBα is a repressor of *bmal1* transcription, while RORα is a *bmal1* activator (Ko and Takahashi, 2006). In this way, *bmal1* levels are further regulated by an antagonism between its own activated gene products. This loop, while containing no direct *Drosophila* orthologs, is functionally equivalent to the vri/pdp1ε pathway in that species (Yu and Hardin, 2006). Other conserved processes include post-translational pathways,

such as substrate phosphorylation by *casein kinase 1 epsilon* (*CK1*ε), a functional homologue of *Drosophila doubletime* (*dbt*) protein (Yu and Hardin, 2006).

Avian Molecular Clocks

Little is known about how molecular clocks function in birds. Nevertheless, clock genes have been cloned in multiple bird species, including chicken, Japanese quail, pigeon, sparrows, and others. Among those discovered are avian orthologs of *clock*, *bmal1*, *bmal2*, *per2*, *per3*, *cry1*, *cry2, and cry4* (Chong et al., 2000; Yoshimura et al., 2000; Brandstätter et al., 2001; Yamamoto et al., 2001; Bailey et al., 2002; Fu et al., 2002; Chong et al., 2003; Yasuo et al., 2003; Mouritsen et al., 2004; Helfer et al., 2006). No counterpart to *per1* has been found in birds.

All presumed "negative" clock gene mRNAs, as well as *bmal* mRNAs, are reported to be rhythmic in chicken and sparrow, although not all of the mRNA transcripts are in phase with their mammalian counterparts (Bell-Pedersen et al., 2005; Helfer et al., 2006). This suggests that there are significant differences in the way that avian and mammalian clocks are transcriptionally regulated. Moreover, in chicken, the same clock genes are differentially regulated in pineal and retina (Bailey et al., 2003; Bailey et al., 2004). Therefore, it seems that the molecular clockworks operating within different pacemakers are unique, even within the same animal. In order to understand the mechanics of the complex avian molecular clock, more functional analyses are needed, as well as a greater understanding of how the clock is regulated at the protein level.

Peripheral Clocks

Ubiquitous Oscillators

Current times have seen a shift in the way circadian zoologists view the organization of biological clocks in animals. A plethora of recent studies (mostly in mammalian models) have demonstrated that, in addition to possessing a neurocephalic circadian axis, multiple peripheral tissues of animals contain self-sustaining circadian oscillators as well. For instance, clock genes are rhythmically expressed in many animal tissues (Oishi et al., 1998; Damiola et al., 2000), and in some cases they can be sustained without damping. One study demonstrated that mPER2::luciferase rhythms in mouse liver and lung could be sustained *in vitro* for more than 20 consecutive days. Moreover, rhythms in peripheral tissue are not abolished by SCN lesions (Yoo et al., 2004). Instead, rhythms in different organs become desynchronized from each other, showing that the SCN coordinates the phasing of clocks intrinsic to these tissues (Yoo et al., 2004; Guo et al., 2005; Guo et al., 2006). Likewise, individual rodent fibroblasts can sustain rhythmic gene expression in culture, and can be transiently synchronized following a serum shock (Welsh et al., 2004; Nagoshi et al., 2004; Stratmann and Schibler, 2006). These and other findings have established that, in animals, circadian clocks are arranged in a hierarchy, where pacemakers, such as the mammalian SCN, synchronize (but do not necessarily drive) the rhythms of "slave" oscillators located in peripheral organs.

Entrainment of Peripheral Clocks

Neuronal pacemakers in most animals entrain primarily by light. In some cases, this may occur via direct exposure of the pacemaker tissue to photic stimuli, as is the case for avian pineal and retinae. For mammals, entrainment relies on second order processing of photic input relayed to the SCN via the retinohypothalamic tract. Peripheral clocks, on the other hand, do not generally entrain to light cues, but by one of two mechanisms: 1) reception of internally derived outputs from the SCN; and 2) exposure to externally derived non-photic stimuli.

Experiments in which immortalized SCN 2.2 cells were co-cultured with NIH 3T3 fibroblasts show that SCN pacemaker cells can drive downstream oscillations in clock gene expression and glucose uptake by secreting a diffusible substance across a semipermeable membrane (Allen et al., 2001). Thus, humoral secretion appears to be at least one mechanism by which the SCN is coupled with peripheral clocks, though some tissues require a neural connection to the SCN in order to for entrainment to occur (Guo et al., 2005). Regulation of serum glucocorticoids may be one indirect method by which the SCN can entrain peripheral oscillators (Balsalobre et al., 2000; Le Minh et al., 2001; Stratmann and Schibler, 2006).

The primary external zeitgeber for some peripheral rhythms, such as those in liver and heart, is food intake. For instance, competing cycles of restricted food availability can uncouple peripheral rhythms in liver and heart from those of the SCN in mice and rats, without phase shifting the SCN itself (Damiola et al., 2000; Hara et al., 2001; Stokkan et al., 2001). While the metabolic entrainment pathway(s) are not

understood, there is evidence that transcriptional activation by the BMAL1/CLOCK complex is sensitive to NAD/NAPD oxidative state, suggesting cellular redox sensing pathways may mediate metabolic entrainment of peripheral clocks (Rutter et al., 2001). Functional CLOCK is not required for metabolic entrainment of at least one peripheral tissue in mice, however (Oishi et al., 2002).

Objectives

Significant progress has been made in understanding how avian clocks are organized, and how multiple pacemakers interact to orchestrate circadian rhythms. Likewise, much work has been done to discover avian orthologs of canonical clock genes and characterize their expression in pacemaker tissues. Still, little is known about how these molecular clock components interact with other pathways to generate overt physiological rhythms, or what constitutes the base ensemble of rhythmic genes in a circadian pacemaker. Moreover, it is not known how central pacemakers regulate clock genes in other avian tissues. This dissertation addresses these issues and presents experimental findings from research conducted on the domestic white leghorn chicken, *Gallus domesticus*.

Our research utilizes both molecular and physiological methods, and we have employed a cell culture model as well as conducted experiments *in vivo*. First, we used microarray analysis to explore circadian regulation of the transcriptome in cultured chicken pinealocytes. We then screened the rhythmically regulated gene population for new candidate clock gene transcripts that are specifically sensitive to a phase shifting

stimulus. Next, we characterized clock gene mRNA expression in multiple central and peripheral tissues, and mapped their tissue specific phase relationships *in vivo*. We also investigated the role of the pineal and the eyes in regulating metabolic and molecular rhythms in these tissues. Finally, we examined temporal regulation of melatonin receptor expression by the pineal, and developed methods for carrying out functional circadian studies in cultured chick cells using RNAi techniques.

In addition to revealing multiple candidate genes of interest expressed in the chick pineal, this work has allowed us to address several hypotheses: 1) the rhythmic chicken pineal transcriptome reduces to a smaller subset of intrinsically rhythmic transcripts *in vitro*; 2) the phasing of clock gene mRNA rhythms is correlated with the phasing of metabolic activity rhythms *in vivo*; and 3) the pineal and eyes regulate rhythms in metabolic activity by influencing clock gene mRNA expression. We show that circadian regulation in the chicken is asymmetric and highly complex, and that circadian oscillations are differentially regulated in multiple tissues, under different lighting conditions, and when in isolation of the circadian network *in vivo*.

CHAPTER II

CIRCADIAN GENOMICS OF THE CHICK PINEAL GLAND *IN VITRO*

Introduction

The chick pineal gland is a heterogeneous tissue consisting of pinealocytes, glia, and lymphocytes, among a few other cell types (Korf, 1994), whose sole reported function is the nightly secretion of the hormone melatonin. The pineal gland serves as part of a multi-oscillatory circadian system (Cassone and Menaker, 1984) and influences other oscillators and downstream processes at least in part via its circadian secretion of melatonin (Cassone and Menaker, 1984; Cassone et al., 1986; Zatz and Mullen, 1988a, 1988b; Cassone et al., 1990).

At the cellular level, the avian pineal gland contains all the components needed for a functional circadian system as it possesses photoreceptors enabling direct entrainment to light (Binkley, 1988; Menaker et al., 1997; Natesan et al., 2002), it contains a circadian oscillator (Deguchi, 1979; Kasal et al., 1979), and it produces a measurable molecular output in the form of rhythmic melatonin biosynthesis and secretion (Kasal et al., 1979; Takahashi et al., 1980). These processes are properties of pinealocytes themselves since they continue *in vitro* as well as *in vivo* (Deguchi, 1979; Kasal et al., 1979; Natesan et al., 2002). The pineal glands of several species of birds rhythmically synthesize melatonin over multiple circadian cycles in both organ culture and dispersed cell cultures, under constant darkness or dim red light (Deguchi 1979; Kasal et al., 1979; Takahashi et al., 1980; Zatz et al., 1988; Murakami et al., 1994).

The biosynthetic pathway for melatonin synthesis has been well characterized, involving four enzymatically catalyzed reactions to produce melatonin from the amino acid tryptophan (Axelrod, 1974). First, tryptophan taken up by pinealocytes is hydroxylated by tryptophan hydroxylase (TrH) to form 5-hydroxytryptophan (5-HTP). 5-HTP is converted to 5-hydroxytryptamine (5-HT) by aromatic amino acid decarboxylase (AADC), and is then acetylated during the night by arylalkylamine-N-acetyltransferase (AANAT) to form N-acetylserotonin (NAS). Finally, NAS is converted into melatonin by hydroxyindole-O-methyltransferase (HIOMT). The mRNAs for *TrH*, *AANAT* and *HIOMT* are rhythmically expressed in the chick pineal gland *in vivo* and *in vitro*, and rhythmic post-transcriptional regulation of these enzymes has been demonstrated (Klein, 1985; Cassone, 1998; Gastel et al., 1998; Bernard et al., 1999; Ganguly et al., 2002) suggesting that the circadian clock within pinealocytes regulates this process at multiple levels of cellular organization.

The molecular basis of the circadian clock mechanism itself is poorly understood in birds, although avian orthologs of most canonical clock genes (i.e., genes thought to comprise the molecular oscillator in mammalian clocks) have been isolated, cloned and characterized (Bailey et al., 2003, 2004). However, the dynamic interactions of these genes and their products have not been systematically studied in as much detail as it has been in mammals. In mammals, the clock mechanism is thought to consist of interlocking feedback loops of “positive” and “negative” clock gene elements, which are regulated at the transcriptional and translational levels, as has been elegantly demonstrated in *Drosophila* and other model systems (Dunlap, 1999; Glossop et al.,

1999; Shearman et al., 2000; Bell-Pedersen et al., 2005). In the mammalian model, *clock*, *bmal1*, and *bmal2* comprise the positive arm of the circadian loop. The protein products of these genes are known to dimerize in the cytoplasm, after which they enter the nucleus and activate transcription of multiple genes by binding to E-box sequences in the promoter regions of target genes. Among those activated target genes are the "negative elements" which include three *period* genes (*per1*, *per2*, and *per3*) as well as two *cryptochrome* genes (*cry1* and *cry2*). In turn, PER and CRY proteins dimerize in the cytoplasm, then enter the nucleus where they inhibit their own transcriptional activation by inhibition of CLOCK/BMAL binding to E-boxes, thus closing the loop.

Previously, our laboratory has utilized high-density cDNA microarray technology to obtain a transcriptional circadian profile of approximately 8,000 pineal-specific chick cDNAs expressed *in vivo* within the pineal gland and retina (Bailey et al., 2003, 2004). This research has revealed a complex circadian orchestration of a diverse array of pineal transcripts, including "clock gene" orthologs, photo-transduction components, immune function genes, and protein processing and trafficking components. Here, we apply our genomic approach to the study of the chick pineal gland *in vitro.* We used microarray analysis to investigate the expression of genes within cultured pinealocytes subjected to both LD and DD cycles. We report that a reduced subset of genes was rhythmically expressed *in vitro* compared to those previously published *in vivo*, and that gene expression rhythms were lower in amplitude, although the functional distribution of the rhythmic transcriptome was largely similar.

Materials and Methods

Cell Culture

All animals were treated in accordance with ILAR guidelines; these procedures have been approved by the Texas A&M University Laboratory Animal Care Committee (AUP no. 2001-163). One-day-old chicks were obtained from Hyline International (Bryan, TX), killed by decapitation, and their pineal glands were removed for cell culture following published protocols (Zatz et al., 1988). Briefly, excised glands were dispersed in trypsin, seeded into 12-well polystyrene tissue culture plates, and maintained in McCoy's 5A modified medium supplemented with 10% chicken serum, 10% fetal bovine serum, and 1% PSN antibiotic cocktail (Gibco/Invitrogen, Carlsbad, CA) in a humidified incubator at 37^{o}C with 5% CO_2. Cells were maintained on a 12-hour light: dark cycle (38 $\mu W/cm^2$ light intensity) for the duration of the culture, until sampling began. In order to maintain optimal growth rates and cell density, fetal bovine serum was left out of the culture medium on the second and third day. On the fourth day and thereafter, the cells were maintained in medium containing 10mM KCl and no serum, as described previously (Zatz et al., 1988).

Experimental Sampling in LD and DD Cycles

On day 6 of the culture, cells were either kept in a 12 hour LD cycle or transferred to DD. Media was collected every four hours for a 24-hour period; sampling began 4 hours after lights on for cells in LD, or 4 hours after the beginning of the subjective light period for cells in DD. When sampling in the dark, infrared viewers

were used. Media was pooled from all plates within each treatment, and stored at –20°C for melatonin RIA analysis. Cells from a single plate were harvested into Trizol reagent (Invitrogen) every four hours, beginning with ZT2 (in LD) or CT2 (in DD), in between time points during which media was being collected, i.e. at ZT/CT 2, 6, 10, 14, 18, 22. Trizol samples from each plate were immediately pooled, homogenized, and then frozen at –80°C for future RNA extraction. Four biological replicates were performed for each experimental timepoint.

Melatonin Radioimmunoassay

Melatonin was measured using radioimmunoassay, which has been validated for chick plasma and cell culture medium (Lamosova et al., 1995). Media samples were mixed with tricine buffered saline and incubated with ^{3}H-radiolabeled melatonin (8,000-10,000 cpm per 100 µl) for 30 min. at room temperature. Samples were then incubated at 4°C overnight with sheep anti-melatonin antibody (Stockgrand Ltd., Surrey, UK) diluted to achieve on an optimal binding range of 20-25%. Bound melatonin was separated from free melatonin by addition of dextran-coated charcoal suspension and centrifugation at 4°C. Supernatant containing the bound antibody fraction was removed, placed into scintillant, and counted on a scintillation counter (Beckman Instruments Inc., Fullerton , CA). Data analysis was performed using ImmunoFit EIA/RIA software (Beckman Instruments Inc). Standard curves were fitted to a 4-parameter logistic function and melatonin levels were calculated as absolute values.

cDNA Microarray Production

Microarrays were constructed from two cDNA libraries that were generated from chick mRNA isolated during midday (ZT6) and midnight (ZT18) as described previously (Bailey et al., 2003). Approximately 4000 cDNA clones from each library (8113 total) are represented in our custom microarray. 100 μm spots were arrayed at 190 micron positional intervals onto poly-L-lysine coated slides using a GeneMachines OmniGrid microarrayer. Dried slides were stored in the dark at room temperature before use in hybridizations.

Microarray Hybridizations

Total RNA was extracted from cell lysates using a Qiagen RNeasy kit (Qiagen, Valencia, CA), then amplified using a MessageAmp II RNA amplification kit (Ambion, Austin, TX). Both total RNA and aRNA samples were analyzed on an Agilent 2100 Bioanalyzer for quantitation and quality control. cDNA was synthesized from randomly primed aRNA using a 3DNA Array 350RP kit (Genisphere, Hatfield, PA) and Superscript II RT-PCR enzyme and reagents (Invitrogen). cDNAs were then modified, concentrated, and hybridized to the array as recommended in the Genisphere users' protocol. Bound cDNA from each timepoint in both the LD and DD cultures were hybridized to Cy5 probes, while cDNA from samples collected at ZT18 or CT18 (from LD and DD cultures, respectively) were hybridized to Cy3 probes, and served as the control for each time series.

All hybridizations were carried out in SDS-based buffer, and slides were washed and dried following each hybridization as recommended (Genisphere). Slides were scanned for Cy5 and Cy3 fluorescence using an Affymetrix 428 array scanner, and .tif images were generated from scans for both channels. All microarray hybridizations were performed twice (N=2 sample replicates) for each experimental group (N=4 biological replicates), giving a total number of 8 replicates for all samples.

Microarray Analysis

The .tif images generated from the scanner were analyzed using GenePixPro (Axon Instruments, Union City, CA) to determine signal and background fluorescence, and a false color image was then generated for each dye. This application was then used to generate .gpr files, which were analyzed using GeneSpring (Silicon Genetics, Palo Alto, CA). Data from the LD and DD series (N=8 per timepoint) were subjected to LOWESS normalization, and each time-point was reported as the normalized ratio of Cy5 to Cy3 intensity, where the ZT/CT 18 time point (for LD and DD, respectively) was designated as the control for each time series. Thus, expression of each gene at a given time-point was reported in terms of relative abundance to its own expression at midnight.

We established a multilevel analysis with different stringencies to determine which genes showed rhythmic expression patterns at different amplitudes. All analyses were based on two criteria: fold-change, and statistically significant variation, of expression levels relative to ZT/CT18. Our first statistical method defined rhythmic

expression as: 1) having a minimum 1.5-fold difference in expression levels for at least one time point relative to midnight; and 2) having a significantly different level of expression for one or more time-points relative to midnight, based on two-sample Students' t-test comparisons. Our second statistical method required that gene expression show an overall statistically significant variation over time based on ANOVA, as well as exhibiting at least a 1.5-fold change in expression levels. In addition, we screened genes that met a 2-fold change requirement using both statistical methods. All filters based on fold-change were performed using a linear ratio interpretation, whereas all statistical filters were based on a log ratio interpretation within the GeneSpring program. The data discussed in this dissertation have been deposited in NCBIs Gene Expression Omnibus (GEO, http://www.ncbi.nlm.nih.gov/geo/) and are accessible through GEO Series accession number GSE5292.

Quantitative Real-Time PCR Analysis

Expression of selected genes from the microarray analysis was validated using quantitative real-time PCR (qPCR), as follows. Pineal culture aRNA was DNase treated, primed with random hexamers, and cDNA was synthesized by reverse transcription using a Superscript II RT PCR kit (Invitrogen). Relative quantitation of selected genes was achieved by performing SYBR green-based real-time PCR using an ABI Prism 7700 Sequence Detection instrument (Applied Biosystems, Foster City, CA). Primers optimized for SYBR green real-time PCR amplification were designed for selected

genes using Primer Express (Applied Biosystems). Primer sequences are listed in Supplemental Table 1.

Standard curves were generated for target gene cDNAs and for *cyclophilin*, which we used as an endogenous reference, and cDNA for each timepoint was run in triplicate for each plate. Target gene expression levels were normalized to the endogenous reference values, and then normalized to a calibrator sample, which consisted of a mix of cDNA from each timepoint. Each plate included a "no template control" reaction (cDNA was replaced with water) as well as an "RT- control" reaction (reverse transcriptase enzyme was replaced with water) to rule out the possibility of genomic contamination.

Statistical Analysis

Time course data for microarray validation were subjected to cosinor analysis utilizing linear harmonic regression (CircWave software; Oster et al., 2006), as well as ANOVA. ANOVA was performed using Sigma Stat software package (Systat Software Inc, Point Richmond, CA).

Results

Pineal Melatonin Rhythms

We measured melatonin secretion by the pineal cultures to monitor physiological output in parallel with the gene expression analysis. Initial pilot studies performed demonstrate the *in vitro* pineal cultures are capable of entrainment to a LD 12:12 cycle.

As expected, cultured pinealocytes exhibited rhythmic melatonin production for at least three days in a LD 12:12 cycle (Fig. 1A), with a phase consistent with previous reports. The melatonin rhythm of pinealocytes used in the array analysis persisted in constant darkness with a reduced amplitude (Fig. 1B).

Rhythmic Transcriptome

In order to select statistically significant rhythmic genes while excluding erratically expressed genes, we used two different statistical filters to screen for rhythmicity (as described in the methods), and present the data here as discrete data sets (Supplemental Tables 2, 3). All sequences, BLAST results, and alignments are listed by reference number and are accessible through the Texas A&M Biology Department's Laboratory for Functional Genomics chicken pineal database at http://enterprise.bio.tamu.edu/index_chick.html.

Using the t-test comparison method, we found that 446 (5.5%) of the cDNAs represented on the array exhibit at least a 1.5-fold amplitude rhythm in LD (Supplemental Table 2). Of these, 191 were unique, classified genes, 216 returned no BLAST hit, and the remainders were redundantly represented cDNAs. The genes showing the greatest redundancy in this data set were *HIOMT* (n = 10), *TrH* (n = 9), *transthyretin* (n = 8), *cystatin c* (n = 5), and *purpurin* (n = 4). The total number of transcripts showing 2-fold rhythmic expression was greatly reduced, representing only 76 genes, or 0.9% of all genes on the array. Of these, 18 were unique, classified genes,

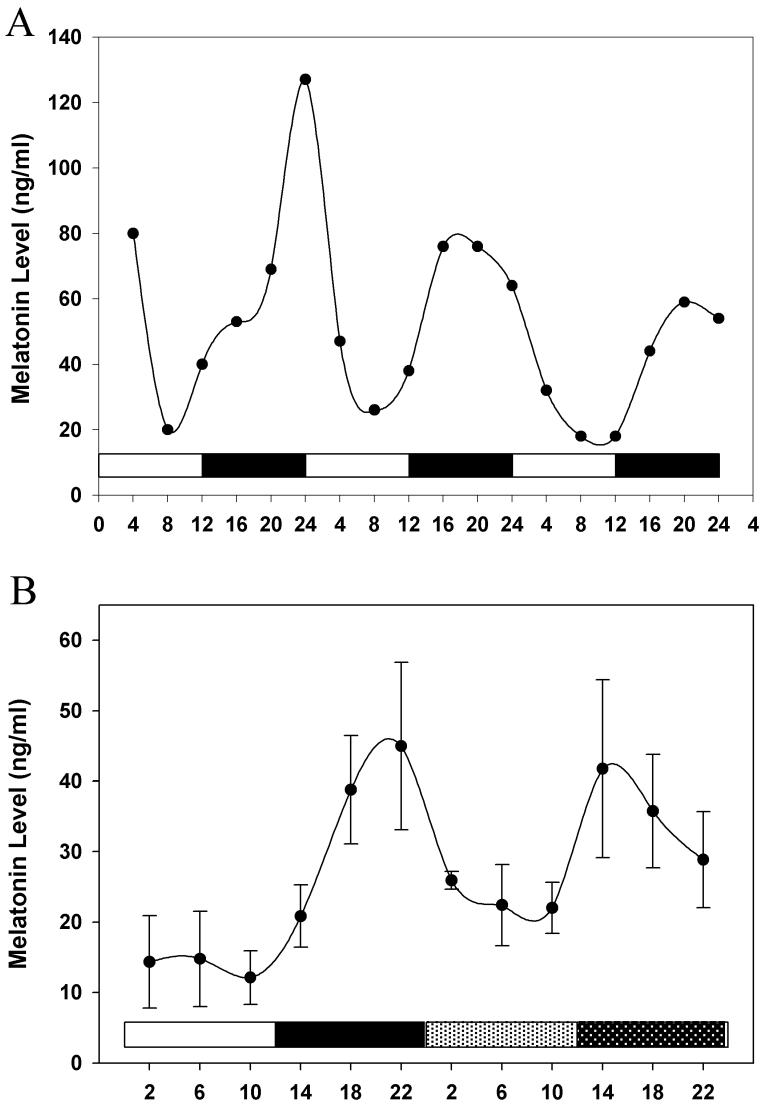

Figure 1. Pineal melatonin rhythms. **A,** Levels of melatonin secreted by chick pinealocytes were measured for 3 days in culture under an LD cycle. White bars indicate the time when lights were on, and black bars indicate the time when lights were off. **B,** Melatonin levels were measured from cultured pinealocytes maintained one day of LD followed by one day of DD. Light hatched bars indicate subjective day, while dark hatched bars indicate subjective night.

while 44 were unknown, with the remainder being redundancies. Not surprisingly, most of the redundant cDNAs were *HIOMT* (n = 7), *TrH* (n = 6), and *purpurin* (n = 4).

Applying the same statistical method to the DD data set, we found that 337 cDNAs (4.2%) exhibit at least a 1.5-fold-amplitude rhythm in DD (Supplemental Table 2). 150 of these were unique, classified genes, 164 were unknown, and the remainders were redundant transcripts. The reduced number of redundant, rhythmic genes in the DD data set likely indicates that some cDNAs, although rhythmic, did not meet our 1.5-fold change criterion. This is supported by the fact that overall transcriptional rhythmicity, and to a lesser extent, melatonin production, was reduced in DD. In fact, only 33 total cDNA's showed at least a 2-fold change in expression in DD, of which 14 were unique, classified genes, and 15 were unknown.

Using ANOVA as a statistical filter, the total number of rhythmically expressed transcripts with a 1.5-fold or greater amplitude in LD was reduced to 187 (2.3%), representing 71 unique, classified genes and 91 unidentified transcripts (Supplemental Table 3). The most commonly repeated cDNAs were again *HIOMT* (n = 9), *TrH* (n = 8), *transthyretin* (n = 5), and *purpurin* (n = 4) with *cystatin c* only being represented twice. While the t-test method was more inclusive overall, 11 out of the 71 classified genes which passed the ANOVA filter alone did not pass the t-test filter. Screening for 2-fold rhythmic expression using the ANOVA statistical filter reduced the list to 76 total genes (0.9%), including 26 unique, classified genes and 39 unknown transcripts. The disparity in the number of genes showing 2-fold or greater rhythmicity in LD as reported using the two different statistical filters was quite low. This was not unexpected, given that genes

cycling with higher amplitude are more likely to show statistical significance using either method. However, 10 of the combined 44 classified genes within the two gene lists were mutually exclusive.

Using the ANOVA-based statistical analysis for the DD data set, we found that a total of 108 (1.3%) transcripts, including 47 unique, classified genes and 54 unidentified transcripts exhibited a 1.5-fold amplitude rhythm (Supplemental Table 3). 17 out of 47 of the classified genes did not pass the t-test filter. Only 22 total transcripts passed our ANOVA-based screen at the 2-fold level, with 11 unique, classified genes and 10 unknown transcripts. However, 15 out of the combined 25 classified genes within these two gene lists were mutually exclusive. Overall, our pineal cultures show a large reduction in the number and amplitude of rhythmic transcripts compared to what has been observed *in vivo* (Fig. 2). In spite of this result, the amplitude of the melatonin secretion rhythm is robust and comparable to that observed in serum of chicken *in vivo* (Pelham, 1975).

Rhythmic Functional Gene Groups

Genes that exhibited 1.5-fold rhythmic expression in LD or DD were classified into one of twenty-one different functional categories using the same schema published previously in our laboratory (Bailey et al., 2003, 2004). This type of analysis permits a comparison of pineal transcriptome regulation *in vivo* and *in vitro*. We performed this analysis on the data set from the t-test based analysis, reasoning that the larger data set would minimize the possibility of sampling error. In both LD and DD, the functional

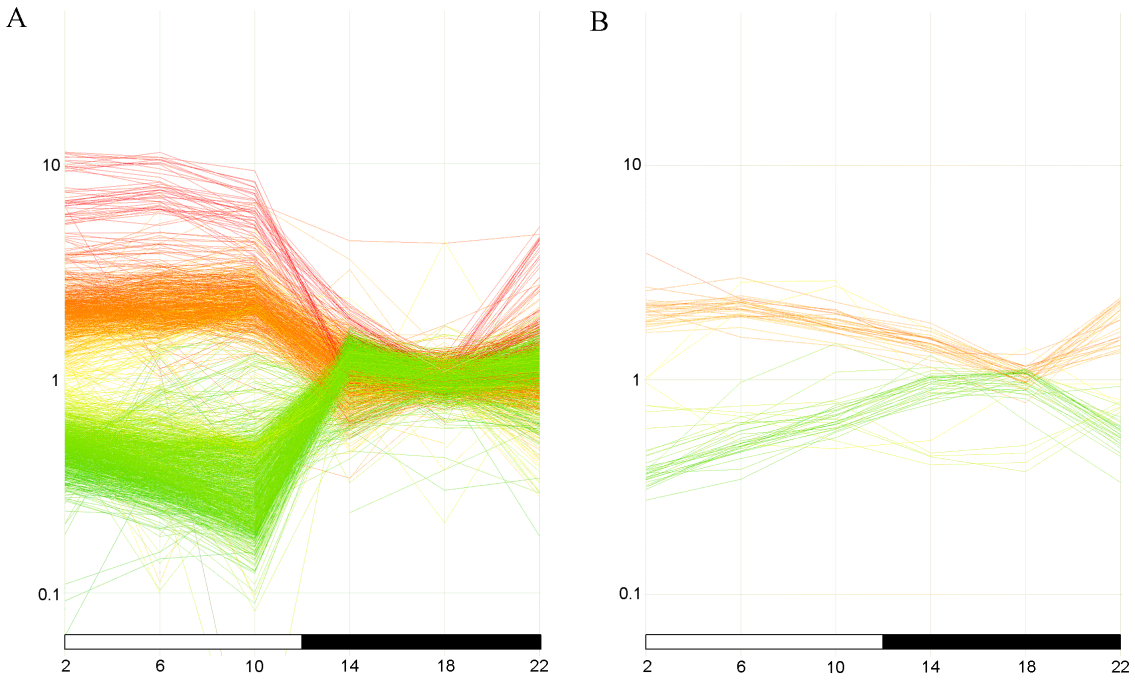

Figure 2. Rhythmic transcripts *in vivo* and *in vitro*. Gene expression profiles are shown for transcripts which cycle with a 2-fold rhythm in pineal *in vivo* (**A**) or in cell culture (**B**) under LD conditions. Statistical filtering of each data set is based on ANOVA as well as t-tests for the cell culture experiment.

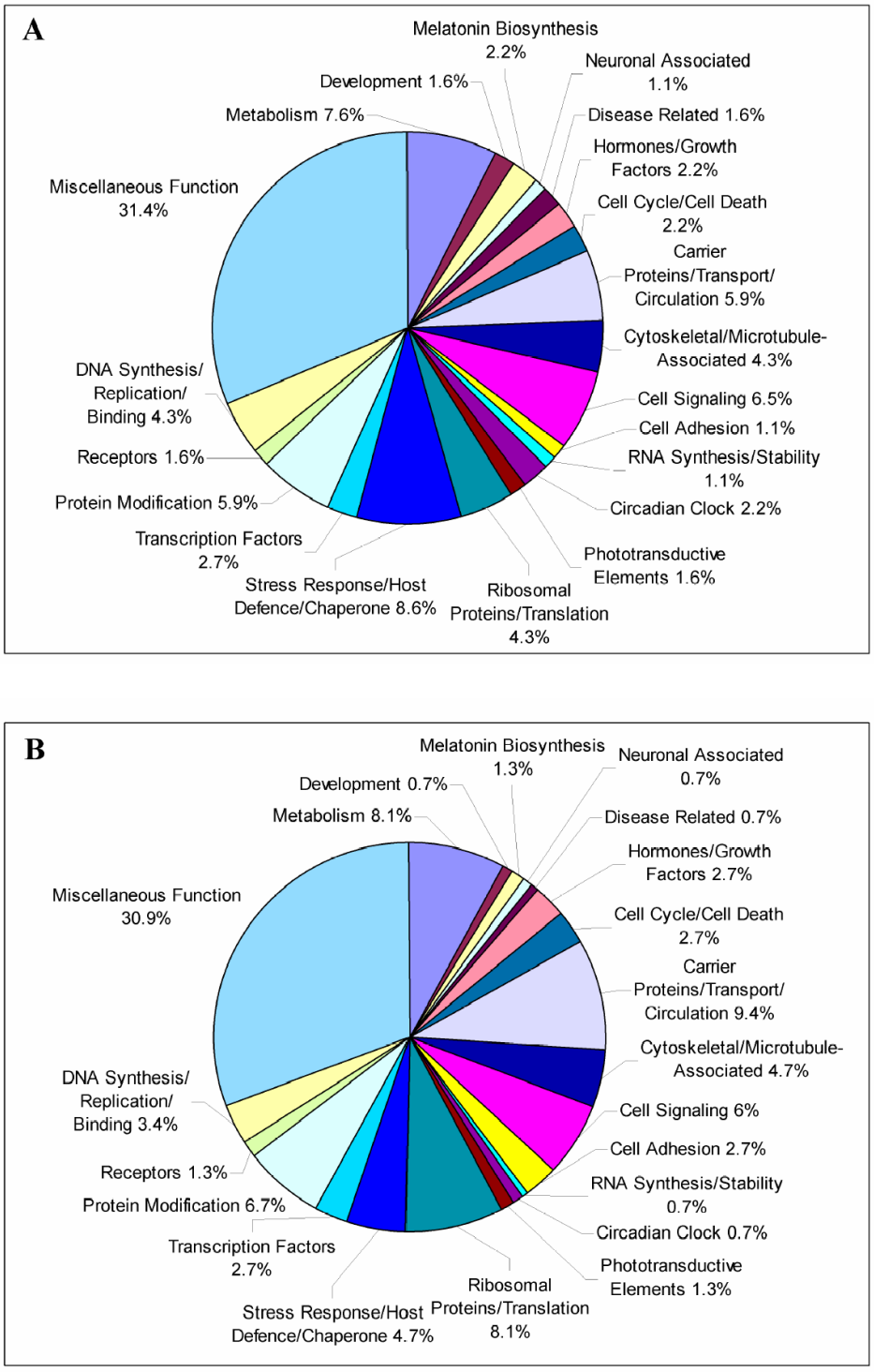

Figure 3. Rhythmic gene functions. Rhythmically transcribed genes were clustered according to proposed function, and the percentage of rhythmic genes representing each category is given under LD (**A**) or DD (**B**) conditions.

groups exhibiting the largest degree of circadian regulation were those associated with protein modification, intermediary metabolism, stress-response/immune function, cellular signaling, transport, and ribosomal proteins/translation (Fig. 3; Supplemental Table 4).

Microarray Validation

To validate the experimental data, the mRNA expression levels of four well characterized genes in the chick pineal gland were analayzed using qPCR techniques. Two genes from the melatonin biosynthesis pathway (*TrH* and *HIOMT*) and two clock genes (*cry1* and *per3*) were chosen for validation under LD conditions. Corroborating the microarray data, melatonin biosynthesis genes exhibited high amplitude circadian rhythms when measured using qPCR. *TrH* expression was rhythmic (array $p_{cosinor} <$ .001; array $p_{ANOVA} < .001$; qPCR $p_{cosinor} < .001$; qPCR $p_{ANOVA} < .001$), with > 2-fold higher mRNA levels at night (Fig. 4A). As expected (Bernard et al., 1999), *HIOMT* expression was approximately antiphase to the *TrH* rhythm, peaking at midday, with a large (~3-fold) amplitude rhythm in LD (array $p_{cosinor} < .001$; array $p_{ANOVA} < .001$; qPCR $p_{cosinor} < .001$; qPCR $p_{ANOVA} < .001$) (Fig. 4B).

The amplitude of clock gene rhythms was reduced compared to those of the melatonin biosynthesis genes. *Cry1* expression was rhythmic (array $p_{cosinor} < .001$; array $p_{ANOVA} < .001$; qPCR $p_{cosinor} = .001$; qPCR $p_{ANOVA} = .003$) with peak expression occurring at ~ZT6 (Fig. 4C). *Per3* mRNA expression was rhythmic in LD (array $p_{cosinor} < .001$; array $p_{ANOVA} < .001$; qPCR $p_{cosinor} < .001$; qPCR $p_{ANOVA} < .001$), with peak

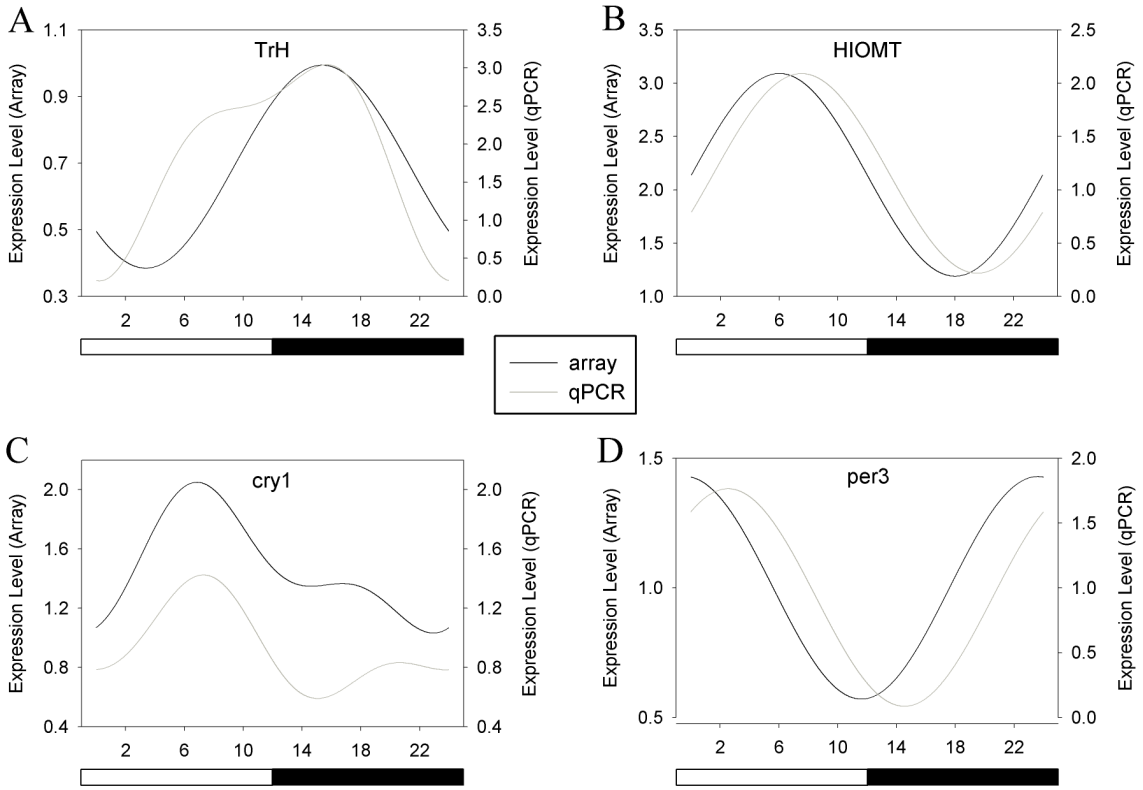

Figure 4. Microarray validation. qPCR was used to validate rhythmic expression of TrH, HIOMT, *cry1*, and *per3* genes under LD conditions (**A-D**, respectively). Cosinor functions fitted to data from microarray analysis using GeneSpring output (black lines) and from qPCR analysis (grey lines) are plotted. Cosinor analysis and ANOVA were performed on each data set. White bars indicate lights on, and black bars indicate lights off.

expression occurring between ZT22-2 (Fig. 4D). The phases of the rhythms of both clock genes, as well as the melatonin biosynthesis genes, were similar when measured using either qPCR or microarray hybridization techniques.

Discussion

Despite maintaining a robust rhythm of melatonin release comparable with previously reported rhythms *in vitro* (Zatz and Mullen, 1988a; Zatz and Mullen 1988b; Zatz et al., 1988) cultured pinealocytes exhibited lower amplitude mRNA rhythms within a diminished population of cycling transcripts as compared to what was reported *in vivo* (Bailey et al., 2003). Based on the two methods of analysis used in this study, our estimates of the number of genes expressing a 1.5-fold or greater rhythm within the pineal *in vitro* vary from ~2-6% of the genome in LD, and ~1-4% in DD, as represented in our array. Less than 1% of all pineal genes represented in our study express a 2-fold or greater amplitude rhythm in LD or DD using either method. While it is impossible to report the number of rhythmically expressed genes with absolute precision, it is likely that the actual proportion of rhythmic genes falls between our two estimates.

Nevertheless, it is clear that the chick pineal undergoes a large reduction in both the number of rhythmically transcribed genes and in the amplitudes of their rhythms *in vitro* as compared to *in vivo*, where a 2-fold or higher amplitude rhythm was observed for ~22% of the total number of transcripts in LD and ~8.5% of the total number of transcripts in DD (Bailey et al., 2003). Such a large reduction in the rhythmicity of the chick pineal transcriptome is surprising, considering that a robust rhythm of melatonin

release is retained in culture and persists in DD (Figure 1). This observation suggests that melatonin synthesis may be one of a small number of outputs from the circadian clock that continues to cycle at high amplitude in the absence of endogenous physiological feedback, and, perhaps, highlights an important disconnect between the melatonin synthesizing machinery and the presumed core oscillator mechanism.

It is not surprising, then, that the largest and most consistent number of high-amplitude rhythmic transcripts were *HIOMT* and *TrH*, two genes involved in the melatonin biosynthesis pathway that are regulated by the circadian clock. Our array analysis did not show *AANAT* mRNA to be rhythmic in constant conditions as it is in other dispersed pinealocyte cultures, although this may be due to our placement of cells under constant darkness, as opposed to constant dim red light, as has been done in other studies utilizing the same culture system (Bernard et al., 1997). *In vivo*, the amplitude of *AANAT* is greatly reduced under DD conditions as well (Bailey et al., 2003). This may suggest that *AANAT*, despite being the rate-limiting enzyme in this pathway, may damp more readily in the absence of physiological stimuli such as norepinephrine, or that it is regulated primarily through post-transcriptional mechanisms. However, *HIOMT* and *TrH*, along with *cystatin*, *transthyretin*, and *purpurin*, had the most abundant number of rhythmic transcripts, consistent with observations *in vivo* (Bailey et al., 2003).

The circadian phases of melatonin biosynthesis gene mRNA's are consistent with previous reports of mRNA regulation of these genes in chick. Orthologs of the clock genes *cry1* and *per3* also exhibited mRNA rhythms consistent with the literature and with their putative role as negative elements. It is worth mentioning that, although the

canonical negative element clock genes were rhythmic, they oscillated with low amplitudes compared to many other genes represented on the array, especially genes involved in melatonin biosynthesis. Therefore, if the "clock genes" are driving all cellular mRNA rhythms, significant amplification steps must occur to produce the more robustly rhythmic outputs. Of course, we have not investigated rhythmicity at the protein level, and it is likely that post-transcriptional mechanisms play a significant role in the regulation of downstream processes by the clock.

Interestingly, the functional clustering of rhythmic genes in pineal culture is remarkably similar to what is observed in the pineal *in vivo*, indicating that the reduction in the number of rhythmic genes in culture is global, rather than selective. The fact that pathways involved in immune-function are widely regulated by the pineal clock *in vitro* supports the notion that the pineal gland may play a more complex role in avian physiology than just the endocrine secretion of melatonin. While circadian control of these pathways may be specific to the pineal, it is also worth noting that genes involved in redox state/metabolism and protein processing appear to be highly regulated by the clock in other systems (Duffield, 2003; Bell-Pederson et al., 2005). Thus, despite high specificity in circadian control at the level of the individual gene, many common functional outputs appear to be regulated by the clock across different species.

Another intriguing observation is the large number of genes we found to be exclusively rhythmic in DD. Our broadest estimate indicates that as many as 73 (~50%) of the unique, classified genes found to be rhythmic in DD are not rhythmic in LD. Similar findings have been published from at least two other laboratories conducting

array studies of *Drosophila* genomics (Lin et al., 2002; Ueda et al., 2002; Duffield, 2003). One explanation for this phenomenon is that LD cycles could mask the rhythmicity of some light-regulated genes. Another explanation is that unknown mechanisms may result in the suppression of rhythmic mRNA regulation under LD cycles, or alternatively, rhythmic gene expression may be triggered under DD conditions. Although these findings have been understated in the literature, we suggest that they are likely more than just an epiphenomenon, and may be an important, global aspect of the complex circadian orchestration of animal genomes. Indeed, one study investigating torpor in mice reported that enzymes involved in lipid catabolism were rhythmic under DD, but not LD conditions, and therefore concluded that constant darkness could function as a circadian signal in these animals (Zhang et al., 2006).

Conclusions

We reveal that pinealocytes, while maintaining robust circadian physiology, exhibit globally reduced transcriptional rhythms *in vitro*. This reduced subset is, however, reflective of the functional distribution of the larger rhythmic transcriptome *in vivo*. While chick clock gene orthologs continue to cycle in culture, they do so at low levels, suggesting that significant signal amplification and/or posttranscriptional regulation must occur if these genes are driving the larger amplitude rhythms seen in the physiological output of the cells, as well as the expression of other more highly rhythmic genes. Further, constant darkness signals the rhythmic expression of multiple gene

transcripts in cultured pinealocytes, indicating that such phenomena may be intrinsic to circadian pacemakers.

CHAPTER III

A FUNCTIONAL SCREEN OF THE RHYTHMIC PINEAL TRANSCRIPTOME: REGULATION BY LIGHT AND NOREPINEPHRINE

Introduction

Chick pinealocytes exhibit all the characteristics of a complete circadian clock, comprising photoreceptive inputs, molecular clockworks and an easily measured rhythmic output, melatonin biosynthesis. These properties make the *in vitro* pineal a particularly useful model for exploring circadian control of gene transcription in a pacemaker tissue, as well as regulation of the transcriptome by primary inputs to the clock (both photic and noradrenergic).

In birds, the pineal gland and the hypothalamic suprachiasmatic nucleus (SCN) are autonomous oscillatory tissues, each comprising a node in a mutually inhibitory neuroendocrine feedback loop (Cassone and Menaker, 1984). In this system, melatonin secreted from the pineal inhibits SCN activity, and noradrenergic efferents from the SCN inhibit pineal melatonin synthesis (Cassone et al., 1986; Zatz and Mullen, 1988a, 1988b; Cassone et al., 1990). Additionally, these structures interact with a third autonomous oscillator, the avian retina, to form a tripartite circadian "clock" which influences downstream processes and peripheral oscillations (Cassone and Menaker, 1984).

The mechanism linking the core circadian oscillator in pinealocytes with the melatonin biosynthetic machinery is not completely understood. As stated above, pinealocytes respond directly to light *in vitro*, and there are at least three separable

pathways by which light affects melatonin levels: 1) acute suppression of melatonin synthesis, 2) decrease in rhythm damping and 3) phase shifting of the circadian pacemaker underlying melatonin rhythms (Zatz et al., 1988). The acute effects of light are mediated, at least in part, by a reduction in cAMP levels, which leads to a decrease in AANAT protein levels as well as a modest decrease in *AANAT* transcription (Zatz and Mullen, 1988a, 1988b; Zatz et al., 1988; Zatz, 1992; Zatz et al., 2000; Ganguly et al., 2002).

In the chick, norepinephrine (NE) released via a polysynaptic pathway originating in the SCN also effects an acute inhibition of melatonin biosynthesis through activation of α_2 adrenergic receptors and a subsequent reduction in intracellular cAMP levels (Binkley, 1988; Zatz, 1996). Thus, it appears that light and NE share a common signal transduction pathway leading to acute inhibition of melatonin biosynthesis. NE does not, however, exert any phase-shifting effects on melatonin biosynthesis rhythms, and therefore sympathetic input, unlike light, does not serve as a Zeitgeber for the chicken pineal clock (Zatz and Mullen, 1988b). Similarly, daily light and/or NE administration decreases damping (or increases the amplitude) of the rhythm of melatonin release via a cAMP-dependent pathway (Cassone and Menaker, 1983; Zatz, 1991). In contrast, the mechanism underlying phase shifting of the pineal oscillator involves different pathway(s) that do not involve cAMP signal transduction (Zatz and Mullen, 1988a, 1988b; Zatz, 1992), and remains unresolved at this time.

Based upon our previously published data (Bailey et al., 2003, 2004) and published reports (Deguchi, 1979; Kasal et al., 1979; Takahashi et al., 1980; Cassone et

al., 1986; Binkley, 1988; Zatz and Mullen, 1988a, 1988b; Zatz et al., 1988; Cassone et al., 1990; Menaker et al., 1997; Natesan et al., 2002), we hypothesize that central clock mechanisms in the chick pineal gland are likely identical or, at least, very similar in the retina and must be retained *in vitro.* Further, light should affect expression of these genes, while norepinephrine should only affect output. Therefore, we employed the pineal-specific microarray developed and used in previous studies from our laboratory (Bailey et al., 2003, 2004) to investigate the effects of 6-hour exposure to light or to norepinephrine on gene expression in free-running cultures during both subjective day and night. This protocol was used as the basis of a screen to identify genes that met the following criteria in cultured pinealocytes: 1) exhibit a rhythmic mRNA expression pattern that persists in constant darkness; 2) are light responsive; and 3) are insensitive to NE administration. These should represent a subset of genes identified in both pineal gland and retina *in vivo* (Bailey et al., 2003, 2004).

Materials and Methods

Cell Culture

All animals were treated in accordance with ILAR guidelines; these procedures have been approved by the Texas A&M University Laboratory Animal Care Committee (AUP no. 2001-163). Chicks were obtained from Hyline International (Bryan, TX) and used to establish pinealocyte cultures as previously described (see Chapter II methods). Cultures were entrained to a LD 12:12 cycle until sampling began.

Light Pulse Experiment

On day 6 of culture, cells were transferred to DD, and given a 6 hour light pulse (38 $\mu W/cm^2$) from either CT12-18 or from CT0-6 the following day, a protocol known to be sufficient to elicit a phase shift in pinealocytes (Zatz and Mullen, 1988b). Control cultures were maintained in DD, and received no light pulse. At CT12 or CT0, cells were washed, the media was changed, and then collected at CT18 or CT6, respectively, for both control cultures and cultures that had received the light pulse. After media was collected, cells were harvested into Trizol, homogenized, and stored at -80^oC. Four biological replicates were performed for each timepoint, for both light exposed and control treatments.

Norepinephrine Experiment

The protocol used in this experiment was the same protocol used in the light pulse experiments, except experimental cultures received norepinephrine-supplemented media ($3x10^{-8}$ M) instead of a light pulse. Control cultures received media lacking norepinephrine. Four biological replicates were performed for each timepoint, for both treatments.

Melatonin Radioimmunoassay

Melatonin levels in collected meadia samples were measured using radioimmunoassay, as described previously (see Chapter II methods). Data analysis and

melatonin quantitation was performed using ImmunoFit EIA/RIA software (Beckman Instruments Inc) as before.

Microarray Hybridizations

Total RNA was extracted, amplified, and reverse transcribed as described previously, and cDNA was processed and hybridized to our custom cDNA microarray (see Chapter II methods) following the Genisphere users' protocol. For the light pulse experiment, cDNA from cells exposed to a light pulse was hybridized to Cy5 probes, while cDNA from control cells was hybridized to both Cy3 and Cy5 probes. Labeling was carried out in the same way for the norepinephrine experiment, where cDNA samples from norepinephrine treated cells served as the experimental channel, and samples that did not receive norepinephrine served as the control channel. As an additional control, dye swaps were carried out for cDNA samples in both the light pulse and norepinephrine experiments.

All hybridizations were carried out in SDS-based buffer. Afterwards, slides were washed and dried, and then scanned (using an Affymetrix 428 array scanner) to generate image files. All microarray hybridizations were performed twice (N=2 sample replicates) for each experimental group (N=4 biological replicates), giving a total number of 8 replicates for all samples.

Microarray Analysis

Image files were quantified using GenePixPro (Axon Instruments, Union City, CA), and these data were then analyzed using GeneSpring software (Silicon Genetics, Palo Alto, CA). Data from both the light pulse and norepinephrine dosage experiments (N=8 per time-point per treatment) were subjected to LOWESS normalization followed by an additional dye-swap normalization step. In these experiments, Cy5 to Cy3 normalized experimental treatments (samples that had received light or NE) were compared to control samples using filters on statistical differences and fold change. Light or NE was considered to have an effect on gene expression if: 1) there was a minimum 1.5 fold difference between experimental and control treatments at CT6 or CT18; and 2) the difference was statistically significant based on a t-test. We also examined genes which showed 2-fold or greater regulation by light or norepinephrine. When using GeneSpring for these analyses, all filters based on fold-change were performed using a linear ratio interpretation, whereas all statistical filters were based on a log ratio interpretation. The data discussed in this publication have been deposited in NCBIs Gene Expression Omnibus (GEO, http://www.ncbi.nlm.nih.gov/geo/) and are accessible through GEO Series accession number GSE5292.

Quantitative Real-Time PCR Analysis

Expression of selected genes from the microarray analysis was validated using quantitative real-time PCR (qPCR), as follows. Pineal culture aRNA was DNase treated, randomly primed, and reverse transcribed as before. Real-time PCR amplification and

detection was performed on an ABI 7500 Fast system (Applied Biosystems, Foster City, CA) using SYBR green master mix. Target gene mRNA levels were determined using the relative quantification method as described previously (see Chapter II methods), using *cyclophilin* as an endogenous control gene. Target and control gene primer sequences are listed in Supplemental Table 1.

Statistical Analysis

Time course data for microarray validation were subjected to cosinor analysis using the CircWave software application, as well as ANOVA. Changes in melatonin levels were subjected to a two-sample t-test. ANOVA and t-tests were performed using Sigma Stat software package (Systat Software Inc, Point Richmond, CA).

Results

Regulation by Light and Norepinephrine

As expected, 6-hour exposure to a light pulse (38 $\mu W/cm^2$) inhibited melatonin release from the cultured pinealocytes at both subjective midday and midnight (Fig. 5). Norepinephrine administration ($3x10^{-8}$ M) significantly decreased melatonin release during the subjective day but not during the subjective night (Fig. 5). A total of 142 (~1.8%) cDNAs were shown to be regulated at least 1.5-fold by light. 50 of these were unique, classified genes, 71 were unknown, and the remainders were redundant cDNAs (Supplemental Table 5). The most abundant light regulated genes were *HIOMT* (n = 10), *TrH* (n = 8), *cystatin* (n = 3), and *purpurin* (n = 4). The only clock gene that was

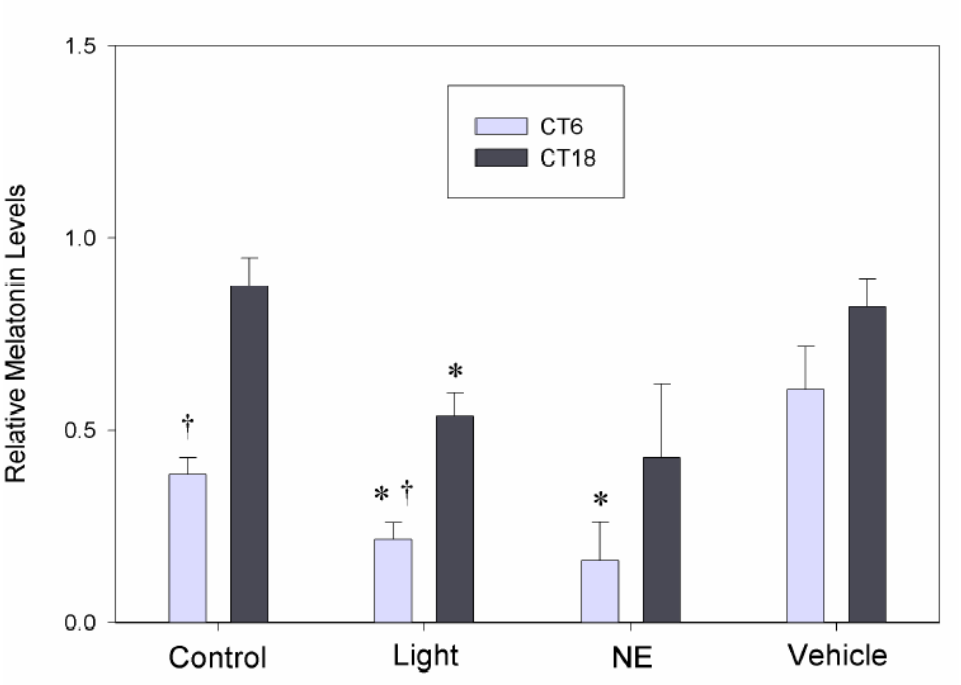

Figure 5. Inhibition of melatonin production by light and norepinephrine. Melatonin levels released into media were measured during mid-subjective day and mid-subjective night for cultures that had received a 6-hr light pulse, those that had received a 6-hr dose of NE (3×10^{-8} M), and for control cultures which had received no light or a vehicle solution. Significant difference ($p < .05$) between experimental treatments and controls for each timepoint is indicated by *. Significant difference ($p < .05$) between CT6 and CT18 timpoints within each treatment group is indicated by †.

shown to be light regulated was *cry1*, which was upregulated by light (at both CT6 and CT18), consistent with previously published data (Yamamoto et al., 2001). Only a small number of transcripts (n = 24) were regulated 2-fold, although these include all the above except purpurin (Supplemental Table 5).

The phototransductive/photoregulatory elements shown to be affected by light were *purpurin* (p*urp*) and *early-undifferentiated retina and lens gene* (e*url*). Other phototransductive/photoregulatory genes represented on our array were rhythmic, but not acutely light-regulated, including *retinal fascin*, *interstitial retinol-binding protein 3* (i*rbp*), and *transducin γ-subunit*. All of these but the last are rhythmic *in vivo* as well (Bailey et al., 2003).

A light pulse applied to pinealocyte cultures during CT0-CT6 affected the expression of a larger number of transcripts than when applied during CT12-CT18, including both induction (CT6, n = 54; CT18, n = 32) and suppression (CT6, n = 50; CT18, n = 30) of specific genes (Supplemental Table 5). The total number of genes influenced by light exposure, however, was similar within a given treatment. In contrast to light exposure, norepinephrine administration had little overall effect on gene expression—only 19 cDNAs showed 1.5-fold regulation by NE (Supplemental Table 6).

Comparative Analysis and Candidate Genes

As part of our screen to identify candidate genes that may play a role in pinealocyte clock function, we compiled non-overlapping unigene lists which fit into combinations of one or more of the following categories, based on t-test analyses: 1)

rhythmic genes with 1.5-fold amplitude expression in LD; 2) rhythmic genes with 1.5-fold amplitude expression in DD; 3) genes regulated 1.5-fold by light; and 4) genes regulated 1.5-fold by norepinephrine (Supplemental Table 7). A summary of the number of genes in each list, ranked in order of decreasing numbers, is displayed in Table 1.

Table 1. Comparative gene list

Gene List	# non-redundant genes
LD only	234
DD only	172
LD, DD	102
Light Only	44
LD, Light	34
LD, DD, Light	27
NE only	14
DD, Light	8
LD, NE	3
DD, NE	1
LD, DD, Light, NE	1
LD, DD, NE	0
LD, Light, NE	0
DD, Light, NE	0
Light, NE	0

Clustered, non-overlapping unigene lists, ranked in order of decreasing gene number. Genes are clustered as follows: LD: rhythmic genes with at least 1.5-fold amplitude mRNA expression in LD; DD: rhythmic genes with at least 1.5-fold amplitude mRNA expression in DD; Light: gene mRNA regulated at least 1.5-fold by light; NE: gene mRNA regulated at least 1.5-fold by norepinephrine.

A nearly equal number of genes that were rhythmic in LD and affected by light were also rhythmic in DD. We consider those genes which met this criteria and were also unaffected by norepinephrine to be candidate “clock-related” genes requiring

Table 2. Candidate gene list

Blast Hit
Cry1*
Cystatin c**
HIOMT**
N-myc downstream regulated 1*
Nuclear factor 1 X protein**
Hypothetical protein DaciDRAFT_2108 [Delftia acidovorans SPH-1]*
Purpurin **
PREDICTED: hypothetical protein [Gallus gallus] cp5764**
Proline-rich protein 15, isoform CRA_a [Rattus norvegicus]*
Unnamed protein product [Tetraodon nigroviridis]**
18 unidentified sequences

List of annotated genes that meet the following criteria: 1) they exhibit a rhythmic expression pattern that persists in constant darkness; 2) they are light regulated; and 3) they are insensitive to NE administration.
* Gene also passed ANOVA in one data set, either LD or DD
** Gene also passed ANOVA in both LD and DD data sets

further analysis (Table 2; Fig. 6). Although *cry1* did not continue to exhibit a significant rhythm in DD under our array analysis, we include it here because qPCR verifies that *cry1* is in fact rhythmic under DD conditions (data not shown), and *cry1* expression is potently induced by light (at CT6) but unaffected by NE at either timepoint (Fig. 6A-B). The mRNA rhythms of these genes under LD conditions correlate well with their regulation by light in all cases, as demonstrated for selected genes (Figs. 6-7). However, some of these genes underwent a complete phase inversion in DD (Fig. 7).

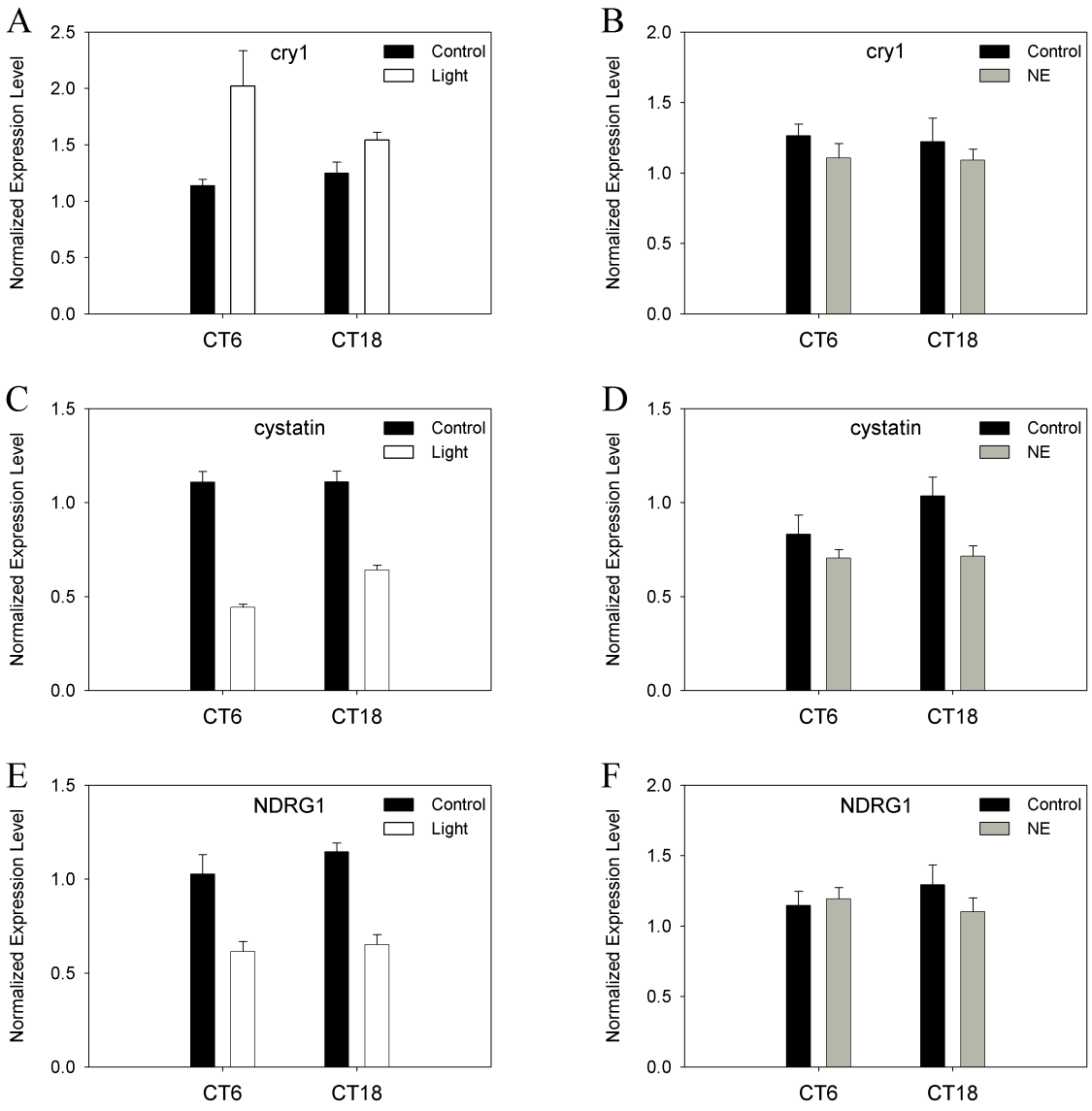

Figure 6. Light regulated, NE-insensitive gene transcripts. Expression data from selected genes that passed the criteria outlined in our screen are plotted here as histograms showing mRNA levels measured after receiving a 6-hour pulse of light (left panel) or 6-hour course of NE supplemented medium (right panel) relative to controls. Histogram plots are based on normalized array data from GeneSpring (Silicon Genetics).

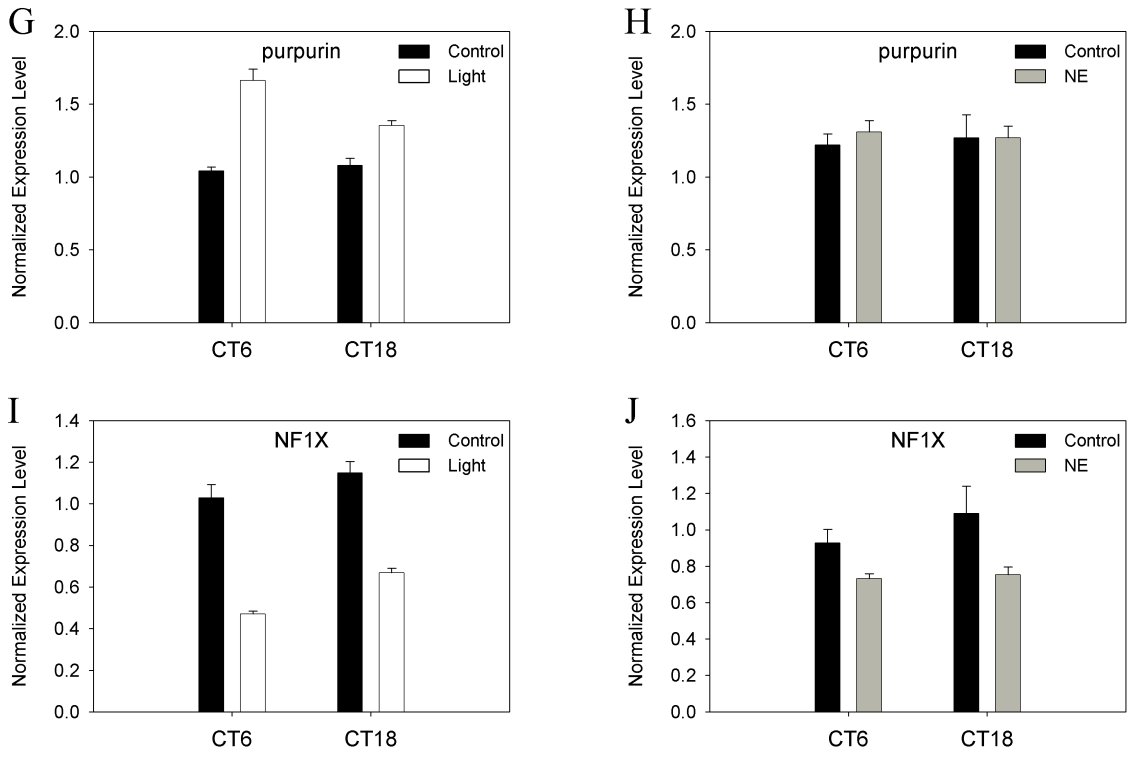

Figure 6 Continued.

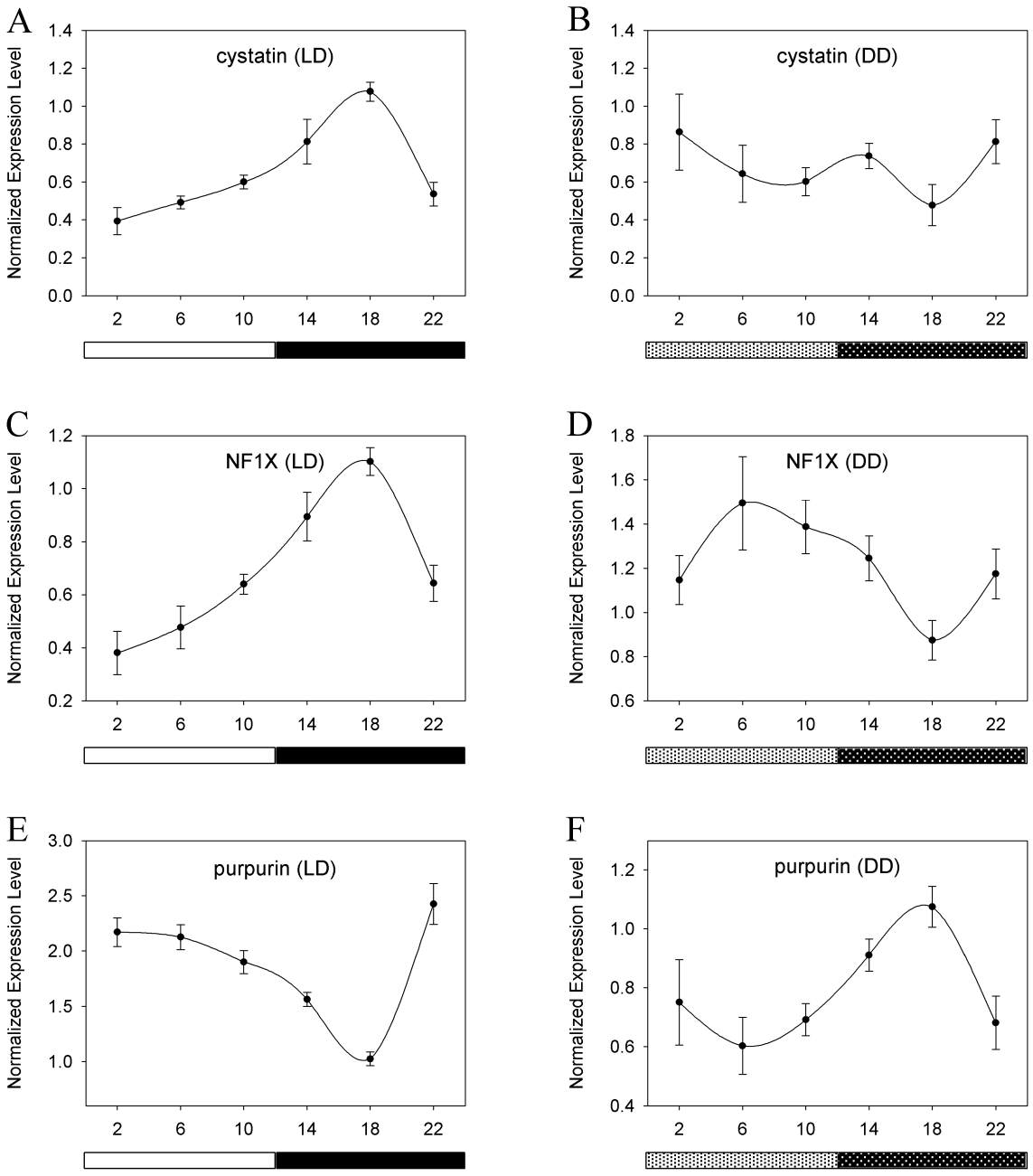

Figure 7. Phase inversions of candidate gene mRNA rhythms in DD. Circadian expression patterns of genes that exhibited phase inversions in expression rhythms when switched from LD to DD are shown here (LD, left panel; DD, right panel).

Array Validation of Selected Genes

We validated the expression of three genes of interest (*cystatin c*, *NF1X*, and *purpurin*) which were identified in our screen. While temporal expression patterns of the genes have not been previously characterized in chick pineal, our microarray analysis reveals they exhibit circadian rhythms *in vitro*. *Cystatin c* exhibited higher expression at night, with a peak occurring around ZT18 as measured using either method (Fig. 8A), although qPCR did not show a significant change in expression using ANOVA (array $p_{cosinor}$ <.001; array p_{ANOVA} <.001; qPCR $p_{cosinor}$ = .043; qPCR p_{ANOVA} = .201). Microarray analysis and qPCR revealed a peak in *NF1X* expression between ZT14-ZT18 (Fig. 8B), although this rhythm was not significant as measured by qPCR, likely due to the detection of a secondary peak at ~ZT2 (array $p_{cosinor}$ <.001; array p_{ANOVA} <.001; qPCR $p_{cosinor}$ = .334; qPCR p_{ANOVA} = .176). *Purpurin* expression was highly rhythmic, with identical phases measured using either method (Fig. 8C; array $p_{cosinor}$ <.001; array p_{ANOVA} <.001; qPCR $p_{cosinor}$ <.001; qPCR p_{ANOVA} <.001).

Discussion

The observation that light had a differential effect on mRNA levels at different times of day suggests that the pineal clock may modulate photo-responsiveness itself as a function of circadian time, such that light has a greater effect at a time when it is normally present as an exogenous stimulus. This is perhaps not surprising given that circadian entrainment by light is dependent on time of day, though our results show that temporal regulation of the light response extends to induction and inhibition of specific

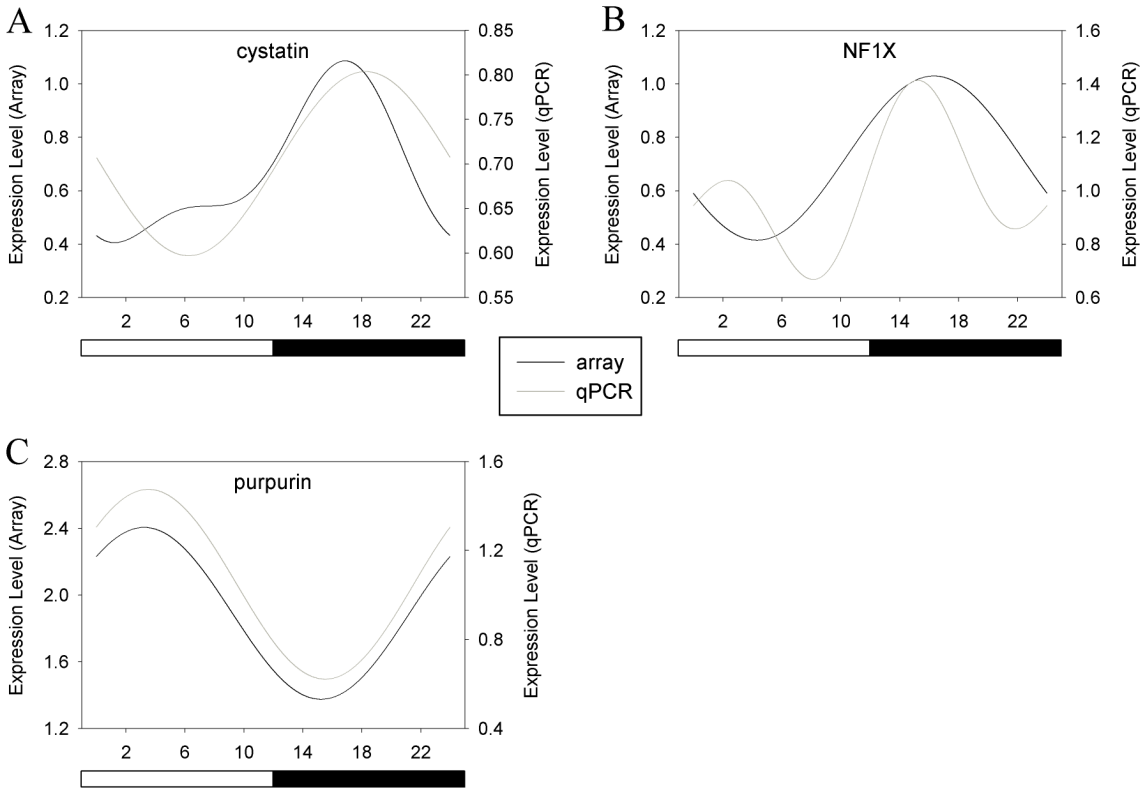

Figure 8. Microarray validation of selected genes. qPCR was used to validate rhythmic expression of cystatin c, NF1X, and purpurin under LD conditions (**A-C**, respectively). Cosinor functions fitted to data from microarray analysis using GeneSpring output (black lines) and from qPCR analysis (grey lines) are plotted. Cosinor analysis and ANOVA were performed on each data set. White bars indicate lights on, and black bars indicate lights off.

gene transcripts. Although the effect of induction/reduction of mRNA by NE is small compared to a light stimulus, they have comparable effects on melatonin production. Thus, if NE has global effects on the chick pineal, it may exert its largest effects at the protein level, with comparatively small effects on gene expression, as is the case for NE's acute inhibition of melatonin biosynthesis (Natesan et al., 2002).

Our comparative analysis revealed that many genes were rhythmic exclusively in LD or DD, or were rhythmic in both. As might be expected, there was significant overlap between genes that were rhythmic in LD only and those that were affected by a light pulse. The rhythmic expression of these genes is therefore probably light-driven, although some may have exhibited low amplitude rhythms in DD that were not detected on the array. Additionally, we found a significant number of genes that were regulated by light, but were not rhythmic in LD. Again, some of these genes may have expressed weak rhythms that went undetected. Another explanation is that light may be masking the endogenous rhythms of some of these genes in LD.

As noted in the results, some of these gene mRNA rhythms underwent a complete phase inversion in DD, suggesting that LD cycles may impose light-driven rhythms for some genes via acute inhibition/induction by light. Nevertheless, we cannot differentiate between acute and phase-shifting effects of light in this analysis, and therefore some of these genes may or may not fit the true criteria expected for clock-related genes. Also, because only one pass sequencing was conducted from the 5′ ends of these genes, some of the "unknown" genes that did not return a significant BLAST hit might be identified with additional sequencing. Some of these may be redundant with

other genes from our analysis. Several of these classified genes are rhythmic in chick retina as well (Bailey et al., 2004), suggesting they may be a ubiquitous component of chick pacemaker tissues. A brief discussion of some of the classified genes from our screen follows.

NF1X

Nuclear factor 1 X-type (*NF1X*) is a transcription factor known to bind the palindromic consensus sequence TTGGC$(N)_5$GCCAA (Nowock et al., 1985), and has been shown to activate replication of adenoviral DNA (Nagata et al., 1983). It is highly conserved in vertebrates, with chicken and hamster orthologs showing 92% amino acid sequence identity (Kruse et al., 1991). *NF1X* is reported to control the expression of a number of different genes in liver (Lichsteiner et al., 1987; Bois-Joyeux and Danan, 1994; Cardinaux et al., 1994; Anania et al., 1995; Garlatti et al., 1996), and is a known repressor of *glutathione S-transferase* (Osada et al., 1997), which is involved in intermediary metabolism of xenobiotics and is also shown to be rhythmic in our study (Supplemental Tables 2, 7). NF1 proteins also exhibit a redox-sensitive regulation of *CYP1A* transcription in humans (Morel and Barouki, 1998). Since CYP1A protein levels alter the oxidative state of the cell, which in turn activates the transcription of multiple transcription factors (Puga et al., 2000), *CYP1A* could provide a direct link between the pineal clock, cellular redox state, and intermediary metabolism if the circadian clock regulated it. Future research exploring a redox dependent regulatory role of *NF1X* within the chick pineal clock is warranted.

Cystatin C

C*ystatin* is a potent cysteine protease inhibitor (Dickinson, 2002) and has been implicated in diverse processes, including immunomodulation. Chicken *cystatin* has also been reported to act as a growth hormone in mouse fibroblasts (Dickinson, 2002). The putative role of *cystatin* in immune function is intriguing, given that many genes associated with the immune system show circadian rhythmicity in the pineal gland *in vivo* (Bailey et al., 2003) as well as *in vitro* (see Chapter II). Furthermore, we hypothesize that cystatin may interact with redox-sensitive pathways at the posttranslational level, since cysteine thiol groups are the primary redox-sensing structures.

NDRG1

N-myc downstream regulated 1 (*NDRG1*) is involved in a wide array of biological processes, including cellular differentiation and stress responses (Piquemal et al., 1999; Agarwala et al., 2000), and is repressed by the *n-myc* and *c-myc* proto-oncogenes. The rhythmic and light inducible expression of *NDRG1* may indicate circadian regulation of *n-myc* itself. This finding would be of interest since N-MYC protein activates transcription via binding to E-boxes (Alex et al., 1992), and subsequently the activation of a large number of genes involved in ribosomal and protein synthesis (Boon et al., 2001), consistent with the result of our functional clustering analysis of pinealocytes *in vitro*.

Additionally, *NDRG1* is reported to be induced by retinoic acid (Piquemal et al., 1999) and to associate with APOLIPOPROTEIN A-I (Hunter et al., 2005). APOLIPO-PROTEIN A-I is a gene product involved in cholesterol transport which we found to be regulated in a circadian fashion within the chick pineal (Supplemental Tables 2, 3, 7). *NDRG1* may therefore couple retinoic acid signaling with circadian regulation of cellular trafficking of lipids in the pineal.

Purpurin

Purpurin belongs to the lipocalin protein family, a diverse group of proteins involved in various processes including immune function and retinoid binding (Flower, 1994). *Purpurin* is known to be synthesized in retinal photoreceptors (Berman et al., 1987), and while its function is not fully understood, it is thought to mediate cellular adhesion and survival (Schubert and LaCorbiere, 1985) as well as having a role in the transport of retinol within the retina (Schubert et al., 1986). These properties make *purpurin* an interesting potential candidate gene for linking visual input or immune response to the pinealocyte clock.

Conclusions

Our combined approach of utilizing a temporal, photic and pharmacological microarray experiment allowed us to identify novel genes linking clock input to clock function within the pineal. Our experimental screen has provided a set of rhythmic genes that are sensitive to light, a potential phase-shift inducing stimulus, but not acute

regulation by norepinephrine. This gene set supplies unique and intriguing candidates for deeper characterization of the circadian system, including knockdown and over-expression experiments that may lead to the identification of genes with novel circadian clock function in avian species.

CHAPTER IV

MODULATION OF CIRCADIAN METABOLIC AND CLOCK GENE mRNA RHYTHMS BY EXTRA-SCN OSCILLATORS

Introduction

Organization of circadian clocks is complex in avian species, consisting of an interplay between three separate oscillators located in the pineal, the eyes, and the avian suprachiasmatic nucleus (SCN) (Gwinner and Brandstätter, 2001; Underwood et al., 2001). It has been proposed that these three structures contain damped oscillators, which interact within a neuroendocrine loop to sustain rhythmicity over multiple cycles (Cassone and Menaker, 1984). Specifically, this model hypothesizes that the avian pineal and retina inhibit SCN activity during the night by secretion of melatonin and/or via neurotransmission, while the SCN inhibits melatonin production in the pineal during the day. There are no known efferent neural connections from the SCN to the retina.

This is only a generalized model for avian species, however, as the specific interactions between circadian oscillators are hierarchical and species dependent. For example, pinealectomy has a greater effect on overt rhythms in passerine birds such as house sparrow than on galliform species such as chicken and quail (Underwood et al., 2001; Bell-Pederson et al., 2005). In the latter two species, the eyes have been demonstrated to play a greater role, as enucleation, but not pinealectomy, abolishes activity rhythms in these animals (Nyce and Binkley, 1977; Underwood, 1994). This regulatory role for avian eyes does not correlate with their contribution to circulating

melatonin, however. For instance, the retinae of quail secrete up to 50% of the plasma levels of melatonin, the pineal being responsible for the remaining half (Underwood, 1994). In contrast, the eyes of chickens release very little, if any, detectable amounts of melatonin in the bloodstream (Reppert and Sagar, 1983; Cogburn et al., 1987).

Radioligand binding studies using 2-[^{125}I]iodomelatonin (IMEL) demonstrate that melatonin binding is widespread in the avian nervous system, most prominently within the visual structures, including the retina and vSCN (Dubocovich and Takahashi, 1987; Rivkees et al., 1989; Cassone et al., 1995). Birds express three melatonin receptor subtypes, Mel_{1A}, Mel_{1B}, and Mel_{1C}, which also have widespread, but differential spatial distributions in the brain (Reppert et al., 1995, 1996; Natesan and Cassone, 2002). Furthermore, melatonin receptor mRNA levels, as well as IMEL binding, are rhythmic in some neuronal structures (Lu and Cassone, 1993b; Natesan and Cassone, 2002).

As an endocrine output of the circadian system, melatonin plays an important role in synchronizing internal rhythms. For instance, melatonin entrains behavioral and metabolic rhythms (as measured by uptake of the metabolic marker 2-deoxy[^{14}C]-glucose, or 2DG) in birds (Lu and Cassone, 1993a; Lu and Cassone, 1993b; Adachi et al., 2002; Cantwell and Cassone, 2002) as well as activity rhythms in mammals and neuronal firing rhythms of mammalian SCN tissue *in vitro* (Redman et al., 1983; Starkey et al., 1995). Less is known about how melatonin influences peripheral tissues, although studies characterizing autoradiographical binding and molecular receptor distribution in birds and mammals suggest melatonin may act on heart, lung, kidney, gut, gonads, and circulatory vasculature, although the density and distribution of these sites is highly

species dependent (Pang et al, 1993; Lee et al., 1995; Wan and Pang, 1995; Pang et al, 1996; Drew et al., 2001; Poon et al., 2001; Naji et al., 2004). In rodents, melatonin is known to regulate the expression of multiple clock genes within the pars tuberalis, a site with a high density of melatonin receptors (Pévet et al., 2006).

In addition to regulating glucose metabolism, circadian clocks are linked to numerous other metabolic processes, including lipogenesis, xenobiotic metabolism, and cellular redox state (Rutter et al., 2001; Duffield, 2003; Wijnen and Young, 2006; Duez and Staels, 2007; Kohsaka and Bass, 2007). Also, circadian mutant mice exhibit a range of metabolic defects, including hyperphagia, obesity, and impaired carbohydrate metabolism (Rudic et al., 2004; Turek et al., 2005; Oishi et al., 2006; Kohsaka and Bass, 2007). These data highlight an intimate linkage between circadian clocks and metabolism. Many of these processes are likely controlled via tissue specific circadian regulatory pathways.

In peripheral tissues, the core transcriptional feedback loops based on the positive and negative regulatory limbs (composed of *bmal*/*clock* and *per*/*cry* genes, respectively) are preserved (Yagita et al., 2001; Stratmann and Schibler, 2006; Hastings et al., 2007). As with pacemaker tissues, these gene products oscillate autonomously, though they dampen over time as a result of desynchronization between individual cellular oscillators (Balsalobre et al., 1998; Yamazaki et al., 2000; Yoo et al., 2004; Guo et al., 2005; Guo et al., 2006). Presumably, it is the oscillations of these canonical clock gene products which drive rhythms in local physiological processes within peripheral tissues.

In both birds and mammals, the SCN coordinates the circadian physiology of multiple organ systems by synchronizing peripheral clocks via both neural and humoral mechanisms (Bell-Pedersen et al., 2005; Stratmann and Schibler, 2006; Kalsbeek et al., 2007). However, it is not known how multiple pacemakers interact to coordinate peripheral oscillators in complex avian systems. In this study, we profile mRNA rhythms of both positive and negative clock genes in multiple central and peripheral tissues in chick, and monitor 2DG uptake as an important circadian output in these tissues. We also investigate the roles of the eyes and the pineal in synchronizing peripheral rhythms, and explore the relationship between metabolic rhythms and transcription of avian clock genes.

Materials and Methods

Animals and Surgeries

All animals were treated in accordance with ILAR guidelines; these procedures have been approved by the Texas A&M University Laboratory Animal Care Committee (AUP no. 2005-110). Male White Leghorn chicks were obtained from Hyline International (Bryan, TX) on the first day post-hatch and maintained on a 12:12 LD cycle in heated brooders with continuously available food and water. Four rounds of surgeries (pinealectomy, enucleation, or sham surgery) were performed 7-8 days post-hatch. Prior to each surgery, chicks were deeply anaesthetized with an intramuscular injection of a ketamine/xylazine (9:1) cocktail (100 mg/kg).

Pinealectomies (n = 72) were performed as follows: anaesthetized chicks were secured in a stereotaxic apparatus, a small mid-sagittal incision was made in the skin above the cranium, and then a small portion of skull was removed using a dental drill to expose the pineal gland. Meninges were cut away using microsurgical Vannas scissors, the pineal was gently removed with forceps, and the opening was packed with gel foam to reduce bleeding. The wound was then closed with surgical suture and treated with a topical antibiotic ointment. For enucleation surgeries, animals (n = 72) were anaesthetized and then bilaterally enucleated using curved iridectomy scissors. To maintain hemostasis, the orbits were packed with gel foam while pressure was applied with surgical gauze, and animals were placed at an angle to allow wound drainage during recovery from the anaesthetic. Sham surgeries (n = 72) were performed exactly the same way as pinealectomies, except that the pineal was left intact. All animals were allowed to recover for one week in LD with food and water provided *ad libitum*.

2DG Injections and Tissue Sampling

As with surgeries, tissue sampling was done in four rounds. After recovery, chickens were kept in LD or placed under DD (n = 108 total, each treatment), and then maintained in those conditions for three days prior to tissue collection. Tissues were then harvested every four hours over six timepoints, beginning two hours after lights on (LD birds) or two hours after the onset of subjective day (DD birds). One hour prior to tissue collection, 3 birds from each surgery group were given intraperitoneal injections of 2-deoxy[^{14}C]glucose (100 μCi/kg; American Radiolabeled Chemicals, St. Louis,

MO). Injections were administered randomly to three groups of three animals over an hour long period, with 20 minute intervals between sets of injections.

Exactly one hour after being injected, animals were killed by CO_2 asphyxiation and the following tissues were excised and frozen on dry ice: telencephalon, diencephalon, optic tectum, liver, and heart. Serum was isolated from trunk blood and then frozen along with tissue samples. After all tissues were harvested, they were transferred to an ultrafreezer for long term storage at -80° C. All injections and euthanizations done at night or under DD were performed in the dark using infrared optical viewers. When harvesting brain tissue during dark phases, a dim red light source was used.

Tissue Processing and 2DG Uptake

Frozen tissue samples (100 mg) were placed into Trizol reagent (Invitrogen) and disrupted using a roto-stator homogenizer. Small aliquots of tissue homogenates and serum samples were placed into scintillant and beta emission was measured using a liquid scintillation counter (Beckman Instruments Inc., Fullerton , CA). 2DG uptake levels were determined based on the specific activity of the isotope (300 mCi/mmol), and then normalized to tissue weight and serum 2DG levels.

Real-Time PCR Analysis

Total RNA was extracted from lysis homogenates using a Qiagen RNeasy kit (Qiagen). RNA was DNase treated, then primed with oligo dT primers using a

Superscript II First Strand Synthesis RT-PCR kit (Invitrogen). Quantitative real-time PCR (qPCR) amplification and detection was performed on an ABI 7500 Fast instrument (Applied Biosystems) using SYBR green master mix. Target gene mRNA levels were determined by the standard curve method of relative quantification, using *cyclophilin* as an endogenous control gene. Every PCR plate included control samples lacking template and samples which lacked reverse transciptase during the cDNA synthesis reaction. Primer sequences are listed in Supplemental Table 1.

Statistical Analysis

All 2DG and qPCR timecourse data were subjected to ANOVA (Sigma Stat software), as well as cosinor analysis utilizing a linear harmonic regression algorithm (CircWave software). F-testing probability values (α) were set to ≤ 0.05, and expression was considered to be rhythmic when a cosine fit was statistically significant ($p \leq 0.05$).

Results

2DG Uptake in Brain

Previous studies utilizing autoradiographical methods show that many avian brain structures exhibit daily or circadian rhythms in 2DG uptake, especially in visual structures and in the vSCN (Lu and Cassone, 1993a; Lu and Cassone, 1993b; Cantwell and Cassone, 2002). To determine whether overt rhythms can be detected in embryonic subdivisions of the brain, we measured 2DG uptake in homogenates of excised telencephalon, diencephalon, and optic tectum. We also investigated whether circadian

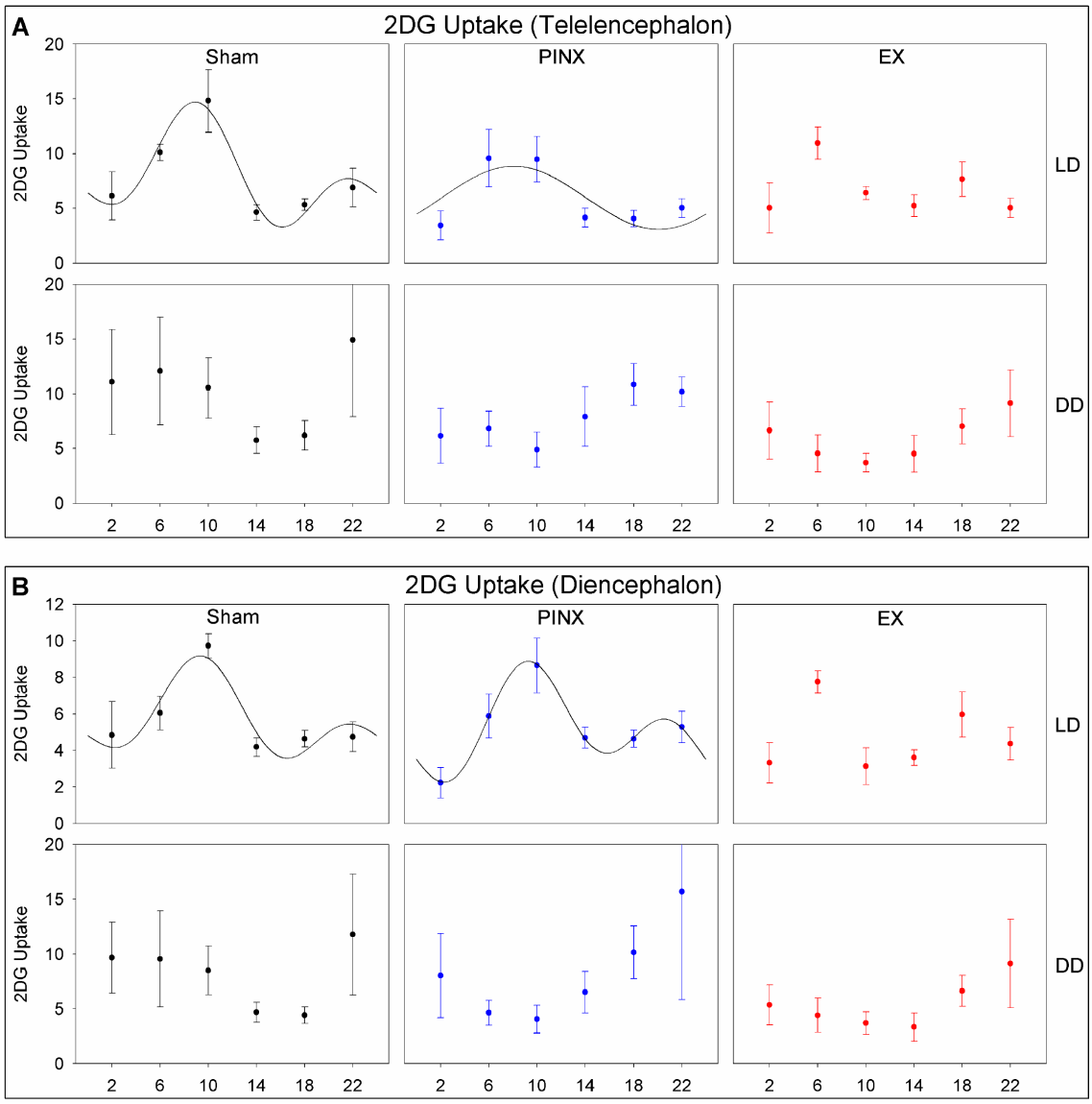

Figure 9. 2DG uptake in brain. 2DG uptake is shown for telencephalon (**A**), diencephalon (**B**), and optic tectum (**C**). Data are plotted as a function of zeitgeber time, or hours after lights on, for birds in LD 12:12 (top row in each panel). For birds in DD (bottom row in each panel), the abscissa displays hours after the onset of the third subjective day. In each panel, the left column indicates sham operated animals, the middle column indicates pinealectomized (PINX) animals, and the right column indicates enucleated (EX) animals. Data points are plotted with SEM at each timepoint in either black, blue, or red color, corresponding to sham, PINX, and EX treatment groups, respectively. For time series that significantly fit a cosine function (α, $p \leq 0.05$), a fitted curve is plotted along with data points in the graph.

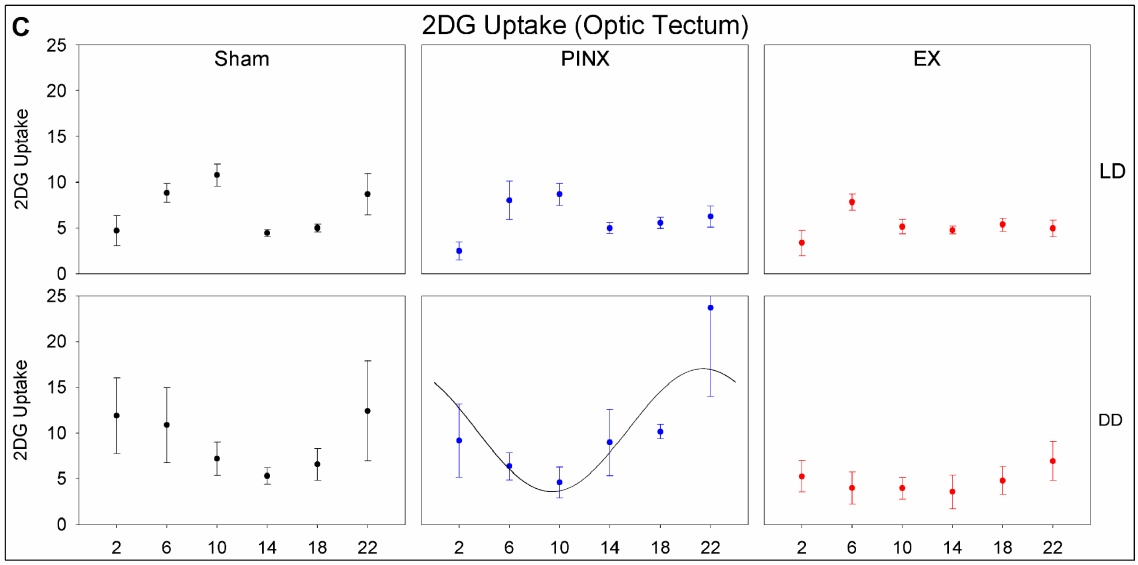

Figure 9 Continued.

rhythms in metabolism persist or dampen after three days of free-running in constant conditions. Finally, we examined the effects of pinealectomy and bilateral enucleation on metabolic rhythms.

2DG uptake rhythms were observed in both forebrain and diencephalon of intact birds under LD, such that uptake occurred during midday, at approximately ZT 8, based on the best fit cosinor wave (Fig. 9A, B; Table 3). This observation corroborates and extends previous reports from our laboratory (Cantwell and Cassone, 2002). Surprisingly, 2DG uptake rhythms were not detected in optic tectum, based on our criteria for cosinor analyses (Fig. 9C; Table 3). However, 2DG uptake in optic tectum did vary significantly over time, as determined by ANOVA. Metabolic rhythms did not persist in any brain tissue after three days in DD, and 2DG uptake was highly variable in the day and during late subjective night. This may indicate that damping of the metabolic rhythms occurred in individual birds, or alternatively, birds may have drifted out of phase from each other, but maintained coherence within individual brain tissues.

Enucleation had a large effect on metabolic rhythms in both rhythmic brain structures, as it abolished 2DG rhythms even under LD conditions (Fig. 9A, B; Table 3). The effects of pinealectomy were more subtle. In telencephlon, pinealectomy had a moderately disruptive effect on the metabolic rhythm, resulting in a 50% decrease in the rhythm amplitude, but with no effect on acrophase. In contrast, pinealectomy had little effect on 2DG uptake rhythms in diencephalon, although the acrophase was delayed considerably (Table 3). This is likely due to the somewhat biphasic shape of the fitted cosinor curve, however. Optic tectum was an aberration in this data set, as rhythmic

2DG uptake was only detected in under constant conditions in pinealectomized animals (Fig. 9C). This may indicate that weak 2DG rhythms occur in the tissue in other treatment groups, but that we were unable to detect them despite having relatively strong statistical power.

Table 3. Cosinor Analysis (2DG Uptake)

Tissue	Sample	Light Cycle	α	Cosinor p-value	ANOVA p-value	Acrophase	Amplitude
Telen	Sham	LD	<.05	.001	.002	8.02 +/- 0.49	5.70
Telen	PinX	LD	<.05	.017	.020	8.08 +/- 0.48	2.88
Telen	EX	LD	.34	.023	.041		
Telen	Sham	DD	.38	.376	.663		
Telen	PinX	DD	.07	.069	.270		
Telen	EX	DD	.10	.092	.448		
Dien	Sham	LD	<.05	.007	.005	8.29 +/- 0.54	2.80
Dien	PinX	LD	<.05	.001	.003	10.75 +/- 0.53*	3.30
Dien	EX	LD	.84	.009	.009		
Dien	Sham	DD	.30	.298	.614		
Dien	PinX	DD	.11	.101	.409		
Dien	EX	DD	.13	.123	.414		
OT	Sham	LD	.17	.003	.006		
OT	PinX	LD	.12	.009	.015		
OT	EX	LD	.42	.066	.042		
OT	Sham	DD	.17	.163	.591		
OT	PinX	DD	<.05	.036	.062	21.31 +/- 0.45	6.73
OT	EX	DD	.34	.334	.758		
Liver	Sham	LD	<.05	.007	.044	17.54 +/- 0.55	0.54
Liver	PinX	LD	<.05	.001	.012	17.28 +/- 0.51	0.81
Liver	EX	LD	<.05	<.001	.004	15.15 +/- 0.51*	0.97
Liver	Sham	DD	.64	.410	.538		
Liver	PinX	DD	.13	.123	.164		
Liver	EX	DD	.91	.114	.150		
Heart	Sham	LD	<.05	.003	.016	14.95 +/- 0.46	15.86
Heart	PinX	LD	<.05	.039	.076	14.45 +/- 0.51	11.05
Heart	EX	LD	<.05	.036	.032	16.60 +/- 0.49*	10.15
Heart	Sham	DD	.89	.896	.945		
Heart	PinX	DD	.25	.249	.619		
Heart	EX	DD	.52	.517	.749		

* Significantly different from sham treatment

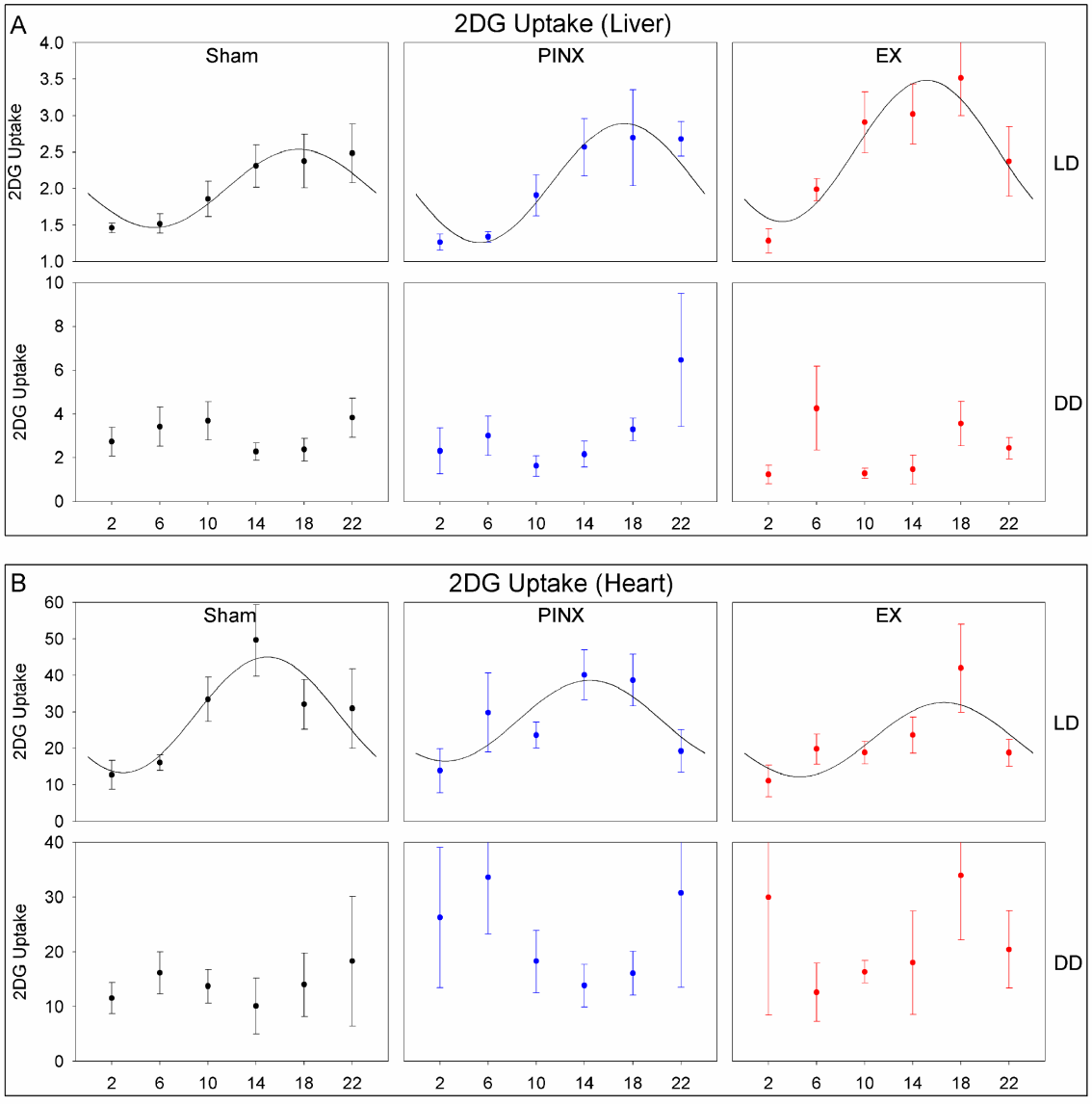

Figure 10. 2DG uptake in peripheral tissues. 2DG uptake is shown for liver (**A**) and heart (**B**). Data are plotted as a function of zeitgeber time, or hours after lights on, for birds in LD 12:12 (top row in each panel). For birds in DD (bottom row in each panel), the abscissa displays hours after the onset of the third subjective day. In each panel, the left column indicates sham operated animals, the middle column indicates pinealectomized (PINX) animals, and the right column indicates enucleated (EX) animals. Data points are plotted with SEM at each timepoint in either black, blue, or red color, corresponding to sham, PINX, and EX treatment groups, respectively. For time series that significantly fit a cosine function (α, $p \leq 0.05$), a fitted curve is plotted along with data points in the graph.

2DG Uptake in Peripheral Tissues

A daily rhythm of 2DG uptake was measured in both liver and heart of intact chickens under LD, but with a considerable delay in phase for both tissues, (Fig. 10). 2DG uptake in liver peaked 9-10 hours after brain metabolic rhythms, while the rhythm was delayed approximately 7 hours in heart (Table 3). The relative amplitude of this rhythm was appreciably greater in heart (~4-fold) compared to liver (<2-fold). As with brain, metabolic rhythms did not persist after three days in constant darkness, for any treatment group.

Surprisingly, surgical removal of the pineal or eyes had opposing effects on metabolic rhythms in these two peripheral tissues. In heart, pinealectomy and enucleation reduced the overall rhythm amplitude, with enucleation having a greater effect (Fig. 10B). In contrast, both surgeries actually increased the rhythm amplitude in liver, with enucleation again producing a greater effect (Fig. 10C).

Table 4. Cosinor Analysis (Clock Gene mRNA Expression)

Tissue	Sample	Light Cycle	α	Cosinor p-value	ANOVA p-value	Acrophase	Amplitude
Telen	bmal1 Sham	LD	<.05	<.001	<.001	11.58 +/- 0.49	0.34
Telen	bmal1 PinX	LD	<.05	<.001	<.001	11.34 +/- 0.50	0.30
Telen	bmal1 EX	LD	<.05	<.001	<.001	11.25 +/- 0.51	0.32
Telen	bmal1 Sham	DD	<.05	<.001	<.001	10.49 +/- 0.53	0.21
Telen	bmal1 PinX	DD	<.05	<.001	.001	9.17 +/- 0.56	0.19
Telen	bmal1 EX	DD	.26	.254	.702		
Telen	cry1 Sham	LD	<.05	<.001	<.001	8.79 +/- 0.52	0.39
Telen	cry1 PinX	LD	<.05	<.001	<.001	8.80 +/- 0.52	0.41
Telen	cry1 EX	LD	<.05	<.001	<.001	8.76 +/- 0.53	0.34
Telen	cry1 Sham	DD	<.05	<.001	<.001	8.29 +/- 0.54	0.51
Telen	cry1 PinX	DD	<.05	.012	.077	7.56 +/- 0.53	0.41
Telen	cry1 EX	DD	.16	.157	.476		
Telen	per3 Sham	LD	<.05	<.001	<.001	22.78 +/- 0.35	0.87
Telen	per3 PinX	LD	<.05	<.001	<.001	22.73 +/- 0.35	1.11

Table 4 Continued.

Tissue	Sample	Light Cycle	α	Cosinor p-value	ANOVA p-value	Acrophase	Amplitude
Telen	per3 EX	LD	<.05	<.001	<.001	22.36 +/- 0.42	0.76
Telen	per3 Sham	DD	<.05	<.001	<.001	21.64 +/- 0.35	1.25
Telen	per3 PinX	DD	<.05	<.001	<.001	22.45 +/- 0.40	0.84
Telen	per3 EX	DD	<.05	.001	.015	22.38 +/- 0.40	0.73
Dien	bmal1 Sham	LD	<.05	<.001	<.001	10.00 +/- 0.49	0.34
Dien	bmal1 PinX	LD	<.05	<.001	<.001	11.09 +/- 0.49	0.31
Dien	bmal1 EX	LD	<.05	<.001	<.001	11.24 +/- 0.51	0.32
Dien	bmal1 Sham	DD	<.05	<.001	<.001	9.40 +/- 0.52	0.27
Dien	bmal1 PinX	DD	.06	.057	.091		
Dien	bmal1 EX	DD	.09	.007	.013		
Dien	cry1 Sham	LD	<.05	<.001	<.001	7.58 +/- 0.51	0.41
Dien	cry1 PinX	LD	<.05	<.001	<.001	9.13 +/- 0.51	0.37
Dien	cry1 EX	LD	<.05	<.001	<.001	8.50 +/- 0.56	0.26
Dien	cry1 Sham	DD	<.05	.006	.032	9.78 +/- 0.53	0.46
Dien	cry1 PinX	DD	<.05	.037	.062	6.55 +/- 0.53*	0.42
Dien	cry1 EX	DD	<.05	.017	.019	5.67 +/- 0.54*	0.46
Dien	per3 Sham	LD	<.05	<.001	<.001	22.53 +/- 0.33	1.15
Dien	per3 PinX	LD	<.05	<.001	<.001	23.24 +/- 0.39	0.89
Dien	per3 EX	LD	<.05	<.001	<.001	21.78 +/- 0.40	0.74
Dien	per3 Sham	DD	<.05	<.001	.010	22.34 +/- 0.42	0.74
Dien	per3 PinX	DD	<.05	.030	.051	21.14 +/- 0.46	0.48
Dien	per3 EX	DD	<.05	<.001	.001	21.56 +/- 0.46	0.68
OT	bmal1 Sham	LD	<.05	<.001	<.001	10.69 +/- 0.50	0.34
OT	bmal1 PinX	LD	<.05	<.001	<.001	10.66 +/- 0.49	0.33
OT	bmal1 EX	LD	<.05	<.001	<.001	11.17 +/- 0.53	0.27
OT	bmal1 Sham	DD	<.05	<.001	<.001	10.96 +/- 0.53	0.26
OT	bmal1 PinX	DD	<.05	.008	.01	11.52 +/- 0.55	0.18
OT	bmal1 EX	DD	<.05	.029	.02	12.05 +/- 0.56	0.14
OT	cry1 Sham	LD	<.05	<.001	<.001	8.68 +/- 0.51	0.39
OT	cry1 PinX	LD	<.05	<.001	<.001	9.29 +/- 0.51	0.37
OT	cry1 EX	LD	<.05	<.001	<.001	9.55 +/- 0.53	0.32
OT	cry1 Sham	DD	<.05	<.001	<.001	8.77 +/- 0.53	0.30
OT	cry1 PinX	DD	<.05	.046	.038	10.32 +/- 0.56	0.23
OT	cry1 EX	DD	<.05	<.001	<.001	8.69 +/- 0.56	0.22
OT	per3 Sham	LD	<.05	<.001	<.001	22.37 +/- 0.31	1.31
OT	per3 PinX	LD	<.05	<.001	<.001	22.13 +/- 0.29	1.18
OT	per3 EX	LD	<.05	<.001	<.001	21.57 +/- 0.45	0.66
OT	per3 Sham	DD	<.05	<.001	<.001	20.79 +/- 0.43	0.56
OT	per3 PinX	DD	<.05	<.001	<.001	21.28 +/- 0.36	0.90
OT	per3 EX	DD	<.05	<.001	.001	21.56 +/- 0.46	0.51
Liver	bmal1 Sham	LD	<.05	<.001	<.001	15.25 +/- 0.39	0.58
Liver	bmal1 PinX	LD	<.05	<.001	<.001	14.67 +/- 0.39	0.58
Liver	bmal1 EX	LD	<.05	<.001	<.001	16.76 +/- 0.43*	0.54
Liver	bmal1 Sham	DD	<.05	<.001	.002	15.23 +/- 0.44	0.63
Liver	bmal1 PinX	DD	<.05	.042	.053	14.72 +/- 0.51	0.31
Liver	bmal1 EX	DD	<.05	.007	.016	14.84 +/- 0.50	0.68
Liver	cry1 Sham	LD	<.05	<.001	<.001	11.41 +/- 0.48	0.53
Liver	cry1 PinX	LD	<.05	<.001	<.001	9.54 +/- 0.50*	0.45
Liver	cry1 EX	LD	<.05	.007	.081	12.13 +/- 0.53	0.42

Table 4 Continued.

Tissue	Sample	Light Cycle	α	Cosinor p-value	ANOVA p-value	Acrophase	Amplitude
Liver	cry1 Sham	DD	.34	.031	.017		
Liver	cry1 PinX	DD	.28	.098	.083		
Liver	cry1 EX	DD	.11	.104	.204		
Liver	per3 Sham	LD	<.05	<.001	<.001	3.44 +/- 0.28	1.24
Liver	per3 PinX	LD	<.05	<.001	<.001	3.24 +/- 0.26	1.43
Liver	per3 EX	LD	<.05	<.001	<.001	5.52 +/- 0.43*	0.76
Liver	per3 Sham	DD	.98	.520	.603		
Liver	per3 PinX	DD	.08	.078	.102		
Liver	per3 EX	DD	<.05	.015	.071	3.36 +/- 0.31	2.08
Heart	bmal1 Sham	LD	<.05	<.001	<.001	10.38 +/- 0.46	0.48
Heart	bmal1 PinX	LD	<.05	<.001	<.001	10.18 +/- 0.46	0.45
Heart	bmal1 EX	LD	<.05	<.001	<.001	11.91 +/- 0.52	0.30
Heart	bmal1 Sham	DD	<.05	.014	.033	10.07 +/- 0.56	0.18
Heart	bmal1 PinX	DD	.05	.054	.258		
Heart	bmal1 EX	DD	.06	.018	.014		
Heart	cry1 Sham	LD	<.05	<.001	<.001	5.42 +/- 0.46	0.64
Heart	cry1 PinX	LD	<.05	<.001	<.001	5.26 +/- 0.45	0.57
Heart	cry1 EX	LD	<.05	<.001	<.001	5.45 +/- 0.55	0.31
Heart	cry1 Sham	DD	<.05	<.001	.001	2.46 +/- 0.51	0.4
Heart	cry1 PinX	DD	.29	.281	.450		
Heart	cry1 EX	DD	.21	.202	.360		
Heart	per3 Sham	LD	<.05	<.001	<.001	0.26 +/- 0.39	0.94
Heart	per3 PinX	LD	<.05	<.001	<.001	23.85 +/- 0.36	1.17
Heart	per3 EX	LD	<.05	<.001	.004	23.12 +/- 0.50	0.44
Heart	per3 Sham	DD	<.05	<.001	<.001	21.94 +/- 0.36	0.97
Heart	per3 PinX	DD	<.05	<.001	<.001	20.79 +/- 0.45	0.73
Heart	per3 EX	DD	.06	.053	.173		

* Significantly different from sham treatment

Clock Gene Expression in Brain

Telencephalon

We measured the temporal expression of mRNA levels of the clock genes *cry1*, *per3*, and *bmal1* in the same three subdivisions of the chicken brain. In telencephalon, all three clock genes exhibited circadian rhythms in mRNA levels. Contrary to the metabolic rhythms, clock gene mRNA rhythms in intact animals persisted for three days in DD, with a similar phase and amplitude to rhythms observed in LD (Fig. 11; Table 4).

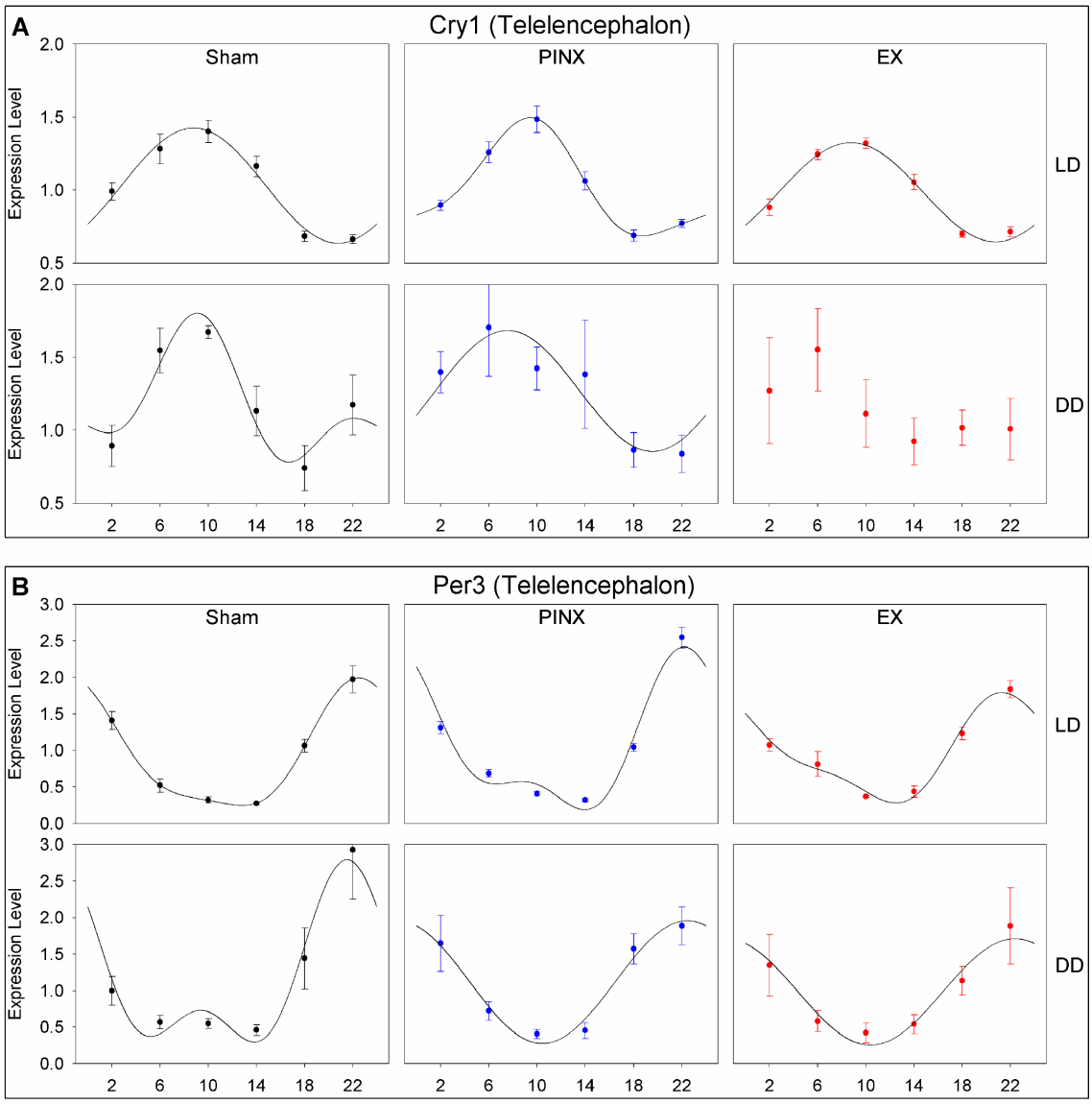

Figure 11. Clock gene expression in telencephalon. mRNA levels of chick *cry1* (**A**), *per3* (**B**), and *bmal1* (**C**) are shown for telencephalon as measured by qPCR. Data are plotted as a function of zeitgeber time, or hours after lights on, for birds in LD 12:12 (top row in each panel). For birds in DD (bottom row in each panel), the abscissa displays hours after the onset of the third subjective day. In each panel, the left column indicates sham operated animals, the middle column indicates pinealectomized (PINX) animals, and the right column indicates enucleated (EX) animals. Data points are plotted with SEM at each timepoint in either black, blue, or red color, corresponding to sham, PINX, and EX treatment groups, respectively. For time series that significantly fit a cosine function (α, $p \leq 0.05$), a fitted curve is plotted along with data points in the graph.

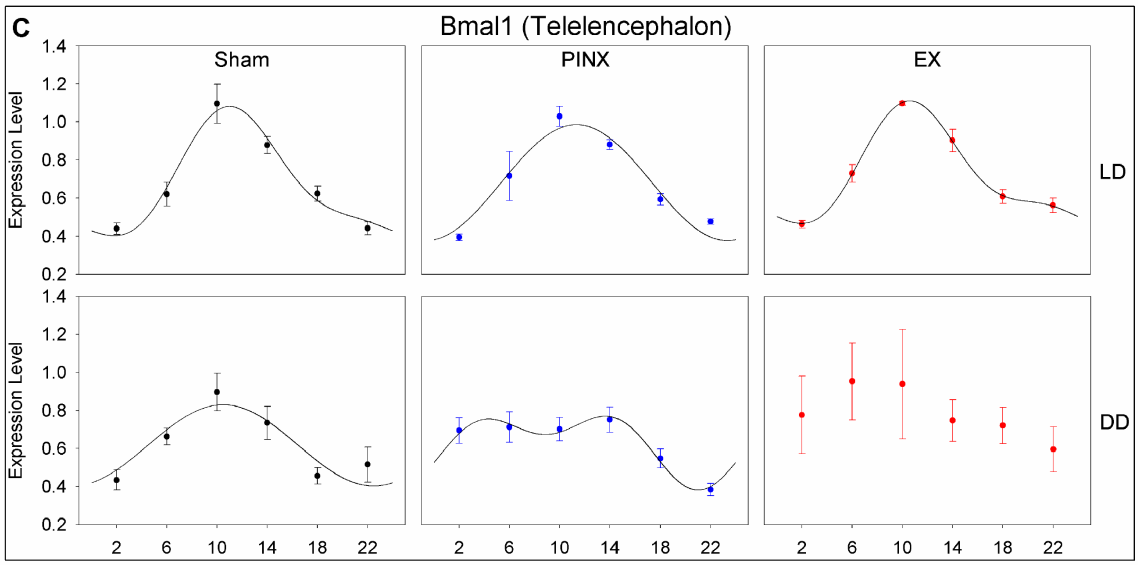

Figure 11 Continued.

Cry1 mRNA levels peaked between mid and late day/subjective day, at around ZT/CT 8-9 (Fig. 11A). *Per3* mRNA levels peaked about 10 hours earlier, during late night, at ZT/CT 22-23 (Fig. 11B). *Bmal1* mRNA peaked just before the day/night transition, approximately antiphase to the *per3* rhythm (Fig. 11C). The phases of these rhythms match clock gene mRNA profiles reported for neural tissues of chick and other avian species (Yoshimura et al., 2000; Okano et al., 2001; Yamamoto et al., 2001; Fukada and Okano, 2002; Bailey et al., 2003; Chong et al., 2003; Helfer et al., 2006).

Surgical interventions affected the clock gene rhythms differentially in telencephalon. Overall, pinealectomy had little effect on telencephalic clock gene expression, resulting in only minor reductions in mRNA rhythm amplitude for *cry1* and *per3* in DD, and actually increasing the amplitude of *per3* in LD (Fig. 11A, B). Additionally, pinealectomy appeared to disrupt, but not abolish, the *bmal1* mRNA rhythm, resulting in a broadened daytime peak (Fig. 11C). Enucleation had a more potent effect, abolishing detectable free-running rhythms of *cry1* and *bmal1* mRNA, and reducing rhythm amplitudes of *cry1* and *per3* mRNA in LD, as well as *per3* under constant darkness (Fig. 11).

Diencephalon

Clock gene expression in diencephalon was very similar to what was observed in telencephalon, although *bmal1* peaked a little earlier in sham animals, and *cry1* peaked later in DD (Fig. 12; Table 4). Also, detectable *bmal1* mRNA rhythms were abolished by both enucleation and pinealectomy (Fig. 12C), though *cry1* rhythmicity persisted (Fig.

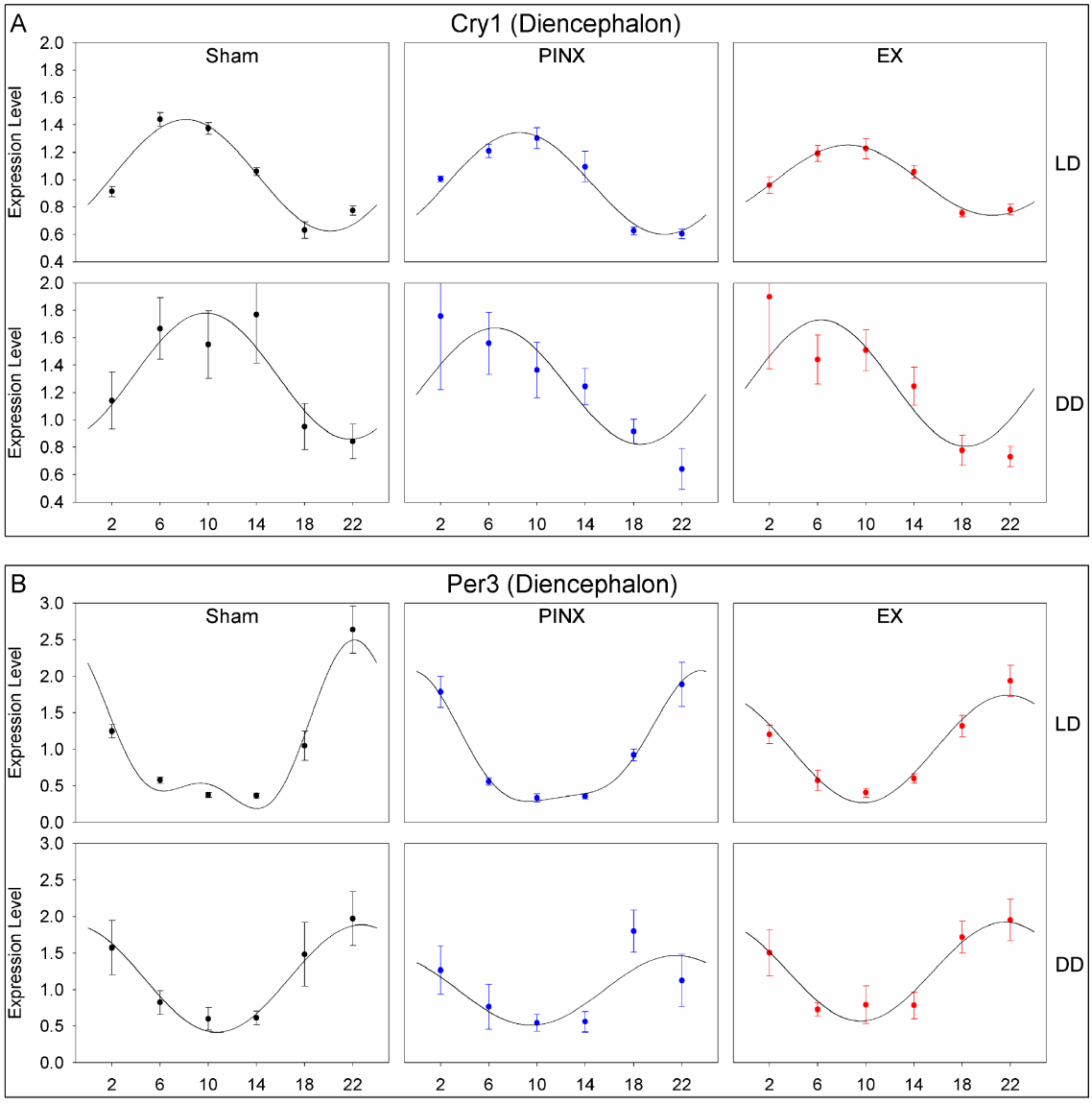

Figure 12. Clock gene expression in diencephalon. mRNA levels of chick *cry1* (**A**), *per3* (**B**), and *bmal1* (**C**) are shown for telencephalon as measured by qPCR. Data are plotted as a function of zeitgeber time, or hours after lights on, for birds in LD 12:12 (top row in each panel). For birds in DD (bottom row in each panel), the abscissa displays hours after the onset of the third subjective day. In each panel, the left column indicates sham operated animals, the middle column indicates pinealectomized (PINX) animals, and the right column indicates enucleated (EX) animals. Data points are plotted with SEM at each timepoint in either black, blue, or red color, corresponding to sham, PINX, and EX treatment groups, respectively. For time series that significantly fit a cosine function (α, $p \leq 0.05$), a fitted curve is plotted along with data points in the graph.

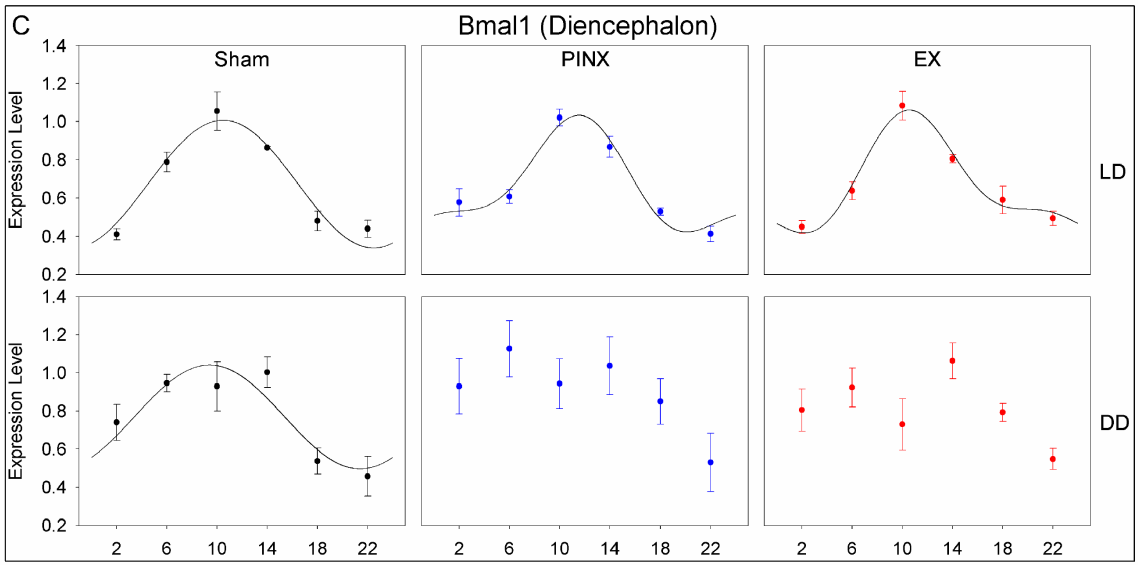

Figure 12 Continued.

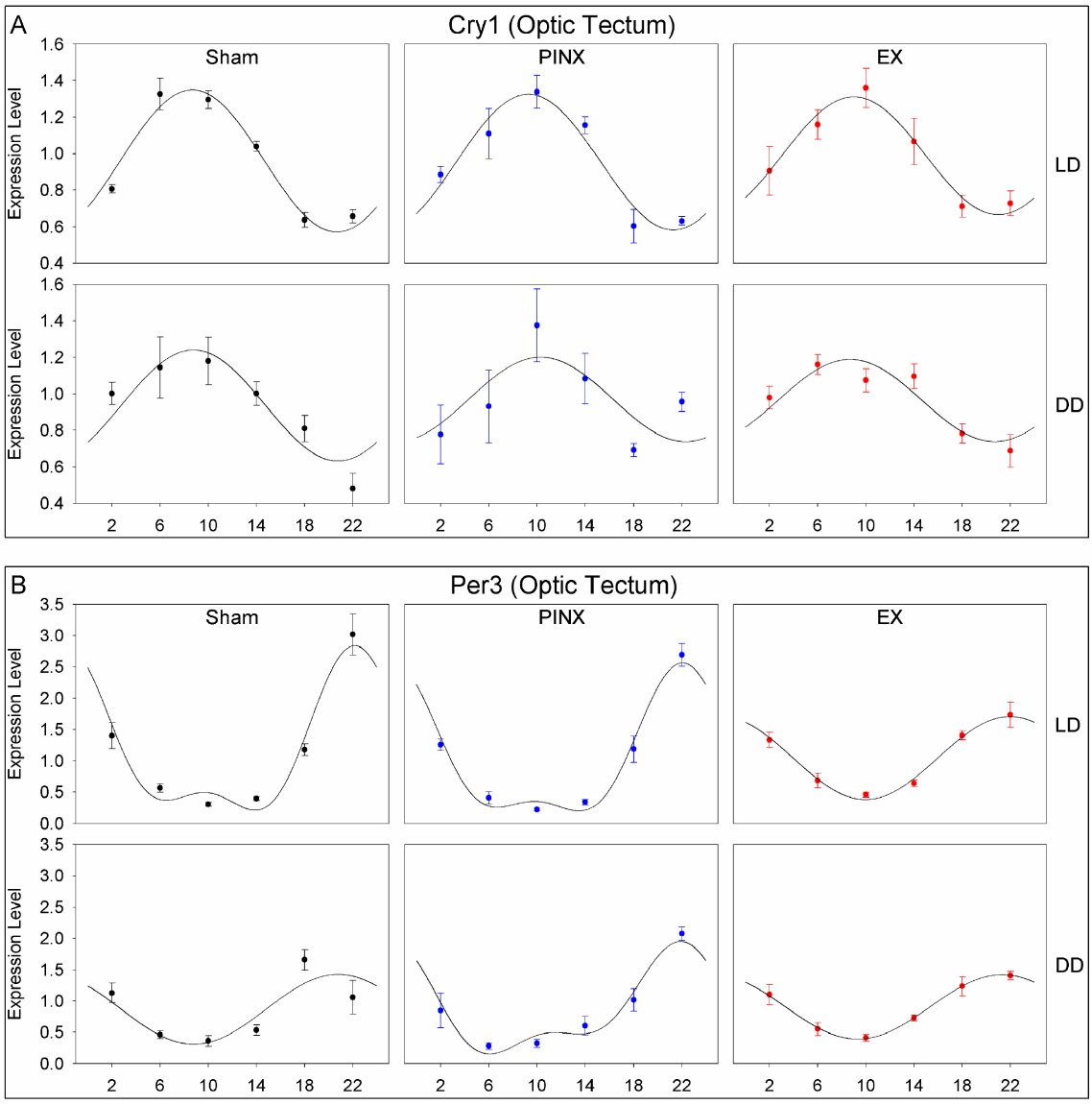

Figure 13. Clock gene expression in optic tectum. mRNA levels of chick *cry1* (**A**), *per3* (**B**), and *bmal1* (**C**) are shown for telencephalon as measured by qPCR. Data are plotted as a function of zeitgeber time, or hours after lights on, for birds in LD 12:12 (top row in each panel). For birds in DD (bottom row in each panel), the abscissa displays hours after the onset of the third subjective day. In each panel, the left column indicates sham operated animals, the middle column indicates pinealectomized (PINX) animals, and the right column indicates enucleated (EX) animals. Data points are plotted with SEM at each timepoint in either black, blue, or red color, corresponding to sham, PINX, and EX treatment groups, respectively. For time series that significantly fit a cosine function (α, $p \leq 0.05$), a fitted curve is plotted along with data points in the graph.

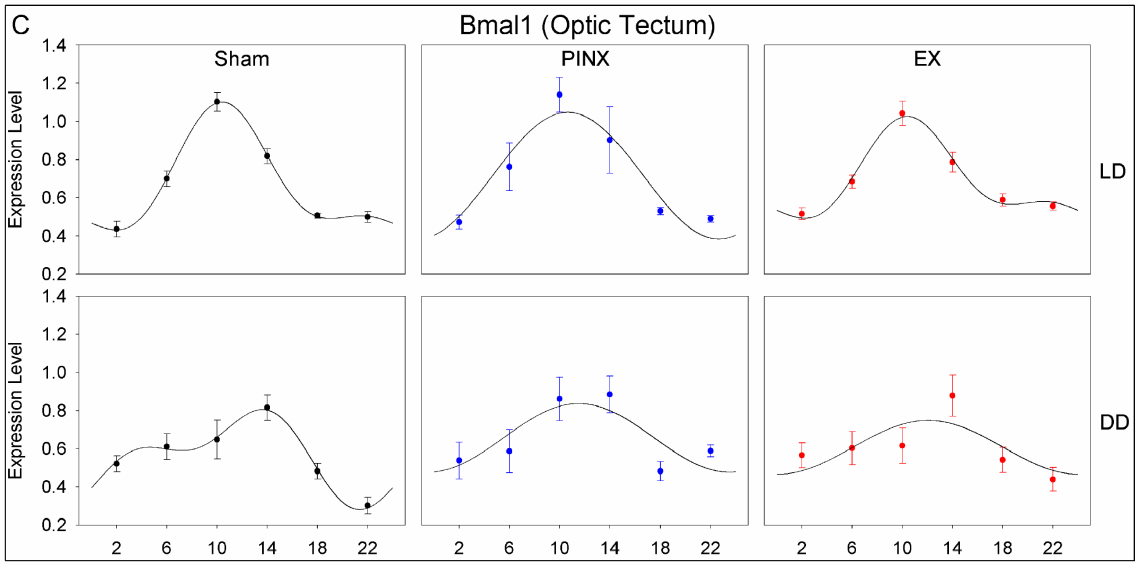

Figure 13 Continued.

12B). The phase of the *cry1* rhythm, however, peaked significantly earlier for animals in both surgery groups, compared to sham birds (Table 4). Generally, where clock gene rhythms were not abolished, either surgery produced a slight disruptive effect by reducing the amplitude of the oscillations.

Optic Tectum

While metabolic rhythms were not detected in the optic tectum of sham birds, all three clock genes exhibited rhythmic mRNA expression in this tissue, with rhythm amplitudes comparable to those measured in telencephalon and diencephalon (Fig. 13; Table 4). The *per3* rhythm amplitude was, however, somewhat reduced in DD compared to other tissues. Overall, as in other brain tissues, pinealectomy and enucleation reduced the amplitude of clock gene rhythms in optic tectum, both in LD and DD. The exception to this was the *per3* rhythm in DD, perhaps because the rhythm amplitude was relatively low in sham animals compared to other brain structures. Enucleation did not abolish any of the clock gene rhythms in optic tectum, although *bmal1* expression was disrupted considerably (Fig. 13C).

Clock Gene Expression in Peripheral Tissues

Liver

We next examined clock mRNA expression in heart and liver. *Cry1*, *per3*, and *bmal1* mRNA levels exhibited daily rhythms in liver, though only the *bmal1* rhythm persisted in DD (Fig 14). The phases of the clock gene rhythms were delayed relative to

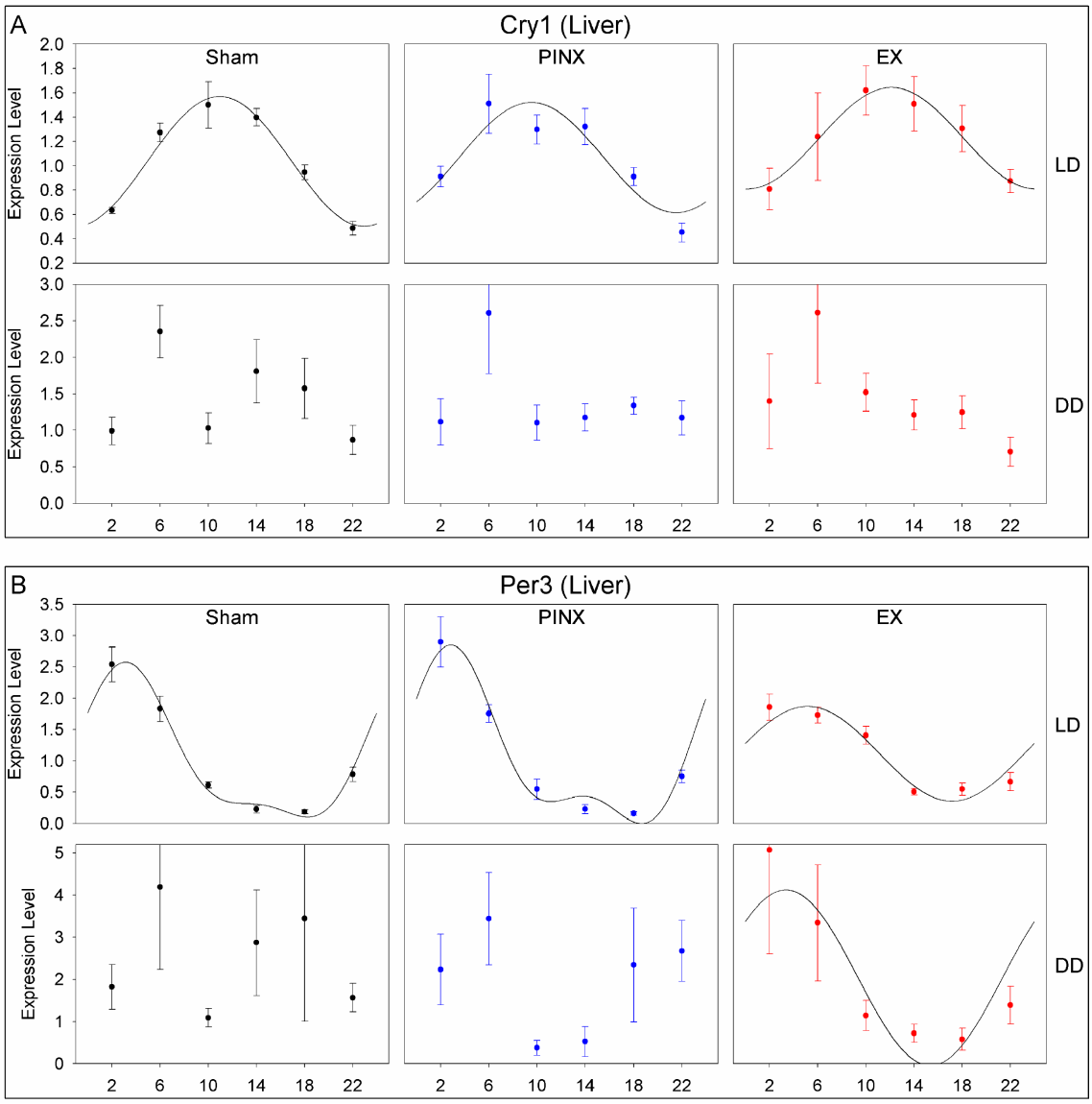

Figure 14. Clock gene expression in liver. mRNA levels of chick *cry1* (**A**), *per3* (**B**), and *bmal1* (**C**) are shown for telencephalon as measured by qPCR. Data are plotted as a function of zeitgeber time, or hours after lights on, for birds in LD 12:12 (top row in each panel). For birds in DD (bottom row in each panel), the abscissa displays hours after the onset of the third subjective day. In each panel, the left column indicates sham operated animals, the middle column indicates pinealectomized (PINX) animals, and the right column indicates enucleated (EX) animals. Data points are plotted with SEM at each timepoint in either black, blue, or red color, corresponding to sham, PINX, and EX treatment groups, respectively. For time series that significantly fit a cosine function (α, $p \leq 0.05$), a fitted curve is plotted along with data points in the graph.

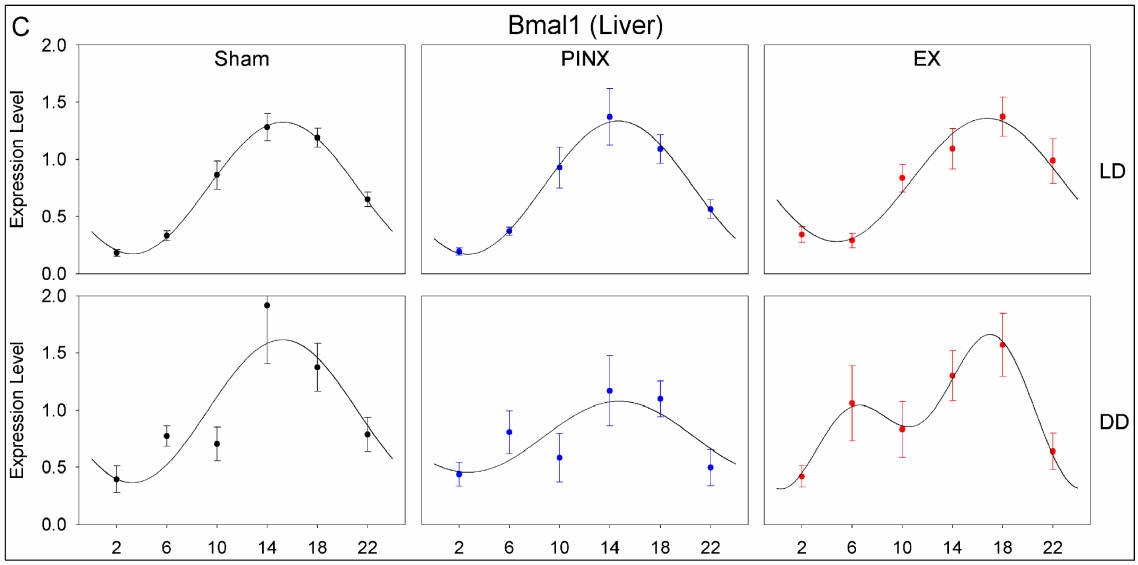

Figure 14 Continued.

brain. *Bmal1* and *per3* mRNA levels in liver peaked approximately 4-5 hours after their peak levels in brain, at ~ZT 15 and ~ZT 3, respectively. *Cry1* mRNA peaked 2-4 hours later, at ~ZT 11 (Table 4).

Hepatic clock gene expression was similar in pinealectomized animals in LD, although the *bmal1* mRNA rhythm amplitude was reduced by about half in DD (Fig. 14C; Table 4). In enucleated animals, *cry1* and *per3* rhythms were attenuated, and *bmal1* expression appeared to be disrupted (Fig. 14; Table 4). Surprisingly, temporal expression of *per3* mRNA levels fit a cosinor function, although these data did not show significant variation over time when analyzed subjected to ANOVA.

Heart

Unlike liver, all three clock genes exhibited circadian rhythms in heart, and these persisted in constant darkness (Fig. 15). Also, these rhythms had a different phase relationship to each other and to brain than was observed in liver. For instance, the phase of the *per3* mRNA rhythm in LD was delayed only 1.5-2 hours with respect to brain (peaking at around ZT 0), less than half the delay observed in liver. In DD, *per3* was approximately in phase with brain rhythms (Fig. 15B; Table 4). Likewise, *bmal1* mRNA rhythms in heart exhibited a similar phase to *bmal1* rhythms in brain structures, both in LD and DD (Fig. 15C; Table 4). Cardiac rhythms of *cry1*, however, were advanced by 2-3 hours in LD and 6-7 hours in DD, with peaks at ZT 5-6 and CT2-3, respectively (Fig. 15A; Table 4).

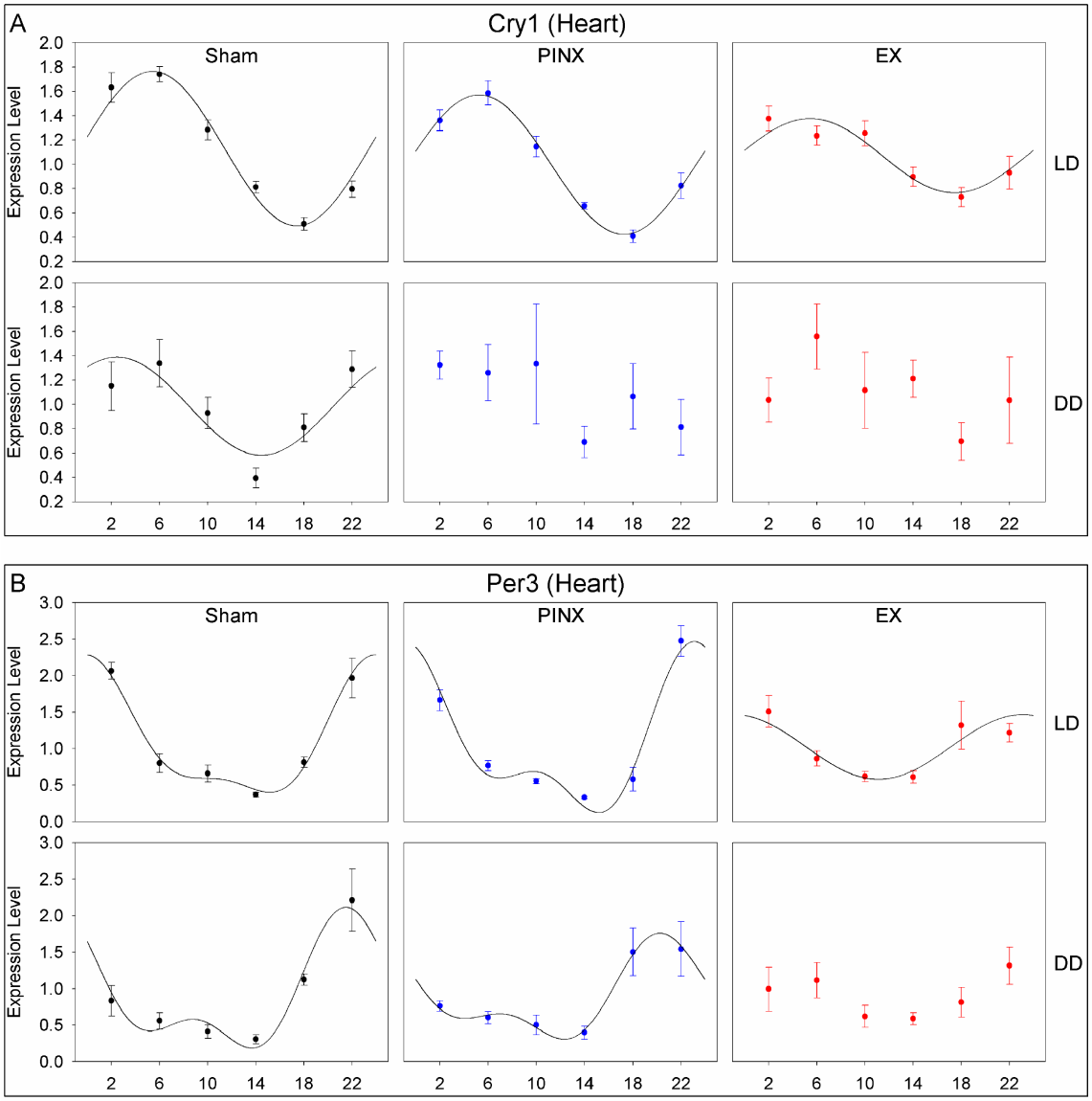

Figure 15. Clock gene expression in heart. mRNA levels of chick *cry1* (**A**), *per3* (**B**), and *bmal1* (**C**) are shown for telencephalon as measured by qPCR. Data are plotted as a function of zeitgeber time, or hours after lights on, for birds in LD 12:12 (top row in each panel). For birds in DD (bottom row in each panel), the abscissa displays hours after the onset of the third subjective day. In each panel, the left column indicates sham operated animals, the middle column indicates pinealectomized (PINX) animals, and the right column indicates enucleated (EX) animals. Data points are plotted with SEM at each timepoint in either black, blue, or red color, corresponding to sham, PINX, and EX treatment groups, respectively. For time series that significantly fit a cosine function (α, $p \leq 0.05$), a fitted curve is plotted along with data points in the graph.

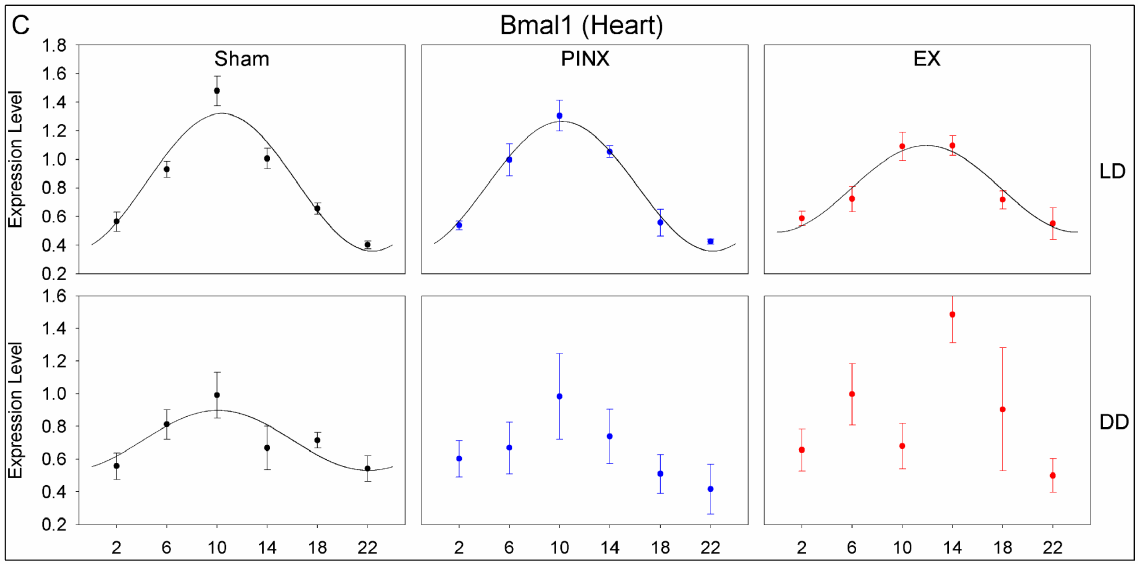

Figure 15 Continued.

Overall, both types of surgery had a greater effect on clock gene rhythms in heart than in liver. While pinealectomized birds had normal clock gene rhythms in LD, significant rhythms could not be detected for either *cry1* or *bmal1* in free-running conditions. Also, the cardiac *per3* mRNA rhythm was diminished in pinealectomized birds under DD, though it was slightly increased for birds in LD (Fig. 15; Table 4). Enucleation had a more potent effect on cardiac tissue, abolishing mRNA rhythms of all three clock genes in DD, and reducing rhythm amplitudes by 40-50% in LD (Fig. 15; Table 4).

Circadian Phase Analysis

To facilitate comparison of circadian phases of metabolic and clock gene rhythms between different tissues, acrophases determined for statistically significant rhythms were plotted onto polar graphs. These graphs reveal that all three brain structures possess a similar pattern of clock gene expression, in which the phases of individual rhythms, along with their respective phase angles, are conserved (Fig. 16). Phases were most tightly clustered in LD, with rhythms dampening or drifting out of phase in DD. Overall, while removal of the pineal or eyes was shown to abolish or reduce the amplitudes of some genes, they did not consistently effect the phasing of clock genes. The only metabolic rhythm detected in brain tissue after three days in DD was in the optic tectum of pinealectomized animals, which was approximately antiphase to the 2DG uptake rhythms detected in other tissues (Fig. 16 C). Interestingly, the phases of the clock gene rhythms in these animals were not significantly different from those in sham animals.

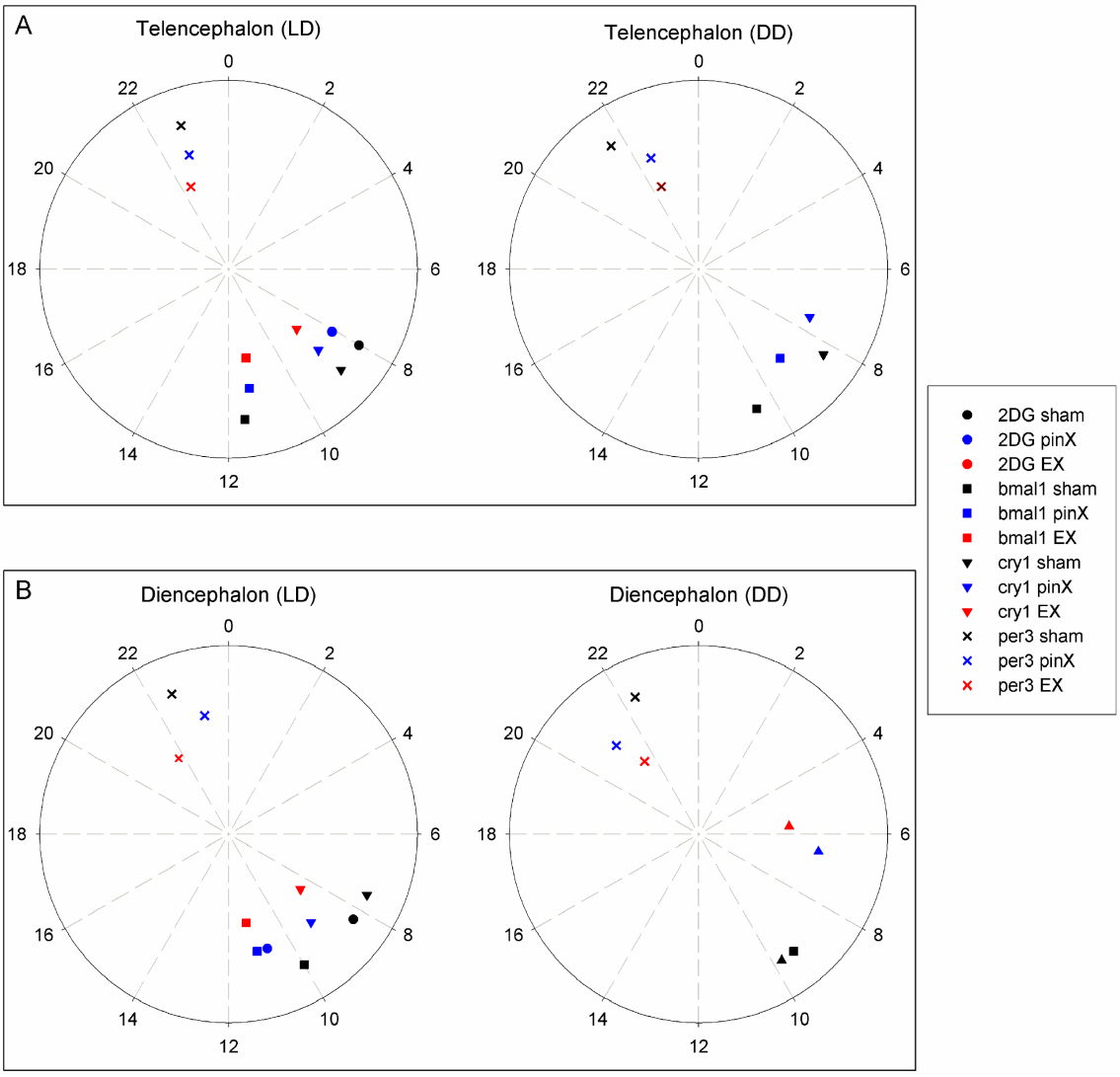

Figure 16. Circadian phase plots for brain. Polar plots show circadian acrophases for statistically significant rhythms as determined by cosinor analysis. Rhythms in 2DG uptake and clock gene mRNA rhythms are plotted for telencephalon (**A**), diencephalon (**B**), and optic tectum (**C**). Rhythms under LD cycles are plotted on the left column of each panel, and rhythms under DD are plotted on the right column. The angular axis (Θ) displays hours after lights on (LD), or hours after the beginning of subjective day (DD). Radial values are shared by data points within common surgical treatment groups. Circadian phases of metabolic and clock gene rhythms are distinguished by shape, whereas surgical treatment groups are distinguished by color (see key).

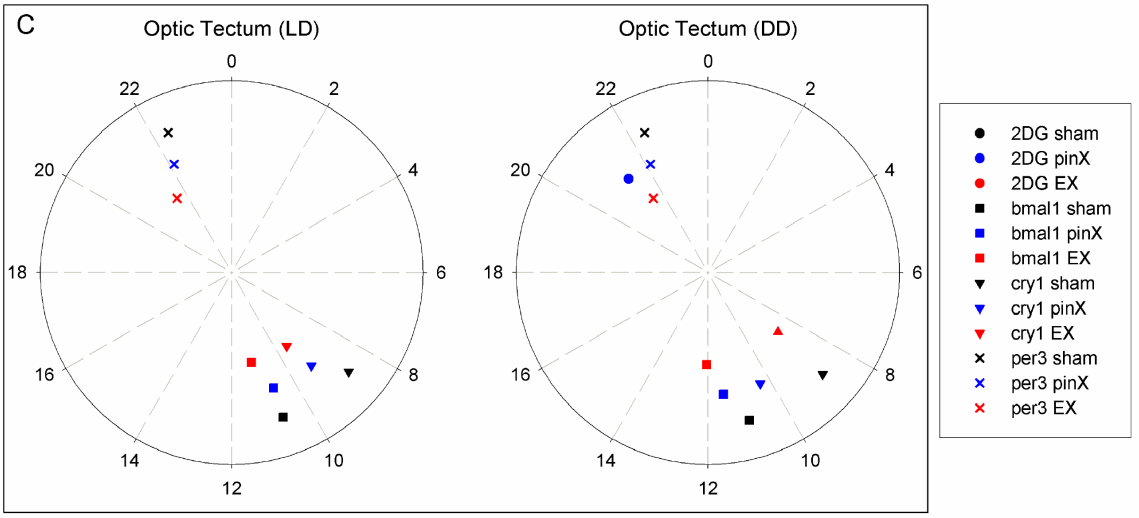

Figure 16 Continued.

In peripheral tissues, the phase angles between different clock gene rhythms and 2DG uptake rhythms was not conserved, and were distinct in liver and heart (Fig. 17). In liver, the phases of *bmal1* and *per3* were both delayed by 4-5 hours in LD, and thus maintained the same phase angle in liver and brain. *Cry1* rhythms, however, exhibited a different phase relationship to other genes in liver and brain. Also, *bmal1* and *per3* were delayed by ~2 hours in enucleated animals, but this was not correlated with a similar shift in 2DG rhythms in these animals (Fig. 17A). In constant darkness, most clock gene mRNAs were not rhythmic, although the few rhythms that were detected maintained a similar phase.

In heart, *bmal1* and *per3* mRNA expression was similarly correlated, having circadian phases coincident with their expression in brain tissues. In contrast, the rhythm in *cry1* was at a different phase angle to the *bmal1* and *per3* rhythms, and to the 2DG uptake rhythm (Fig. 17B). Moreover, although all clock genes were rhythmic in heart, the phases of these rhythms became desynchronized in DD.

Discussion

Metabolism is controlled by the circadian clock in animals, allowing them to synchronize bioenergetic processes with anticipated daily activities. For instance, plasma levels of glucose as well as glucose uptake are controlled by the clock in many species, and are higher during the day or night in diurnal or nocturnal animals, respectively (la Fleur, 2003). One exception is the SCN, where glucose utilization is higher during the day in both diurnal and nocturnal species (Refinetti, 2005). In this

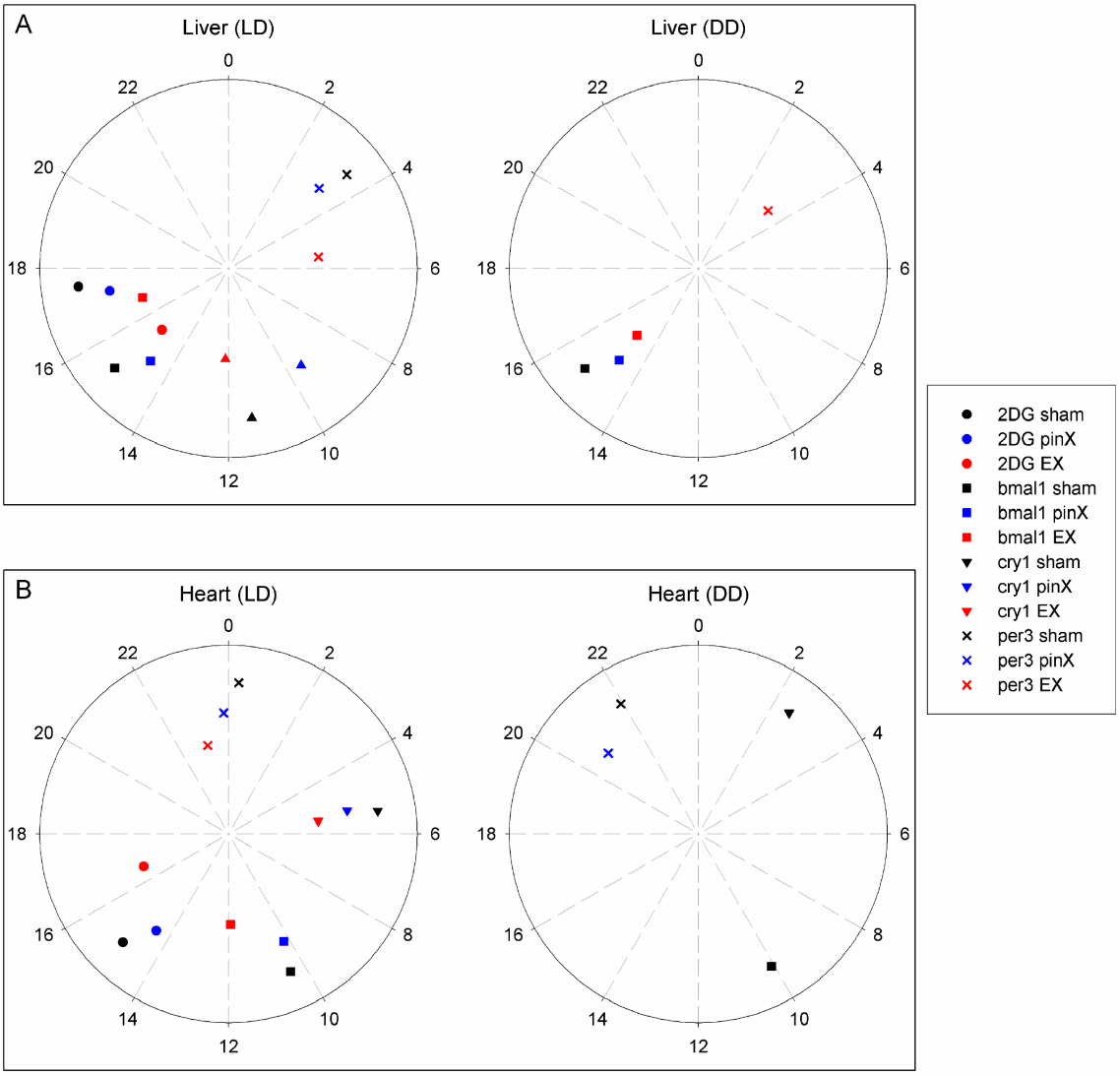

Figure 17. Circadian phase plots for peripheral tissues. Polar plots show circadian acrophases for statistically significant rhythms as determined by cosinor analysis. Rhythms in 2DG uptake and clock gene mRNA rhythms are plotted for liver (**A**) and heart (**B**). Rhythms under LD cycles are plotted on the left column of each panel, and rhythms under DD are plotted on the right column. The angular axis (Θ) displays hours after lights on (LD), or hours after the beginning of subjective day (DD). Radial values are shared by data points within common surgical treatment groups. Circadian phases of metabolic and clock gene rhythms are distinguished by shape, whereas surgical treatment groups are distinguished by color (see key).

study, we demonstrate that overt daily rhythms of 2DG uptake occur in at least two subdivisions of the chicken brain, as well as in at least two different peripheral organs. In brain, uptake was high during the day (with a peak at ~ZT 8), as has been reported for the SCN in house sparrows and mammals (Schwartz et al., 1980; Cassone, 1988; Schwartz, 1990), as well as other brain structures in chickens (Cantwell and Cassone, 2002). Moreover, we show that both heart and liver exhibit rhythms in 2DG uptake, which are phase delayed by up to 10 hours compared to brain. These nocturnal rhythms did not persist in constant darkness, however, and may therefore be indirectly affected by light stimulation. Similar findings have been made in chick brain, where multiple anatomical brain regions, including six visual structures, exhibited daily rhythms. However, these rhythms persisted in constant darkness in only two such structures (Cantwell and Cassone, 2002).

Surprisingly, one of the structures in which circadian rhythms of 2DG uptake has been reported is optic tectum. In our study, optic tectum was the only brain structure in which metabolic rhythms were not detected even in LD. However, examination of the data suggest 2DG may be rhythmic, but that greater statistical power is needed to resolve these rhythms from background variation. Secondly, the previous study utilized autoradiographic techniques to measure rhythms in specific structures, whereas our methods measure 2DG uptake in whole tissue samples. Therefore non-uniformly distributed 2DG uptake rhythms in tissue may have resulted in a diminished signal:noise ratio with our technique. Also, we measured 2DG uptake after three days in DD, not one day as in the previous study. It is therefore likely that these metabolic rhythms are weak

circadian rhythms which had damped out by the third day. Indeed, autoradiographical data reveal considerable dampening of the rhythms had occurred after one day in DD (Cantwell and Cassone, 2002).

Alternatively, it is possible that 2DG uptake was still rhythmic in these tissues by the third day in DD, but that individual chickens had drifted out of phase, resulting in an artifact of apparent arrythmicity. However, this seems unlikely, given that the mRNA rhythms of most clock genes were easily detectable, and still in phase with rhythms measured under LD. This could, however, suggest that 2DG rhythms are less tightly coupled with the clock under DD, and can therefore drift out of phase from other clock components.

In any case, it is interesting that 2DG uptake rhythms were delayed by 7-10 hours in peripheral tissues, such that uptake peaked at night, when chickens are less active. Unlike some species, plasma glucose levels in chicks do not vary throughout the day (Raheja, 1973), suggesting that overall glucose utilization is reduced in these peripheral organs during the period of activity. It is unclear what adaptive benefit this may have for a diurnal species such as chicken.

Another interesting observation was that the 2DG uptake rhythms in heart and liver were not phase locked to the clock gene mRNA rhythms, or to rhythms in brain. Similar findings were reported for NIH3T3 cells entrained by co-culture with SCN cells. In that study, 2DG uptake rhythms in fibroblasts lagged SCN uptake rhythms by four hours, while *per2* mRNA levels were delayed by 12 hours (Allen et al., 2001). While we observe a different lag time in peripheral clock gene and metabolic rhythms, both

studies demonstrate that the phase of molecular clock gene oscillations do not predict the phase of the presumed output of this molecular clock.

Regulation of metabolic and clock gene rhythms in peripheral tissues may occur as a result of endocrine signals from the SCN, or via autonomic efferents originating in the SCN (Bartness et al., 2001; la Fleur 2003; Hastings et al. 2007). The pineal likely regulates peripheral clocks via the nightly secretion of melatonin. This regulation may occur solely through an indirect influence of melatonin on the SCN (Lu and Cassone, 1993a; Lu and Cassone, 1993b; Starkey et al., 1995), or it may also result from direct action of melatonin on peripheral tissues. Functional melatonin receptors have been detected in heart (Pang et al., 1998, 2002) but not liver of chicken, and western analyses from our laboratory confirm these data (unpublished data). In contrast, as the retinae do not contribute to circulating melatonin levels in chicks (Reppert and Sagar, 1983; Cogburn et al., 1987), regulation by the eyes must involve only neural connections, either indirectly via the retinohypothalamic tract (RHT), or through other unknown pathways.

Chickens are able to entrain to a 12:12 light:dark cycle equally well using only their eyes or pineal, as animals in all three surgical groups exhibited daily rhythms in clock gene expression in all structures examined. However, our data reveal differential effects of surgical removal of the pineal or eyes on brain and peripheral rhythms, suggesting the roles of these pacemakers are not entirely redundant, and may involve regulation that is independent of the SCN. Overall, enucleated animals exhibited greater disruptions in both clock gene and metabolic rhythms compared with pinealectomized

animals, with some rhythms being abolished (see Figs. 9A, B; 11A, C). Enucleation abolished rhythms of 2DG uptake in brain even under an LD cycle, while clock gene mRNA levels were still rhythmic, though some were only reduced in amplitude in LD. This disconnect suggests that either: 1) there are parallel pathways by which the eyes reinforce circadian oscillators and their output; or, 2) a minimum amplitude in clock gene transcriptional rhythms is necessary to drive rhythms in clock controlled metabolic output. Moreover, enucleation actually increased the amplitude of 2DG and *per3* rhythms in liver (Figs. 10A, 14B). This may indicate that central pacemakers can actually inhibit endogenous rhythms in this organ, perhaps allowing for tighter coupling between liver and brain rhythms.

Pinealectomy had a disruptive, but overall more subtle effect on rhythms in brain and peripheral tissues, consistent with reported behavioral effects (Nyce and Binkley, 1977; McGoogan and Cassone, 1999). Multiple rhythms disrupted by enucleation were similarly affected by pinealectomy (Figs. 9A; 10A, B; 11B; 12B, C; 15A-C), however, suggesting the eyes and the pineal have similar reinforcing effects. It is therefore tempting to speculate that the eyes and pineal effect overt rhythms solely through their partially redundant roles as components in a neuroendocrine loop with the SCN, the pineal acting as a weaker element. However, SCN independent regulation by the pineal cannot be ruled out, given that melatonin receptor distribution is widespread in the brain and many peripheral tissues (Rivkees et al., 1989; Pang et al., 1993). Additionally, injections of melatonin into chick brain have been reported to cause acute suppression of 2DG uptake in some structures when administered during the day (Cassone and Brooks,

1991; Cantwell and Cassone, 2002). However, our data do not support a similar endogenous role for melatonin in the long term, as 2DG uptake levels were not elevated in any tissues in pinealectomized chickens.

A final point of consideration is that this current study provides the most in depth characterization of avian clock gene expression to date, which has allowed us to make two important observations. First, a comparative analysis of metabolic rhythms and clock gene expression demonstrates that the transcriptional clockwork (along with a presumed circadian output) is organized in a similar fashion throughout multiple brain tissues. Thus, it will be interesting to see if functional anatomical differences in molecular clockworks will be found in the brains of birds, as has been documented for the mammalian forebrain (Reick et al., 2001).

Secondly, our study reveals that in liver and heart, this canonical transcriptional ensemble is structured differently, not only between these two organs, but also between brain and periphery. Particularly, *bmal1* and *per3* mRNA rhythms appear to be phase locked, whereas *cry1* expression is not. The antiphasic relationship between *bmal1* and *per3* is consistent with their putative roles as positive and negative elements of the avian feedback loop. *Cry1*, however, is transcriptionally connected to the loop in a tissue specific manner. Whether this differential regulation is a product of control by specific neuroendocrine pathways or is intrinsic to peripheral tissues is unclear. It will also be of importance to characterize any tissue specific post-transcriptional processes as well.

CHAPTER V

SUMMARY AND SIGNIFICANCE

The body of work presented in this dissertation expands current understanding of the roles extra SCN oscillators play in the circadian biology of chickens. Herein, we demonstrate the usefulness of a pineal cell culture model as a tool for transcriptional profiling and as a functional genomic screen. These studies describe the base rhythmic transcriptome that is presumably sufficient to drive circadian oscillations in the pineal, an important circadian pacemaker in birds. Furthermore, we have revealed transcriptional changes elicited in pineal culture after exposure to different exogenous stimuli, and have generated a list of candidate genes that should be characterized to investigate their potential roles in circadian clock function. Finally, we demonstrate that circadian clocks are organized differently in the brain and periphery of chickens, and that the eyes and pineal reinforce the rhythmic properties of these tissues.

Genomic Properties of the Pineal Pacemaker *In Vitro*

Rhythmic Transcriptome is Reduced but Functionally Conserved

In Chapter II, we demonstrated that the number and amplitude of gene transcripts oscillating in the chicken pineal is dramatically reduced in culture when compared to freshly excised pineals. As in other studies (Bailey, 2003; Duffield, 2003; Bailey 2004), a reduction in rhythmic transcripts also occurred when animals were placed into DD. *In vivo*, approximately one fifth of all transcripts from the pineal cDNA library exhibit 2-

fold rhythms in LD, while in DD this number reduces to approximately 8%. *In vitro*, we observe 1.5-fold rhythms in a maximum of 6% of all transcripts in LD and in less than 4% of those in DD. Only the most robustly oscillating mRNA species exhibit rhythms of 2-fold or more *in vitro,* especially in DD.

These data indicate that chick pineal cells undergo a global reduction in transcriptional rhythms *ex vivo*, despite the autonomous nature of the pineal organ. It is known that clocks reside within individual pinealocytes, each of which are capable of entrainment and rhythmic melatonin release in culture (Nakahara et al., 1997). Coherent pineal rhythms must therefore result from synchronization between cells, perhaps through coupling between functional gap junctions known to occur between pinealocytes *in vivo* (Berthoud et al., 2000). Thus, the observed depression in the rhythmic pineal transcriptome may be explained by two alternate (but not mutually exclusive) mechanisms: 1) the clocks within individual pineal cells dampen in culture; or 2) a loss of coherence occurs as a result of desynchronization.

Our data provide evidence allowing us to differentiate between these two mechanisms, and strongly favor the first explanation. The study presented in Chapter II provides an interesting and unexpected result, demonstrating that while transcriptional rhythms are reduced, rhythmic pineal output is preserved in culture. This is evidenced by the robust melatonin rhythms we measured from cultured pineals, which are comparable in amplitude to plasma melatonin rhythms measured *in vivo* (Cogburn et al., 1987), and to similar *in vitro* pineal preparations (Zatz and Mullen, 1988a, 1988b; Zatz et al., 1988). This result cannot solely be explained by cellular desynchronization,

because such a mechanism would be predicted to result in an equal reduction in all cellular rhythms measured. Though melatonin rhythms will damp in culture after a period of time in the absence of reinforcement from the neuroendocrine network (Cassone and Menaker 1983, 1984; Natesan et al., 2002), our data suggest that global transcriptional rhythms damp at a much faster rate. More direct evidence that dampening occurs within individual pinealocytes could be obtained by performing single cell real time PCR to measure mRNA rhythm amplitudes in isolated cells from culture. Of course this approach would not allow for measurement of large mRNA populations as is done with microarray techniques.

Still, a functional clock must continue to reside in the reduced pineal transcriptome, given that melatonin biosynthesis continues to oscillate in normal fashion. This raises the possibility that: 1) robust melatonin biosynthesis is maintained as a result of amplification steps despite a weakened oscillator; or 2) proteomic regulation compensates for weakened transcriptional rhythms. Though most clock gene mRNA rhythms are reduced *in vitro*, mRNA products of two genes involved in the melatonin biosynthesis pathway (HIOMT and TrH) are comparable to *in vivo* levels (Chapter II), suggesting that amplification of selected clock outputs may occur. Alternatively, the rhythmic proteome may not reflect these changes seen in mRNA rhythms. For instance, one study of the mouse hepatic proteome showed that as many as 20% of liver proteins undergo rhythmic changes in protein levels, though mRNA levels were rhythmic for only half of these genes (Reddy et al., 2006). More work is needed to understand what rhythmic changes occur in clock proteins as well as the pineal proteome as a whole.

Despite dramatic reductions in the number of rhythmic pineal transcripts *in vitro*, the functional clustering is similar, with the majority of cycling gene products of known function being involved in metabolism, stress/immune response, transport, and protein synthesis and modification. (see Chapter II and Bailey et al., 2003). These same classes of clock controlled genes are found to be regulated in species as diverse as mouse and *Neurospora* (Lewis et al., 2002; Panda et al., 2002; Ueda et al., 2002; Duffield, 2003; Vitalini et al., 2006), and within both the pineal and retina of chicken *in vivo* (Bailey et al., 2003; 2004). Such strong conservation in circadian control over these processes suggests that the output of clocks, like the oscillators themselves, are fundamental to a great diversity of life. There is far less conservation, however, in the individual genes that are regulated by circadian clocks, even between different tissues within the same organism. For instance, only one gene product, cytochrome c oxidase, exhibits a circadian rhythm in *Neurospora*, and in chick retina and pineal (*in vivo* and *in vitro*).

Our microarray study also revealed that significant populations of transcripts are exclusively rhythmic under LD or DD conditions, with nearly 50% of the unique transcripts cycling in free running conditions being arrhythmic in LD (see Chapters II, III). Whilst these results are surprising, similar findings have been reported in at least two independent circadian genomics studies in *Drosophila* (Lin et al., 2002; Ueda et al., 2002; Duffield, 2003). Another study reported that circadian regulation of specific metabolic pathways in mice occurs only in DD (Zhang et al., 2006). Moreover, it was found that this regulation required functional *mper1* and *mper2* genes, though global transcriptional rhythms were not investigated. Other published DNA microarray studies

have not reported such phenomena either because similar results were not found, or because similar investigations were not carried out. Some researchers may be cautious in interpreting such data, as such findings might be regarded as artifactual . However, the fact that similar findings have been reported for multiple species and tissues and using multiple quantitative techniques suggests these phenomena are real, and, in at least some cases are dependent upon functional clock gene expression (Zhang et al., 2006).

Moreover, if such gene regulation does indeed occur under constant conditions, then caution must be taken when interpreting expression of genes that are only rhythmic in LD. Many such rhythms have been reported in chicken and other organisms, and include both gene expression and physiological processes (see Chapter II, III, IV; Cantwell and Cassone, 2002; Bailey et al., 2003; Duffield, 2003; Bailey et al., 2004). Traditionally, such rhythmic processes are considered to be "light driven". However, the recent reports discussed above reveal the possibility that at least some apparently "driven" rhythms may in fact result from some type of circadian "switch" mechanism. This may account for gene transcripts which we found to be rhythmic in LD, but where mRNA levels were not shown to change when measuring after a light pulse (Chapter III).

Another explanation for why some genes appear to be rhythmically regulated in LD but not DD is based on the limitations of mRNA quantitation. As many molecular rhythms tend to damp in DD (see above), rhythmic gene expression may fall below the sensitivity threshold needed to measure them, especially when using less sensitive microarray techniques. In any case, we find that the functional distribution of genes is

remarkably similar between these exclusively rhythmic groups (Chapter II). This perhaps suggests that the chick pineal can switch between different, but redundant pathways when exposed to different environmental cycles.

The Pineal as an Immune Organ

Daily changes observed in immunological signaling of the pineal both *in vivo* and *in vitro* add further evidence to a body of research that characterizes the pineal as a component of the immune system in both birds and mammals. A growing literature has revealed a host of immuno-stimulatory effects of melatonin in both birds and mammals (Majewski et al., 2005; Carrillo-Vico et al., 2006), thus identifying the pineal as a daily and seasonal circadian effector of immune function. In addition, the chicken pineal is now recognized to be a functional lymphoid organ, with most lymphocytes sequestered in specialized tissue known as pineal-associated lymphoid tissue (PALT), typically located in the periphery of the pineal. Lymphocytes are widely distributed throughout the pineal, however, with some lymphocytes residing within follicles containing pinealocytes (Cogburn and Glick, 1981, 1983; Mosenson and McNulty, 2006). Infiltration of lymphocytes into the pineal is dependent on lymphopoietic activity of the bursa and thymus, and varies over a 24 hour period under an LD cycle as well (Mosenson and McNulty, 2006). This infiltration is age-dependent, however, and does not occur in chicks until after one week post-hatch (Cogburn and Glick, 1981). Therefore, rhythmic expression in immune gene transcripts cannot be attributed to lymphocytes in our study, since pineals were harvested from one day old chicks.

An alternative possible source of expression from immune response genes are microglia, which have recently been identified in chick pineal (Mosenson and McNulty, 2006). Microglia are known to secrete several factors which we found to be rhythmic in pineal cultures, including MHC class I and MHC class II associated proteins, and cathepsin L (Supplemental Tables 2, 7; Banati et al., 1993; Chen et al., 2002). Also, rhythmic expression of chemokine (C-X-C motif) ligand 14 mRNA, a chemotactic factor specific to monocytes (Sleeman et al., 2000), was measured in pineal cultures (Supplemental Tables 2, 7). However, rhythmic expression of other molecules specific to lymphocytes, such as NK lysin (Hong et al, 2006), was also observed (Supplemental Tables 2, 7), perhaps suggesting that small numbers of lymphocytes are present in young chick. Alternatively, pinealocytes themselves may express these genes, implicating a novel immune role for these cells, in addition to the overall role of the pineal as lymphoid organ.

Pineal Inputs and Genomic Screening

In chapter III we showed that light affected mRNA levels of many genes, whereas norepinephrine had a comparatively small effect on gene transcription. Therefore, lack of norepiniphrine input, as the only known endogenous chemical modulator of the pineal, does not immediately account for the reduction in the rhythmic pineal transcriptome *ex vivo*. Rather, the restoration of rhythmic pineal transcripts to *in vivo* levels may involve an indirect mechanism which requires one or more cycles of rhythmic NE exposure, as, perhaps, has been demonstrated for entrainment of astocyte

metabolism by melatonin in culture (Adachi et al., 2002). Alternatively, other heretofore unidentified neurotransmitters or other chemical species may act on the pineal in intact animals.

In contrast to norepinephrine, light significantly influenced the expression of many genes in pineal. We found that a light stimulus affected expression of more genes when given during the day, a time when exogenous light sources are normally present, than when given during the evening, although some mRNA levels were similarly effected at both times of day. This result suggests that pineal photo-responsiveness is also regulated by the circadian clock, such that pinealocytes can anticipate and efficiently react to diurnal light exposure. A likely source of this change in sensitivity is rhythmic mRNA or protein expression of functional photoreceptors and/or other photoregulatory elements. Several rhythmic candidates are *retinal fascin*, *interstitial retinol-binding protein 3* (i*rbp*), *transducin γ-subunit*, and *purpurin* (Chapter III). *Purpurin*, a protein involved in retinol transport (Schubert et al., 1986), is especially interesting since it peaks during the day in LD and exhibits among the highest amplitude pineal mRNA rhythms *in vitro*.

Purpurin is also interesting because it meets all criteria of our genomic screen (Chapter III), and is also highly rhythmic in the pineal *in vivo*, as well as in retina (Bailey et al., 2003; 2004). Because rhythmic expression of *purpurin* is localized within two types of photoreceptive pacemaker tissues, and because it is a photoregulatory element that continues to cycle *in vitro*, *purpurin* is an excellent candidate gene linking

input with clock function. Because many lipocalins are involved in immune function, however, *purpurin* should also considered a candidate for this role in the pineal.

Other potential molecular links between immune/stress response and the circadian clock in the pineal are *cystatin c* and *NF1X*, as discussed in Chapter III. *NF1X* is a transcription factor that controls expression of a variety of genes in liver (Lichsteiner et al., 1987; Bois-Joyeux and Danan, 1994; Cardinaux et al., 1994; Anania et al., 1995; Garlatti et al., 1996) and also regulates xenobiotic response pathways in humans (Morel and Barouki, 1998). *NF1X* may interact with several other components of xenobiotic metabolism found to be rhythmic in pineal or retina, including *cytochrome P450*, *aryl hydrocarbon receptor*, and *heat shock protein 90* (Bailey et al., 2003; 2004). Of particular interest is the finding that *NF1X* activity is affected by cellular redox potential (Morel and Barouki, 1998), presumably via modification of conserved cysteine residues required for DNA binding activity (Novak et al., 1992; Bandyopadhyay and Gronostajski, 1994). DNA binding of some clock gene proteins has been shown to depend on cellular redox state (Rutter et al., 2001), which suggests metabolism can modulate the circadian clock. Moreover, various xenobiotics have been shown to regulate the transcription of multiple clock genes (Claudel et al., 2007). As a redox sensing regulator of xenobiotic metabolism, *NF1X* can both respond to, and alter, the cellular redox state. Therefore, *NF1X* might link the circadian clock with metabolic processes in the pineal.

In this regard, it is worth revisting another candidate from our screen, *cystatin c*. Since cystatin c is a cysteine protease inhibitor (Dickinson, 2002), we postulate that it

could regulate redox dependent *NF1X* activity, or perhaps other such proteins with cysteine thiol residues. For example, cystatin c is known to inhibit several cathepsin proteases, and cathepsins are rhythmic in both pineal and retina (Supplemental Tables 2, 7; Bailey et al., 2004). However, cystatin may also be involved in immunomodulation, or other processes (Dickinson, 2002).

The Pineal and Eyes as System Pacemakers

Clock Genes and Metabolism

In Chapter IV, we described rhythms in metabolism and clock genes in chick tissues, and explored the role of the pineal, as well as that of another extraocular pacemaker, the eyes, in regulating these rhythms *in vivo*. We found that 2DG uptake was rhythmic in LD, but not DD, and these rhythms peaked during the day in at least two anatomically different brain tissues, as has been previously reported (Cantwell and Cassone, 2002). These rhythms were phase delayed in peripheral tissues, peaking during mid or early night in liver and heart, respectively (Chapter IV). These nocturnal metabolic rhythms are perplexing, given that chickens are more active during the day. Indeed, diurnal rhythms in feeding, locomotor activity, body temperature, and heart rate have been recorded in chickens (McNally, 1941; Sturkie, 1963; Winget et al., 1968; Savory et al., 2006). However, unlike mammals, blood pressure is negatively correlated with heart rate in chickens, such that it is higher during the night (Savory et al., 2006). This suggests that circadian regulation of cardiovascular function is complex, and not all cardiac parameters can be directly correlated with daily glucose uptake rhythms. Also,

reports of diurnal variations in liver glycogen content are mixed, and may be influenced by feeding activity (Sollburger, 1964; Twiest and Smith, 1970; Raheja, 1973). Furthermore, the chicks used in our study were considerably younger than those used in previous studies, and it is not known what developmental changes may occur in hepatic physiology of young chicks. However, our study shows clear nocturnal rhythms of hepatic glucose uptake, which likely correlates with a concomitant increase in glycogenesis.

Interestingly, 2DG uptake rhythms were not phase locked to clock gene mRNA rhythms. It is unknown what the phase relationships between clock gene proteins and 2DG uptake rhythms are. Therefore, this may indicate that post-transcriptional regulation varies between brain, heart, and liver. On the other hand, control of cellular metabolism by the molecular oscillator may be organized differently in specialized tissues. A third possibility is that rhythms of metabolic uptake are independent of the molecular oscillator regulating clock gene expression. However, surgical pinealectomy and enucleation perturbed rhythms in both clock gene mRNA and 2DG uptake. In contrast, 2DG uptake actually increased after both surgeries in liver, and this did not correlate with changes in clock gene expression. Also, we show that 2DG uptake levels damp much more quickly than clock gene mRNA rhythms. Thus, there is a disconnect between rhythms of clock gene transcription and glucose uptake, and their regulation by system pacemakers.

Our study reveals further complexity in the way that oscillators are organized in different tissues. Transcriptional clock gene loops and associated metabolic rhythms are

similarly organized in the three brain structures examined, but differ in at least two peripheral tissues (Chapter IV). This may reflect specializations that have evolved in peripheral clocks, and perhaps allows for greater plasiticity needed to orchestrate local physiological rhythms independent of other organismal processes. In particular, we find that *bmal1* and *per3* mRNA rhythms are phase locked across multiple tissue types, whereas *cry1* expression is independent. The antiphasic relationship of *bmal1* and *per3* rhythms supports a conserved role for these genes as positive and negative elements. Conversely, there may be a tissue specific role for *cry1*, demonstrating that fundamental differences exist in the organization of chicken molecular oscillators.

Pineal, Retina, and Melatonin Interactions

Overall, we found that the eyes have a similar, if greater role in reinforcing physiological and molecular rhythms than the pineal gland. This result is consistent with studies that compare effects of enucleation and pinealectomy on rhythms of activity in chickens (Nyce and Binkley, 1977;McGoogan and Cassone, 1999). Thus, as system pacemakers, the eyes are hierachically dominant over the pineal in chick, although perhaps less so than in quail.

Since the melatonin synthesized in the retinae of chickens is not secreted into the blood (Reppert and Sagar, 1983; Cogburn et al., 1987), the eyes must regulate body rhythms via direct neural connections to the SCN or other target tissues. On the other hand, the pineal may influence distant rhythms directly through binding of melatonin in target tissues, or indirectly via melatonin's actions on the SCN. One study reported an

acute inhibition of 2DG uptake levels in some brain structures after injecting melatonin into the brain (Cantwell and Cassone, 2002). Our study does not support such a direct role for melatonin in the long-term, as 2DG uptake was not increased in pinealectomized animals. Thus, acute inhibition by melatonin cannot completely account for 2DG uptake rhythms, which must be driven by other mechanisms. It is likely that control of 2DG uptake is determined by an interaction of acute and circadian (or light driven) processes to determine the overall rhythmic waveform, at least in some tissues.

Melatonin signaling is widespread throughout chick tissues (Pang et al., 1993; 1998; 2002), and appears to be highly complex, as receptor proteins are themselves rhythmic in both brain and retina (Appendix A). Additionally, regulation of melatonin receptor rhythms is differential and tissue-specific. For instance, the MEL_{1C} rhythm in diencephalon peaks during the day and persists in constant darkness, whereas the rhythm in retina is antiphase and is not rhythmic in DD. Furthermore, pinealectomy abolishes this rhythm in retina, but only disrupts the rhythm in diencephalon (Appendix A). Thus, melatonin signaling is determined by a mosaic overlay of rhythmic ligand and receptor interactions that are driven by, and in turn feed into, multiple circadian oscillators.

Future Directions

The studies presented here reveal new insights into the organization of circadian pacemakers in chicken, and provide new avenues of exploration to extend this body of research. A logical next step for characterizing circadian pacemakers is to develop and implement methods of genetic manipulation in order to allow for functional genomic

studies. Since genetic tools are limited for avian species, RNAi or overexpression techniques are the most promising methods available. While RNAi methods are not well established in chicken (Hernández and Bueno, 2005), a wide variety of techniques for delivery and execution of RNAi in mammalian cells are available and should be explored in chick and other avian species. Genetic knockdown experiments should focus on determining what role, if any, avian clock gene orthologs have in regulating pineal physiology, including rhythmic melatonin biosynthesis. Additionally, the various candidate genes identified in this dissertation should be characterized in order to determine whether they might also play a role in circadian processes within the pineal. These studies should be carried out in avian pacemaker tissues both *in vivo* and *in vitro*, though current cell culture models are an ideal starting place.

To date, we have worked to develop multiple RNAi methods in several chicken cell lines, with only limited success. Vector based RNAi using transient or lentiviral mediated delivery of shRNA has offered the most promise thus far. Some of this work is presented in Appendix B. Besides the pineal cultures utilized in our current studies, retinal tissue cultures have been established (Ko et al., 2001) and are suitable targets for RNAi studies as well. Furthermore, because lentiviral transduction can occur in non-mitotic cells, lentiviral mediated shRNA would be suitable for carrying out functional molecular studies *in vivo*. Protocols have been developed for *in vivo* lentiviral gene delivery to mammalian brain and eyes, for instance (Takahashi, 2004; Watson et al., 2004).

In conjunction with these functional molecular studies, it will be necessary to characterize the temporal profiles of clock gene proteins, as well other proteins of interest which may be identified in genomic screens. As discussed earlier, characterization of transcriptional genomic regulation alone may belie a complete representation of the clock controlled proteome. Currently our laboratory is in the process of generating and testing antibodies suitable for use in immunohistochemistry and western analyses. These antibodies will aid in characterizing protein expression of clock genes as well as other genes of interest, and will be useful in bridging the regulatory gap between transcription and function. No doubt such studies will become ever more important as the fledgling field of circadian proteomics matures over the next couple decades.

Finally, our findings provide further evidence that the pineal is a circadian immunoregulatory organ, a novel role that is distinct from its known function as a melatonin-releasing exocrine gland. How this role is realized on the cellular and systemic levels is unknown, thus providing many investigational opportunities. In particular, such opportunities might include: characterizing genes involved in immune function; isolating heterogenous cell types in the pineal; manipulating target genes of interest; and immune-challenging animals to determine loss or enhancement of immune function.

Final Conclusions

In conclusion, we demonstrate that extra SCN pacemakers have redundant roles in reinforcing the circadian system of chickens, though the eyes are hierarchically superior to the pineal in this role. The pineal, in turn, likely regulates other local processes independent of its role as a systemic pacemaker. The set of clock controlled genes in the chicken pineal, or the circadian transcriptome, is reduced but functionally conserved *in vitro*, and supports an endogenous role for the pineal as an immune organ as well as a circadian pacemaker. Moreover, the pineal transciptome, while responding considerably to light, is negligibly influenced by transient exposure to norepinephrine, suggesting a more complex regulation of the pineal occurs *in vivo*. Overall, these data demonstrate that circadian rhythms in gene transcript levels and cellular processes are differentially regulated in the pineal, brain, and peripheral tissues of chick. Collectively, these studies reveal an ever expanding complexity in the hierarchical asymmetry of avian circadian clocks.

REFERENCES

Adachi A, Hasegawa M, Ebihara S (1995) Measurement of circadian rhythms of ocular melatonin in the pigeon by *in vivo* microdialysis. Neuroreport 7:286-288.

Adachi A, Natesan AK, Whitfield-Rucker MG, Weiqum SE, Cassone VM (2002) Functional melatonin receptors and metabolic coupling in cultured chick astrocytes. Glia 39:268-278.

Agarwala KL, Kokame K, Kata H, Miyata T (2000) Phosphorylation of RTP, an ER stress-responsive cytoplasmic protein. Biochem Biophys Res Commun 272:641-647.

Alex R, Sozeri O, Meyer S, Dildrop R (1992) Determination of the DNA sequence recognized by the bHLH-zip domain of the N-myc protein. Nucleic Acids Res 20:2257-2263.

Allen G, Rappe J, Earnest DJ, Cassone VM (2001) Oscillating on borrowed time: diffusible signals from immortalized suprachiasmatic nucleus cells regulate circadian rhythmicity in cultured fibroblasts. J Neurosci 21:7937-7943.

Anania F, Potter J, Rennie-Tankersley L, Mezey E (1995) Effects of acetaldehyde on nuclear protein binding to the nuclear factor I consensus sequence in the alpha 2(I) collagen promoter. Hepatology 21:1640-1648.

Aschoff J, Fatranská M, Giedke H, Doerr P, Stamm D, Wisser H (1971) Human circadian rhythms in continuous darkness: entrainment by social cues. Science 171:213-215.

Axelrod J (1974) The pineal gland: a neurochemical transducer. Science 184:1341-1348.

Bailey MJ, Cassone VM (2004) Opsin photoisomerases in the chick retina and pineal gland: characterization, localization and circadian regulation. Invest Opthalmol Vis Sci 45:769-75.

Bailey MJ, Chong NW, Xiong J, Cassone VM (2002) Chickens' cry2: molecular analysis of an avian cryptochrome in retinal and pineal photoreceptors. FEBS Lett 513:169–174.

Bailey MJ, Beremand PD, Hammer R, Bell-Pedersen D, Thomas TL, Cassone VM (2003) Transcriptional profiling of the chick pineal gland, a photoreceptive circadian oscillator and pacemaker. Mol Endocrinol 17:2084-2095.

Bailey MJ, Beremand PD, Hammer R, Reidel E, Thomas TL, Cassone VM (2004) Transcriptional profiling of circadian patterns of mRNA expression in the chick retina. J Biol Chem 279:52247-52254.

Balsalobre A, Damiola F, Schibler U (1998) A serum shock induces circadian gene expression in mammalian tissue culture cells. Cell 93:929-937.

Balsalobre A, Brown SA, Marcacci L, Tronche F, Kellendonk C, Reichardt HM, Schutz G, Schibler U (2000) Resetting of circadian time in peripheral tissues by glucocorticoid signaling. Science 289:2344-2347.

Banati RB, Rothe G, Valet G, Kreutzberg GW (1993) Detection of lysosomal cysteine proteinases in microglia: flow cytometric measurement and histochemical localization of cathepsin B and L. Glia 7:183-191.

Bandyopadhyay S, Gronostajski RM (1994) Identification of a conserved oxidation-sensitive cysteine residue in the NF1 family of DNA-binding proteins. J Biol Chem 269:29949-29955.

Barrett RK, Underwood H (1991) Retinally perceived light can entrain the pineal melatonin rhythm in Japanese quail. Brain Res 563:87-93.

Bartness TJ, Song CK, Demas GE (2001) SCN efferents to peripheral tissues: implications for biological rhythms. J Biol Rhythms 16:196-204.

Bell-Pedersen D, Cassone VM, Earnest DJ, Golden SS, Hardin PE, Thomas TL, Zoran MJ (2005) Circadian rhythms from multiple oscillators: lessons from diverse organisms. Nat Rev Genet 6:544-556.

Berman P, Gray P, Chen E, Keyser K, Ehrlich D, Karten H, LaCorbiere M, Esch F, Schubert D (1987) Sequence analysis, cellular localization, and expression of a neuroretina adhesion and cell survival molecule. Cell 51:135-142.

Bernard M, Klein DC, Zatz M (1997) Chick pineal clock regulates serotonin N-acetyltransferase mRNA rhythm in culture. Proc Natl Acad Sci USA 94:304-309.

Bernard M, Guerlotte J, Greve P, Grechez-Cassiau A, Iuvone MP, Zatz M, Chong NW, Klein DC, Voisin P (1999) Melatonin synthesis pathway: circadian regulation of the genes encoding the key enzymes in the chicken pineal gland and retina. Reprod Nutr Dev 39:325-334.

Berthoud VM, Hall DH, Strahsburger E, Beyer E, Sáez JC (2000) Gap junctions in the chicken pineal gland. Brain Res 861:257-270.

Binkley S (1988) The pineal. Englewood Cliffs, NJ: Prentice-Hall.

Binkley S, Hryshchyshyn M, Reilly K (1979) N-acetyltransferase activity responds to environmental lighting in the eye as well as in the pineal gland. Nature 281:479-481

Bois-Joyeux B, Danan JL (1994) Members of the CAAT/enhancer-binding protein, hepatocyte nuclear factor-1 and nuclear factor-1 families can differentially modulate the activities of the rat alpha-fetoprotein promoter and enhancer. Biochem J 301:49-55.

Boon K, Caron HN, van Asperen R, Valentijn L, Hermus MC, van Sluis P, Roobeek I, Weis I, Voute PA, Schwab M, Versteeq R (2001) N-myc enhances the expression of a large set of genes functioning in ribosome biogenesis and protein synthesis. The EMBO Journal 20:1383-1393.

Brandstätter R, Abraham U, Albrecht U (2001) Initial demonstration of rhythmic per gene expression in the hypothalamus of a non-mammalian vertebrate, the house sparrow. Neuroreport 12:1167–1170.

Brooks DS, Cassone VM (1992) Daily and circadian regulation of 2-[125I]iodomelatonin binding in the chick brain. Endocrinology 131:1297-1304.

Bünning E (1977) The physiological clock, Ed 2. New York: Springer Verlag.

Cantwell EL, Cassone VM (2002) Daily and circadian fluctuation in 2-deoxy[^{14}C]-glucose uptake in circadian and visual system structures of the chick brain: effects of exogenous melatnonin. Brain Res Bull 57:603-11.

Cantwell EL, Cassone VM (2006a) Chicken suprachiasmatic nuclei: I. Efferent and afferent connections. J Comp Neurol 496:97-120.

Cantwell EL, Cassone VM (2006b) Chicken suprachiasmatic nuclei: II. Autoradiographic and immunohistochemical analysis. J Comp Neurol 499:442-57.

Cardinaux JR, Chapel S, Wahli W (1994) Complex organization of CTF/NF-I, C/EBP, and HNF3 binding sites within the promoter of the liver-specific vitellogenin gene. J Biol Chem 269:32947-32956.

Carrillo-Vico A, Reiter RJ, Lardone PJ, Herrera JL, Fernández-Montesinos R, Guerrero JM, Pozo D (2006) The modulatory role of melatonin on immune responsiveness. Curr Opin Investig Drugs 7:423-431.

Cassone VM (1988) Circadian variation of [14C]2-deoxyglucose uptake within the suprachiasmatic nucleus of the house sparrow, *Passer domesticus*. Brain Res 459:178-182.

Cassone VM (1998) Melatonin's role in vertebrate circadian rhythms. Chronobiol Int 5:457-473.

Cassone, VM, Brooks DS (1991) The sites of melatonin action in the house sparrow brain. J Exp Zool 260: 302-309.

Cassone VM, Menaker M (1983) Sympathetic regulation of chicken pineal rhythms. Brain Res 272:311-317.

Cassone VM, Menaker M (1984) Is the avian circadian system a neuroendocrine loop? J Exp Zool 232:539-549.

Cassone VM, Moore RY (1987) Retinohypothalamic projections and suprachiasmatic nucleus of the house sparrow, *Passer domesticus*. J Comp Neurol 266:171-182.

Cassone VM, Takahashi JS, Blaha CD, Lane RF, Menaker M (1986) Dynamics of noradrenergic circadian input to the chicken pineal gland. Brain Res 384:334-341.

Cassone VM, Roberts MH, Moore RY (1987) Melatonin inhibits metabolic activity in the rat suprachiasmatic nuclei. Neurosci Lett 81:29-34.

Cassone VM, Forsyth AM, Woodlee GL (1990) Hypothalamic regulation of circadian noradrenergic input to the chick pineal gland. J Comp Physiol A 167:187-192.

Cassone, VM, Brooks DS, Kelm TA (1995) Comparative distribution of 2-[^{125}I]iodomelatonin binding in the brains of diurnal birds: outgroup analysis with turtles. Brain Behav Evol 45:241-256.

Chen L, Yang P, Kijlstra A (2002) Distribution, markers, and functions of retinal microglia. Ocul Immunol Inflamm 10:27-39.

Chong NW, Bernard M, Klein DC (2000) Characterization of the chicken serotonin N-acetyltransferase gene. Activation via clock gene heterodimer/E box interaction. J Biol Chem 275:32991-32998.

Chong NW, Chaurasia SS, Haque R, Klein DC, Iuvone PM (2003) Temporal-spatial characterization of chicken clock genes: circadian expression in retina, pineal gland, and peripheral tissues. J Neurochem 85:851-60.

Claudel T, Gaspard C, Saumet A, Gachon F (2007) Crosstalk between xenobiotics metabolism and circadian clock. FEBS Lett 581:3626-3633.

Cogburn LA, Glick B (1981) Lymphopoiesis in the chicken pineal gland. Am J Anat 162:131-142.

Cogburn LA, Glick B (1983) Functional lymphocytes in the chicken pineal gland. J Immunol 130:2109-2112.

Cogburn LA, Wilson-Placentra S, Letcher LR (1987) Influence of pinealectomy on plasma and extrapineal melatonin rhythms in young chickens (*Gallus domesticus*). Gen Comp Endocrinol 68:343-356.

Daan S, Pittendrigh CS (1976) A functional analysis of circadian pacemakers in nocturnal rodents: II. The variability of phase response curves. J Comp Physiol A 106:253-266.

Dai F, Yusuf F, Farjah GH, Brand-Saberi B (2005) RNAi-induced targeted silencing of developmental control genes during chicken embryogenesis. Dev Biol 285:80-90.

Damiola F, Le Minh N, Preitner N, Kornmann B, Fleury-Olela F, Schibler U (2000) Restricted feeding uncouples circadian oscillators in peripheral tissues from the central pacemaker in the suprachiasmatic nucleus. Genes Dev 14:2950-2961.

DeCoursey PJ (1960) Daily light sensitivity rhythm in a rodent. Science 131:33-55.

Deguchi T (1979) A circadian oscillator in cultured cells of chicken pineal gland. Nature 282:94-96.

Dickinson DP (2002) Salivary (SD-type) cystatins: over one billion years in the making—but to what purpose? Crit Rev Oral Biol Med 13:485-508.

Dohlman HG, Thorner J, Caron MG, Lefkowitz RJ (1991) Model systems for the study of seven-transmembrane-segment receptors. Annu Rev Biochem 60:653-688.

Drew JE, Barrett P, Mercer JG, Moar KM, Canet E, Delagrange P, Morgan PJ (2001) Localization of the melatonin-related receptor in the rodent brain and peripheral tissues. J Neuroendocrinol 13:453-458.

Dubocovich ML, Takahashi JS (1987) Use of 2-[^{125}I]iodomelatonin to characterize melatonin binding sites in the chicken retina. Proc Natl Acad Sci USA 84:3916-3920.

Duez H, Staels B (2007) Rev-erb alpha gives a time cue to metabolism. FEBS Lett 582:19-25.

Duffield GE (2003) DNA Microarray analyses of circadian timing: the genomic basis of biological time. J Neuroendocrinol 15:991-1002.

Duncan MJ, Heller KS, Purvis CC, Massey BT, Stetson MH (1993) Investigations of the regulation of specific 2-[^{125}I]iodomelatonin binding sites in Siberian hamsters by endogenous and exogenous melatonin. Brain Res 631:107-113.

Dunlap JC (1999) Molecular bases for circadian clocks. Cell 96:271-290.

Ebihara S, Kawamura H (1981) The role of the pineal organ and the suprachiasmatic nucleus in the control of circadian locomotor rhythms in the Java sparrow, *Padda oryzivora*. J Comp Physiol 141:207-214.

Ebihara S, Uchiyama K, Oshima I (1984) Circadian organization in the pigeon, *Columba livia*: the role of the pineal organ and the eye. J Comp Physiol A 154:59-69.

Ebihara S, Oshima I, Yamada H, Goto M, Sato K (1987) Circadian organization in the pigeon. In: Comparative aspects of circadian clocks (Hiroshige T, Honma K, eds), pp 84-94. Sapporo, Japan: Hokkaido Univ Press.

Ebisawa T, Karne S, Lerner MR, and Reppert SM (1994) Expression cloning of a high-affinity melatonin receptor from xenopus dermal melanophores. Proc Natl Acad Sci USA 91:6133-6137.

Edery I, Rutila JE, Rosbash M (1994) Phase shifting of the circadian clock by induction of the *Drosophila* period protein. Science 263:237-240.

Flower DR (1994) The lipocalin protein family: a role in cell regulation. FEBS Lett 354:7-11.

Fu Z, Inaba M, Noguchi T, Kato H (2002) Molecular cloning and circadian regulation of cryptochrome genes in Japanese quail (Coturnix coturnix japonica). J Biol Rhythms 17:14–27.

Fuchs JL (1983) Effects of pinealectomy and subsequent melatonin implants on activity rhythms in the house finch (*Carpodacus mexicanus*). J Comp Physiol 153:413-419.

Fukada Y, Okano T (2002) Circadian clock system in the pineal gland. Mol Neurobiol 25:19-30.

Gallego M, Virshup DM (2007) Post-translational modifications regulate the ticking of the circadian clock. Nat Rev Mol Cell Biol 8:139-148.

Ganguly S, Coon SL, Klein DC (2002) Control of melatonin synthesis in the mammalian pineal gland: the critical role of serotonin acetylation. Cell Tissue Res 309:127-137.

Garlatti M, Aggerbeck M, Bouguet J, Barouki R (1996) Contribution of a nuclear factor 1 binding site to the glucocorticoid regulation of the cytosolic aspartate aminotransferase gene promoter. J Biol Chem 271:32629-32634.

Gastel JA, Rosebloom PH, Rinaldi PA, Weller JL, Klein DC (1998) Melatonin production: proteasomal proteolysis in serotonin N-acetyltransferase regulation. Science 279:1358-1360.

Gaston S, Menaker M (1968) Pineal function: the biological clock in the sparrow? Science 160:1125-1127.

Gauer F, Masson-Pévet M, Pévet P (1992a) Density of melatonin receptors in the rat suprachiasmatic nucleus: a possible implication of melatonin action. J Neuroendocrinol 4:455-459.

Gauer F, Masson-Pévet M, Pévet P (1992b) Pinealectomy and constant illumination increase the density of melatonin binding sites in the pars tuberalis of rodents. Brain Res 575:32-38.

Gauer F, Masson-Pévet M, Stehle J, Pévet P (1994) Daily variations in melatonin receptor density of rat pars tuberalis and suprachiasmatic nuclei are distinctly regulated. Brain Res 641:92-98.

George SR, Lee SP, Varghese G, Zeman PR, Seeman P, Ng GYK, O'Dowd BF (1998) A transmembrane domain-derived peptide inhibits D1 dopamine receptor function without affecting receptor oligomerization. J Biol Chem 273:30244-30248.

Glossop NR, Lyons LC, Hardin PE (1999) Interlocked feedback loops within the *Drosophila* circadian oscillator. Science 286:766-768.

Guo H, Brewer JM, Champhekar A, Harris RB, Bittman EL (2005) Differential control of peripheral circadian rhythms by suprachiasmatic –dependent neural signals. Proc Natl Acad Sci USA 102:3111-3116.

Guo H, Brewer JM, Lehman MN, Bittman EL (2006) Suprachiasmatic regulation of circadian rhythmis of gene expression in hamster peripheral organs: effects of transplanting the pacemaker. J Neurosci 26:6406-6412.

Gwinner E (1978) Effects of pinealectomy on circadian locomotor activity rhythms in European starlings, *Sturnus vulgaris*. J Comp Physiol 126:123-129.

Gwinner E, Brandstätter R (2001) Complex bird clocks. Philos Trans R Soc Lond B Biol Sci 356:1801-1810.

Hamm HE, Menaker M (1980) Retinal rhythms in chicks: circadian variation in melatonin and serotonin N-acetyltransferase activity. Proc Natl Acad Sci USA 77:4998-5002.

Hara R, Wan K, Wakamatsu H, Aida R, Moriya T, Akiyama M, Shibata S (2001) Restricted feeding entrains liver clock without participation of the suprachiasmatic nucleus. Genes Cells 6:269-278.

Hardin PE (2005) The circadian timekeeping system of *Drosophila*. Curr Biol 15:R714-722.

Harvey AJ, Speksnijder G, Baugh LR, Morris JA, Ivarie R (2002) Expression of exogenous protein in the egg white of transgenic chickens. Nat Biotechnol 20:396-399.

Hastings M, O'Neill JS, Maywood JS (2007) Circadian clocks: regulators of endocrine and metabolic rhythms. J Endocrinol 195:187-198.

Helfer G, Fidler AE, Vallone D, Foulkes NS, Brandstätter R (2006) Molecular analysis of clock gene expression in the avian brain. Chronobiol Int 23:113-127.

Hernández VH, Bueno D (2005) RNA interference is ineffective as a routine method for gene silencing in chick embryos as monitored by fgf8 silencing. Int J Biol Sci 1:1-12.

Hong YH, Lillehoj HS, Dalloul RA, Min W, Miska KB, Tuo W, Lee SH, Han JY, Lillehoj EP (2006) Molecular cloning and characterization of chicken NK-lysin. Vet Immunol Immunopathol 110:339-347.

Hunter M, Angelicheva D, Tournev I, Ingley E, Chan DC, Watts GF, Kremensky I, Kalaydjieva L (2005) NDRG1 interacts with APO A-I and A-II and is a functional candidate for the HDL-C QTL on 8q24. Biochem Biophys Res Commun 332:982-92.

Iigo M, Furukawa K, Hattori A, Hara M, Ohtani-Kaneko R, Suzuki T, Tabata M, Aida K (1995) Effects of pinealectomy and constant light exposure on day-night changes of melatonin binding sites in the goldfish brain. Neurosci Lett 197:61-64.

Kalmus H (1940) Diurnal rhythms in the axolotl larva and in *Drosophila*. Nature 145:72-73.

Kalsbeek A, Kreier F, Fliers E, Sauerwein HP, Romijn JA, Buijs RM (2007) Minireview: circadian control of metabolism by the suprachiasmatic nuclei. Endocrinology 148:5635-5639.

Kasal CA, Menaker M, Perez-Polo Jr (1979) Circadian clock in culture: N-acetyltransferase activity of chick pineal glands oscillates *in vitro*. Science 203:656-658.

Klein DC (1985) Photoneural regulation of the mammalian pineal gland. Ciba Found Symp 117:38-56.

Ko CH, Takahashi JS (2006) Molecular components of the mammalian circadian clock. Hum Mol Genet 15:R271-277.

Ko GY, Ko ML, Dryer SE (2001) Circadian regulation of cGMP-gated cationic channels of chick retinal cones. Erk MAP Kinase and Ca2+/calmodulin-dependent protein kinase II. Neuron 29:255-266.

Ko GY, Ko ML, Dryer SE (2003) Circadian phase-dependent modulation of cGMPgated channels of cone photoreceptors by dopamine and D2 agonist. J Neurosci 23:3145-3153.

Kohsaka A, Bass J (2007) A sense of time: how molecular clocks organize metabolism. Trends Endocrinol Metab 18:4-11.

Konopka RJ, Benzer S (1971) Clock mutants in *Drosophila melanogaster*. Proc Natl Acad Sci USA 68:2112-2116.

Korf HW (1994) The pineal organ as a component of the biological clock. Phylogenetic and ontogenetic considerations. Ann NY Acad Sci 719:13-42.

Kruse U, Oian F, Sippel AE (1991) Identification of a fourth nuclear factor 1 gene in chicken by cDNA cloning: NF1X Nucleic Acids Res 19:6641.

la Fleur SE (2003) Daily rhythms in glucose metabolism: supriachiasmatic nucleus output to peripheral tissue. J Neuroendocrinol 15:315-322.

Lamosova D, Zeman M, Mackova M, Gwinner E (1995) Development of rhythmic melatonin synthesis in cultured pineal glands and pineal cells isolated from chick embryo. Experientia 51:970-975.

Le Minh N, Damiola F, Tronche F, Schutz G, Schibler U (2001) Glucocorticoid hormones inhibit food-induced phase-shifting of peripheral circadian oscillators. Embo J 20:7128-7136.

Lee PP, Shiu SY, Chow PH, Pang SF (1995) Regional and diurnal studies of melatonin and melatonin binding sites in the duck gastro-intestinal tract. Biol Signals 4:212-224.

Lewis ZA, Correa A, Schwerdtfeger KL, Xle X, Gomer RH, Thomas T, Ebbole DJ, Bell-Pedersen D (2002) Overexpression of white collar-1 (WC-1) activiates circadian clock-associated genes, but is not sufficient to induce most light-regulated gene expression in *Neurospora crassa*. Mol Microbiol 45:917-931.

Lichtsteiner S, Wuarin J, Schibler U (1987) The interplay of DNA-binding proteins on the promoter of the mouse albumin gene. Cell 51:963-973.

Lin Y, Han M, Shimada B, Wang L, Gibler TM, Amarakone A, Awad TA, Stormo GD, Van Gelder RN, Taghert PH (2002) Influence of the period-dependent circadian clock on diurnal, circadian, and aperiodic gene expression in *Drosophila* melanogaster. Proc Natl Acad Sci USA 99:9562-9567.

Liu R, Yuan H, Sugamori KS, Hamadanizadeh A, Lee FJS, Pang SF, Brown GM, Pristupah ZB, Niznik HB (1995) Molecular and functional characterization of a partial cDNA encoding a novel chicken brain melatonin receptor. FEBS Lett 374:273-278.

Lu J, Cassone VM (1993a) Daily melatonin administration synchronizes circadian patterns of brain metabolism and behavior in pinealectomized house sparrows, *Passer domesticus*. J Comp Physiol A 173:775-782.

Lu J, Cassone VM (1993b) Pineal regulation of circadian rhythms of 2-deoxy[^{14}C]glucose uptake and 2[^{125}I]iodomelatonin binding in the visual system of the house sparrow, *Passer domesticus*. J Comp Physiol A 173:765-774.

Majewski P, Adamska I, Pawlak J, Barańska A, Skwarło-Sońta K (2005) Seasonality of pineal gland activity and immune functions in chickens. J Pineal Res 39:66-72.

McGoogan JM (2000) Melatonin regulation of circadian rhythms in retinal physiology in chicks. Ph.D. dissertation. Texas A&M University, College Station.

McGoogan JM, Cassone VM (1999) Circadian regulation of chick electroretinogram: effects of pinealectomy and exogenous melatonin. Am J Physiol 277:R1418-1427.

McMillan (1972) Pinealectomy abolishes the circadian rhythm of migratory restlessness. J Comp Physiol 79:105-112.

McMillan JP, Keatts HC, Menaker M (1975) On the role of eyes and brain photoreceptors in the sparrow: entrainment to light cycles. J Comp Physiol 102:251-256.

McNally EH (1941) Heart rate of the domestic fowl. Poult Sci 20:266-271.

Morel Y, Barouki R (1998) Down-regulation of cytochrome P450 1A1 gene promoter by oxidative stress—critical contribution of nuclear factor 1. J Biol Chem 273: 26969-26976.

Mosenson JA, McNulty JA (2006) Characterization of lymphocyte subsets over a 24-hour period in Pineal-Associated Tissue (PALT) in the chicken. BMC Immunol 7:1.

Mouritsen H, Janssen-Bienhold U, Liedvogel M, Feenders G, Stalleicken J, Dirks P, Weiler, R (2004) Cryptochromes and neuronal-activity markers colocalize in the retina of migratory birds during magnetic orientation. Proc Natl Acad Sci USA 101:14294–14299.

Menaker M (1972) Nonvisual light reception. Sci Am 3:22-29.

Menaker M, Moreira LF, Tosini G (1997) Evolution of circadian organization in vertebrates. Braz J Med Biol Res 30:305-313.

Moore RY (1996) Neural control of the pineal gland. Behav Brain Res 73:125-130.

Murakami N, Nakamura H, Nishi R, Marumoto N, Nasu T (1994) Comparison of circadian oscillation of melatonin release in pineal cells of house sparrow, pigeon and Japanese quail, using cell perfusion systems. Brain Res 651:209-214.

Nagata K, Guggenheimer RA, Hurwitz J (1983) Specific binding of a cellular DNA replication protein to the origin of replication of adenovirus DNA. Proc Natl Acad Sci USA 80:6177-6181.

Nagoshi E, Saini C, Bauer C, Laroche T, Naef F, Schibler U (2004) Circadian gene expression in individual fibroblasts: cell-autonomous and self-sustained oscillators pass time to daughter cells. Cell 119:693-705.

Naji L, Carillo-Vico A, Guerrero JM, Calvo JR (2004) Expression of nuclear melatonin receptors in mouse peripheral organs. Life Sci 74:2227-2236.

Nakahara K, Murakami N, Nasu T, Kuroda H, Murakami T (1997) Individual pineal cells in chick possess photoreceptive, circadian clock and melatonin-synthesizing capacities *in vitro*. Brain Res 774:242-245.

Natesan AK, Cassone VM (2002) Melatonin receptor mRNA localization and rhythmicity in the retina of the domestic chick, *Gallus domesticus*. Vis Neurosci 19:265-274.

Natesan A, Geetha L, Zatz M (2002) Rhythm and soul in the avian pineal. Cell Tissue Res 309:35-45.

Norgren RB, Silver R (1989) Retinohypothalamic projections and the suprachiasmatic nucleus in birds. Brain Behav Evol 34:73-83.

Norgren RB, Silver R (1990) Distribution of vasoactive intestinal peptide-like and neurophysin-like immunoreactive neurons and acetylcholineterase staining in the ring dove hypothalamus with emphasis on the question of an avian suprachiasmatic nucleus. Cell Tissue Res 259:331-339.

Novak A, Goyal N, Gronostajski RM (1992) Four conserved cysteine residues are required for the DNA binding activity of nuclear factor I. J Biol Chem 267:12986-12990.

Nowock J, Borgmeyer U, Puschel AW, Rupp RA, Sippel AE (1985) The TGGCA protein binds to the MMTV-LTR, the adenovirus origin of replication, and the BK virus enhancer. Nucleic Acids Res 13:2045-2061.

Nyce J, Binkley S (1977) Extraretinal photoreception in chickens: entrainment of the circadian locomotor activity rhythm. Photochem Photobiol 25:529-531.

Oishi K, Sakamoto K, Okada T, Nagase T, Ishida N (1998) Antiphase circadian expression between BMAL1 and Period homologue mRNA in the suprachiasmatic nucleus and peripheral tissues of rats. Biochem Biophys Res Commun 253:199-203.

Oishi T, Yamao M, Kondo C, Haida Y, Masuda A, Tamotsu S (2001) Multiphotoreceptor and multioscillator system in avian circadian organization. Microsc Res Tech 53:43-47.

Oishi K, Miyazaki K, Ishida N (2002) Functional CLOCK is not involved in the entrainment of peripheral clocks to the restricted feeding: entrainable expression of mper2 and BMAL1 mRNAs in the heart of CLOCK mutant mice on Jcl: ICR background. Biochem Biophys Res Commun 298:198-202.

Oishi K, Atsumi G, Sugiyama S, Kodomari I, Kasamatsu M, Machida K, Ishida N (2006) Disrupted fat absorption attenuates obesity induced by a high-fat diet in clock mutant mice. FEBS Lett 580:127-130.

Okano T, Yamamoto K, Okano K, Hirota T, Kasahara T, Sasaki M, Takanaka Y, Fukada Y (2001) Chicken pineal clock genes: implication of BMAL2 as a bidirectional regulator in circadian clock oscillation. Genes Cells 6:825-836.

Osada S, Ikeda T, Xu M, Nishihara T, Imagawa M (1997) Identification of the transcriptional repression domain of nuclear factor 1-A. Biochem Biophys Res Commun 238: 744-747.

Oshima I, Yamada H, Goto M, Sato K, Ebihara S (1989) Pineal and retinal melatonin is involved in the control of circadian locomotor activity and body temperature rhythms in the pigeon. J Comp Physiol A 166:217-226.

Oster H, Damerow S, Hut RA, Eichele G (2006) Transcriptional profiling in the adrenal gland reveals circadian regulation of hormone biosynthesis genes and nucleosome assembly genes. J Biol Rhythms 21:350-361.

Panda S, Antoch MP, Miller BH, Su AI, Schook AB, Straume M, Schultz PG, Kay SA, Takahashi JS, Hogenesch JB (2002) Coordinated transcription of key pathways in the mouse by the circadian clock. Cell 109:307-320.

Pang SF, Dubocovich ML, Brown GM (1993) Melatonin receptors in peripheral tissues: a new area of melatonin research. Biol Signals 2:177-180.

Pang CS, Tang PL, Song Y, Brown GM, Pang SF (1996) 2-[125I]Iodomelatonin binding sites in the quail heart: characteristics, distribution and modulation by guanine nucleotides and cations. Life Sci 58:1047-1057.

Pang CS, Xi SC, Yau MYC (1998) Melatonin receptors in the chick heart: modulation on isoproterenol stimulated cAMP level. Biol Signals Recept 7:268-269.

Pang CS, Xi SC, Brown GM, Pang SF, Shiu SY (2002) 2[125I]Iodomelatonin binding and interaction with beta-adrenergic signaling in chick heart/coronary artery physiology. J Pineal Res 32:243-252.

Pant K, Chandola-Saklani A (1992) Pinealectomy and LL abolished circadian perching rhythms but did not alter circannual reproductive or fattening rhythms in finches. Chronobiol Int 9:413-420.

Pelham RW (1975) A serum melatonin rhythm in chickens and its abolition by pinealectomy. Endocrinology 96:543-546.

Peters JL, Earnest BJ, Tjalkens RB, Cassone VM, Zoran M (2005) Modulation of intercellular calcium signaling by melatonin in avian and mammalian astrocytes is brain region-specific. J Comp Neurol 493:370-380.

Pévet P, Agez L, Bothorel B, Saboureau M, Gauer F, Laurent V, Masson-Pévet M (2006) Melatonin in the multi-oscillatory mammalian circadian world. Chronobiol Int 23:39-51.

Pierce ME, Sheshberadaran H, Zhang Z, Fox LE, Applebury ML, Takahashi JS (1993) Circadian regulation of iodopsin gene expression in embryonic photoreceptors in retinal cell culture. Neuron 10:579-584.

Piquemal D, Joulia P, Balaguer A, Basset A, Marti J, Commes T (1999) Differential expression of the RTP/Drg1/Ndr1 gene product in proliferating and growth arrested cells. Biochim Biophys Acta 1450:364-373.

Pittendrigh CS (1954) On temperature independence in the clock system controlling emergence time in *Drosophila*. Proc Natl Acad Sci USA 40:1018-1029.

Pittendrigh CS (1960) Circadian rhythms and the organization of living things. Cold Spring Harbor Symp Quant Biol 25:159-184.

Pittendrigh CS (1961) On temporal organization in living systems. In: Harvey lectures series 56, pp 93-175. New York: Academic Press.

Pittendrigh CS (1981a) Circadian systems: general perspective. In: Handbook of behavioral neurobiology, biological rhythms: volume 4 (Aschoff J, ed), pp 57-77. New York: Plenum Press.

Pittendrigh CS (1981b) Circadian systems: entrainment. In: Handbook of behavioral neurobiology, biological rhythms: volume 4 (Aschoff J, ed), pp 95-124. New York: Plenum Press.

Pittendrigh CS, Minis DH (1964) The entrainment of circadian oscillations by light and their role as photperiodic clocks. The American Naturalist 118:261-285.

Poon AM, Choy EH, Pang SF (2001) Modulation of blood glucose by melatonin: a direct action on melatonin receptors in mouse hepatocytes. Biol Signals Recept 10:367-379.

Provencio I, Rodriquez IR, Jiang G, Hayes WP, Moreira EF, Rollag MD (2000) A novel human opsin in the inner retina. J Neurosci 20:600-605.

Puga A, Barnes SJ, Chang C, Zhu H, Nephew KP, Khan SA, Shertzer HG (2000) Activation of transcription factors activator protein-1 and nuclear factor-kB by 2,3,7,8-tetrachlorodibenzo-*p*-dioxin. Biochem Pharm 59:997-1005.

Rada JA, Wiechmann AF (2006) Melatonin receptors in chick ocular tissues: implications for a role of melatonin in ocular growth regulation. Invest Opthalmol Vis Sci 47:25-33.

Raheja KL (1973) Comparison of diurnal variations in plasma glucose, cholesterol, triglyceride, insulin and in liver glycogen in younger and older chicks (*Gallus domesticus*). Comp Biochem Physiol 44:1009-1014.

Reddy AB, Karp NA, Maywood ES, Sage EA, Deery M, O'Neill JS, Wong GK, Chesham J, Odell M, Lilley KS, Kyriacou CP, Hastings MH (2006) Circadian orchestration of the hepatic proteome. Curr Biol 16:1107-1115.

Redman J, Armstrong S, Ng KT (1983) Free-running activity rhythms in the rat: entrainment by melatonin. Science. 219:1089-1091.

Refinetti R (2005) Circadian physiology, Ed 2. Boca Raton, FL: CRC Press.

Reick M, Garcia JA, Dudley C, McKnight SL (2001) NPAS2: an analog of clock operative in the mammalian forebrain. Science 293:437-438.

Reppert SM (1997) Melatonin receptors: molecular biology of a new family of G protein-coupled receptors. J Biol Rhythms 12:528-531.

Reppert SM, Sagar SM (1983) Characterization of the day-night variation of retinal melatonin content in the chick. Invest Ophthalmol Vis Sci 24:294-300.

Reppert SM, Weaver DR (2002) Coordination of circadian timing in mammals. Nature 418:935-941.

Reppert SM, Weaver DR, Ebisawa T (1994) Cloning and characterization of a mammalian melatonin receptor that mediates reproductive and circadian responses. Neuron 13:1177-1185.

Reppert SM, Weaver DR, Cassone VM, Godson C, Kolakowski LF (1995) Melatonin receptors are for the birds: molecular analysis of two receptor subtypes differentially expressed in chick brain. Neuron 15:1003-1015.

Reppert SM, Weaver DR, Godson C (1996) Melatonin receptors step into the light: cloning and classification of subtypes. Trends Pharmacol Sci 17:100-102.

Rivkees SA, Cassone VM, Weaver DR, Reppert SM (1989) Melatonin receptors in chick brain: characterization and localization. Endocrinology 125:363-368.

Rudic RD, McNamara P, Curtis AM, Boston RC, Panda S, Hogenesch JB, Fitzgerald GA (2004) BMAL1 and CLOCK, two essential components of the circadian clock, are involved in glucose homeostasis. PLoS Biol 2:e377.

Rutter J, Reick M, Wu LC, McKnight SL (2001) Regulation of clock and NPAS2 DNA binding by the redox state of NAD cofactors. Science 293:510-514.

Savory CJ, Kostal L, Nevison IM (2006) Circadian variation in heart rate, blood pressure, body temperature, and EEG of immature broiler breeder chickens in restricted-fed and ad libitum-fed states. Br Poult Sci 47:599-606.

Schubert D, LaCorbiere M (1985) Isolation of an adhesion-mediating protein from chick neural retina adherons. J Cell Biol 101:1071-1077.

Schubert D, LaCorbiere M, Esch F (1986) A chick neural retina adhesion and survival molecule is a retinal-binding protein. J Cell Biol 102:2295-2301.

Schwartz WJ, Davidsen LC, Smith CB (1980) *In vivo* metabolic activity of a putative circadian oscillator, the rat suprachiasmatic nucleus. J Comp Neurol 189:157-167.

Schwartz WJ (1990) Different *in vivo* metabolic activities of suprachiasmatic nuclei of Turkish and golden hamsters. Am J Physiol 259:R1083-1085.

Shearman LP, Sriram S, Weaver DR, Maywood ES, Chaves I, Zheng B, Kume K, Lee CC, van der Horst GT, Hastings MH, Reppert SM (2000) Interacting molecular loops in the mammalian circadian clock. Science 288:1013-1019.

Shimizu T, Cox K, Karten HJ, Britto LRG (1994) Cholera toxin mapping of retinal projections in pigeons (*Columba livia*), with emphasis on retinohypothalamic connections. Vis Neurosci 11:441-446.

Simpson SM, Follett BK (1981) Pineal and hypothalamic pacemakers: their role in regulating circadian rhythmicity in Japanese quail. J Comp Physiol 144:381-389.

Sleeman MA, Fraser JK, Murison JG, Kelly SL, Prestidge RL, Palmer DJ, Watson JD, Kumble KD (2000) B cell- and moocyte-activating chemokine (BMAC), a novel non-ELR alpha-chemokine. 12:677-689.

Sollburger A (1964) The control of circadian glycogen rhythms. Ann NY Acad Sci 117:519-554.

Song Y, Pang CS, Ayre EA, Brown GM, Pang SF (1996) Melatonin receptors in the chicken kidney are up-regulated by pinealectomy and linked to adenylate cyclase. Endocrinol 135:128-133.

Starkey SJ, Walker MP, Beresford IJ, Hagan RM (1995) Modulation of the rat suprachiasmatic circadian clock by melatonin *in vitro*. Neuroreport 6:1947-1951.

Stephan FK (2002) The “other” circadian system: food as a Zeitgeber. J Biol Rhythms 17:284-292.

Stokkan KA, Yamazaki S, Tei H, Sakaki Y, Menaker M (2001) Entrainment of the circadian clock in the liver by feeding. Science 291:490-493.

Stratmann M, Schibler U (2006) Properties, entrainment, and physiological functions of mammalian peripheral oscillators. J Biol Rhythms 21:494-506.

Sturkie PD (1963) Heart rate of chickens determined by radio telemetry during light and dark periods. Poult Sci 42:797-798.

Sweeney BM (1987) Rhythmic phenomena in plants, Ed 2. New York: Academic Press.

Takahashi M (2004) Delivery of genes to the eye using lentiviral vectors. In: Gene delivery to mammalian cells: volume 2: viral gene transfer techniques (Heiser WC, ed), pp 439-449. Totowa, NJ: Humana Press.

Takahashi JS, Menaker M (1982) Role of the suprachiasmatic nuclei in the circadian system of the house sparrow, *Passer domesticus*. J Neurosci 2:815-828.

Takahashi JS, Hamm H, Menaker M (1980) Circadian rhythms of melatonin release from individual superfused chicken pineal glands *in vitro*. Proc Natl Acad Sci USA 77:2319-2322.

Toller GL, Nagy E, Horvath RA, Klausz B, Rekasi Z (2006) Circadian expression of bmal1 and serotonin-N-acetyltransferase mRNAs in chicken retina cells and pinealocytes *in vivo* and *in vitro*. J Mol Neurosci 28:143-150.

Turek FW, Joshu C, Kohsaka A, Lin E, Ivanova G, McDearmon E, Laposky A, Losee-Olson S, Easton A, Jensen DR, Eckel RH, Takahashi JS, Bass J (2005) Obesity and metabolic syndrome in circadian clock mutant mice. Science 308:1043-1045.

Twiest G, Smith CJ (1970) Circadian rhythm in blood glucose level of chickens. Comp Biochem Physiol 32:371-375.

Ueda HR, Matsumoto A, Kawamura M, Iino M, Tanimura T, Hashimoto S (2002) Genome-wide transcriptional orchestration of circadian rhythms in *Drosophila*. J Biol Chem 277:14048-14052.

Underwood H (1990) The pineal and melatonin: regulators of circadian function in lower vertebrates. Experientia 46:120-128.

Underwood H (1994) The circadian rhythm of thermoregulation in Japanese quail. I. Role of the eyes and pineal. J Comp Physiol A 175:639-653.

Underwood H, Binkley S, Siopes T, Mosher K (1984) Melatonin rhythms in the eyes, pineal bodies, and blood of Japanese quail (*Coturnix coturnix japonica*). Gen Comp Endocrinol 56:70-81.

Underwood H, Steele CT, Zivkovic B (2001) Circadian organization and the role of the pineal in birds. Microsc Res Tech 53:48-62.

Vitalini MW, de Paula RM, Park WD, Bell-Pedersen D (2006) The rhythms of life: circadian output pathways in *Neurospora*. J Biol Rhythms 21:432-444.

Wan Q, Pang SF (1995) 2-[125I]iodomelatonin binding sites in the quail liver: characterization and the effect of guanosine 5'-O-(3-thiotriphosphate). Biol Signals 4:24-31.

Watson DJ, Karolewski BA, Wolfe JH (2004) Stable gene delivery to CNS cells using lentiviral vectors. In: Gene delivery to mammalian cells: volume 2: viral gene transfer techniques (Heiser WC, ed), pp 413-428. Totowa, NJ: Humana Press.

Welsh DK, Yoo SH, Liu AC, Takahashi JS, Kay SA (2004) Bioluminescence imaging of individual fibroblasts reveals persistent, independently phased circadian rhythms of clock gene expression. Curr Biol 14:2289-2295.

Wijnen H, Young M (2006) Interplay of circadian clocks and metabolic rhythms. Annu Rev Genet 40:409-448.

Winget CM, Card DH, Pope JM (1968) Circadian oscillations of three parameters at defined light intensities and color. J Appl Physiol 24:401-406.

Yagita K, Tamanini F, van Der Horst GT, Okamura H (2001) Molecular mechanisms of the biological clock in cultured fibroblasts. Science 292:278-281.

Yamamoto K, Okano T, Fukada Y (2001) Chicken pineal cry genes: light-dependent upregulation of ccry1 and ccry2 transcripts. Neurosci Lett 313:13–16.

Yamazaki S, Numano R, Abe M, Hida A, Takahashi R, Ueda M, Block GD, Sakaki Y, Menaker M, Tei H (2000) Resetting central and peripheral circadian oscillators in transgenic rats. Science 288:682-685.

Yasuo S, Watanabe M, Okabayashi N, Ebihara S, Yoshimura T (2003) Circadian clock genes and photoperiodism: comprehensive analysis of clock gene expression in the mediobasal hypothalamus, the suprachiasmatic nucleus, and the pineal gland of Japanese Quail under various light schedules. Endocrinology 144:3742–3748.

Yoo SH, Yamazaki S, Lowrey PL, Shimomura K, Ko CH, Buhr ED, Siepka SM, Hong HK, Oh WJ, Yoo OJ, Menaker M, Takahashi JS (2004) PERIOD2::LUCIFERASE real-time reporting of circadian dynamics reveals persistent circadian oscillations in mouse peripheral tissues. Proc Natl Acad Sci USA 101:5699-5700.

Yoshimura T, Suzuki Y, Makino E, Suzuki T, Kuroiwa A, Matsuda Y, Namikawa T, Ebihara S (2000) Molecular analysis of avian circadian clock genes. Brain Res Mol Brain Res 78:207–215.

Yoshimura T, Yasuo S, Suzuki Y, Makino E, Yokota Y, Ebihara S (2001) Identification of the suprachiasmatic nucleus in birds. Am J Physiol Regulatory Integrative Comp Physiol 280:1185-1189.

Yu W, Hardin PE (2006) Circadian oscillators of *Drosophila* and mammals. J Cell Sci 119:4793-4795.

Yuan H, Pang SF (1992) [^{125}I]iodomelatonin binding sites in the chicken brain: diurnal variation and effect of melatonin injection or pinealectomy. Biol Signals 1:208-218.

Zatz M (1991) Light and norepinephrine similarly prevent damping of the melatonin rhythm in cultured chick pineal cells: regulation of coupling between the pacemaker and overt rhythms? J Biol Rhythms 6:137-147.

Zatz M (1992) Does the circadian pacemaker act through cyclic AMP to drive the melatonin rhythm in chick pineal cells? J Biol Rhythms 7:301-311.

Zatz M (1996) Melatonin rhythms: trekking toward the heart of darkness in the chick pineal. Cell Dev Biol 7:811-820.

Zatz M, Mullen DA (1988a) Photoendocrine transduction in cultured chick pineal cells. II. Effects of forskolin, 8-bromocyclic AMP, and 8-bromocyclic GMP on the melatonin rhythm. Brain Res 453:51-62.

Zatz M, Mullen DA (1988b) Two mechanisms of photoendocrine transduction in cultured chick pineal cells: pertussis toxin blocks the acute but not the phase-shifting effects of light on the melatonin rhythm. Brain Res 453:63-71.

Zatz M, Mullen DA, Moskal JR (1988) Photoendocrine transduction in cultured chick pineal cells: effects of light, dark, and potassium on the melatonin rhythm. Brain Res 438:199-215.

Zatz M, Gastel JA, Heath JR III, Klein DC (2000) Chick pineal melatonin synthesis: light and cyclic AMP control abundance of serotonin N-actyltransferase protein. J Neurochem 74:2315-2321.

Zhang J, Kaasik K, Blackburn MR, Lee CC (2006) Constant darkness is a circadian metabolic signal in mammals. Nature 439:340-343.

APPENDIX A

MEL_{1C} RECEPTOR PROTEIN EXPRESSION IN BRAIN AND RETINA

Introduction

The pineal hormone melatonin has been implicated in diverse physiological processes, including those regulating daily circadian timing, seasonal reproduction, thermoregulation, and cellular metabolism. In contrast to the situation in mammals, high affinity binding sites for the radiolabeled melatonin agonist, 2-[^{125}I] iodomelatonin (IMEL) (Dubocovich and Takahashi, 1987), are widespread in the avian brain (Rivkees et al., 1989; Cassone et al., 1995; Reppert et al., 1995), particularly in areas associated with vision. Biochemical characterization of IMEL binding indicate that melatonin receptors are of high affinity with one or two binding sites associated with a G_i-GTP binding protein (Rivkees et al., 1989; Reppert et al., 1995).

Genes encoding three melatonin receptors have been isolated, cloned, and characterized from chick brain (Liu et al., 1995; Reppert et al., 1995). The first of these receptor subtypes, designated Mel_{1A}, has been cloned from both birds (Reppert et al., 1995) and mammals (Reppert et al., 1994). Another receptor subtype, Mel_{1C}, has also been cloned from chickens, and shares high peptide sequence similarity with the melatonin receptor originally isolated from a Xenopus melanophore cDNA library (Ebisawa et al., 1994; Reppert et al., 1995). The Mel_{1B} receptor has not been characterized as fully as the other two sub-types in birds; however, mRNA encoding this receptor is highly expressed in chick retina (Natesan and Cassone, 2002). The Mel_{1A} and

Mel_{1C} receptors are 68% identical, and the predicted gene products have nearly identical molecular weights (~40 kD) and isoelectric points (~9.5). Both receptors have putative amino-terminal, N-linked glycosylation sites, extracellular disulfide bonds, and other features that place them in the G-protein associated seven transmembrane domain receptor protein superfamily (Reppert, 1997). Expression of the receptors in eukaryotic cells yields IMEL binding kinetics that are similar to *in vivo* data with dissociation constant (K_D) values in the pM range and maximal binding (B_{max}) values in the fmol/mg protein range. In spite of sequence and pharmacological similarities, however, Mel_{1A} and Mel_{1C} mRNA are differentially expressed in specific tissues of the chick brain (Reppert et al., 1995), suggesting different functional roles for melatonin occur within different tissues.

Melatonin receptor binding varies temporally as well as anatomically. There is a daily and circadian rhythm in IMEL binding in many visual and auditory structures of the chick brain, such that binding is higher during the day than at night, in both LD and DD conditions (Brooks and Cassone, 1992). Removal of circulating melatonin by pinealectomy does not abolish the IMEL binding rhythm in either house sparrows (Lu and Cassone, 1993b) or chickens (Yuan and Pang, 1992), although the level of binding is increased. While these data provide some insight into the physiological action of melatonin, characterization of receptor proteins will allow further elucidation of the spatial and time dependent role of melatonin. To investigate the distribution of melatonin receptor proteins, we utilize antiserum that shows specific immunoreactivity to the Mel_{1C} receptor sub-type (McGoogan, 2000; Peters et al., 2005). The present study

describes the temporal expression of this receptor in chick diencephalon and retina. We also examine the effects of pinealectomy on these temporal profiles.

Materials and Methods

Animals and Surgeries

Male White Leghorn chicks (Hy-Line International) were obtained on the first day post-hatch and maintained on a 12:12 LD cycle in heated brooders with continuously available food and water. All surgeries were performed 3-7 days post-hatch. Chicks were deeply anaesthetized with a ketamine/xylazine injections (100 mg/kg; im) and secured in a stereotaxic apparatus. Pinealectomies (n = 90) and sham surgeries (n = 90) were performed as described earlier (Chapter IV). All animals were allowed to recover for one week in LD with food and water provided *ad libitum*.

Tissue Sampling

Tissues were taken every four hours for one day in LD and two days in DD. Five chicks per timepoint were euthanized with CO_2 gas, and then decapitated. Brain and eyes were removed, and diencephalon and retina were dissected out and placed into cold protein extraction buffer (Edery et al., 1994). Following each dissection, tissue samples were immediately sonicated in buffer, then protein was extracted by centrifugation and frozen for storage.

Western Blot Analysis

Samples were quantified using a standard colorimetric protein assay (Sigma Total Protein Reagent), separated by SDS-PAGE, then electroblotted onto a nitrocellulose membrane and probed with polyclonal primary antibody at 1:1000 fold dilution in blocking buffer (1% non-fat dry milk in PBS). Blots were washed in PBS and incubated with goat anti-rabbit secondary antibody conjugated to horseradish peroxidase at a dilution of 1:500 in blocking buffer. After a second wash, blots were treated with a solution of diaminobenzidine in PBS (1 mg/ml) and activated with 30% hydrogen peroxide. After optimal staining occurred, blots were given a final wash and allowed to dry.

Band Quantification and Statistics

Dried blots were scanned and quantitatively analyzed using Sigma Scan software. Mean band densities taken from 5 blots were measured for each timepoint and normalized to the highest density band. A one-way analysis of variance was performed on each data set, followed by a *post hoc* analysis using the Bonferroni t-test.

Results

An immunoreactive band of 40 kD was consistently observed in western blots of diencephalon and retina, which corresponds to the predicted molecular weight of melatonin receptors (Reppert, 1997). MEL_{1C} levels were rhythmic in diencephalon, with peak values occuring during the early day and a relatively short period in DD (Fig. 18A)

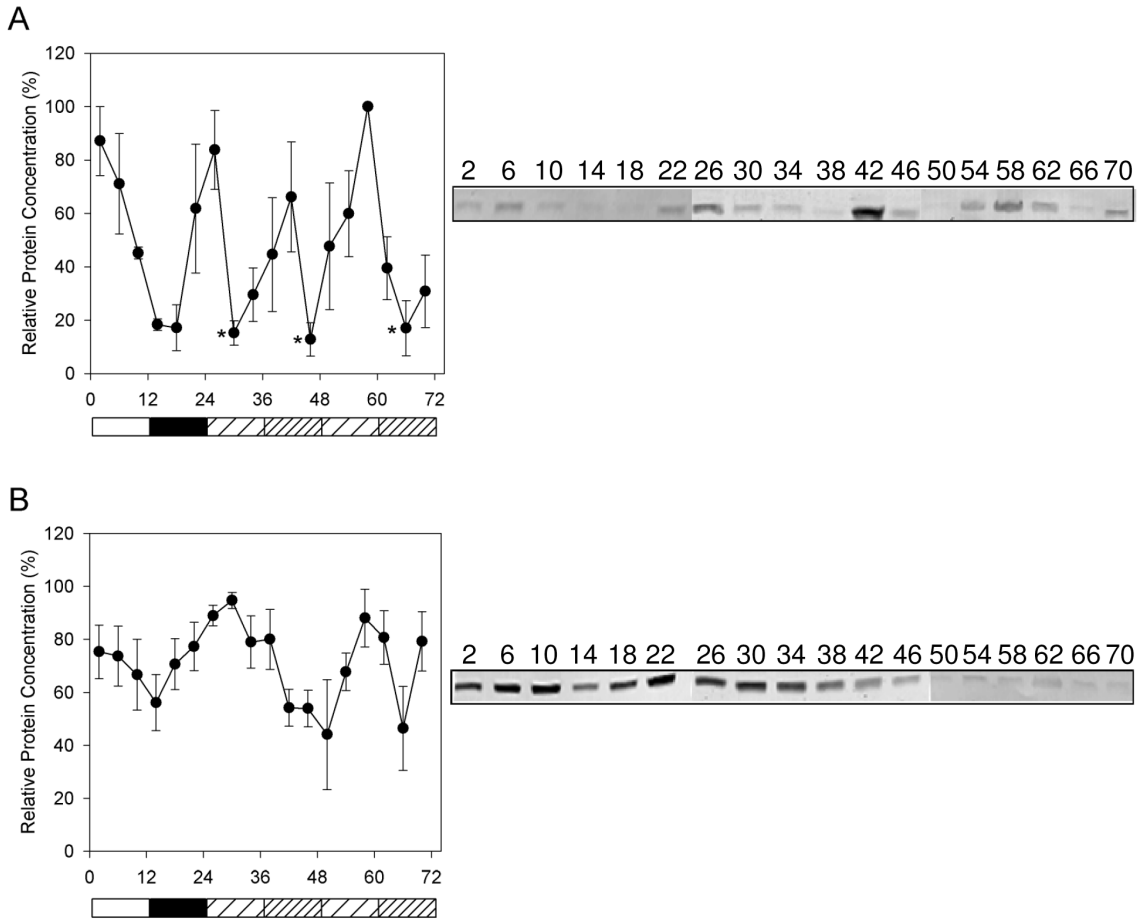

Figure 18. Mel_{1C} receptor protein in diencephalon. Relative quantitative levels of Mel_{1C} protein are plotted for one day in LD, followed by two days in DD in sham (**A**) or pinealectomized (**B**) chickens. The abscissa indicates hours after onset of lights during the first cycle. Open bars indicate lights on (LD), black bars indicate lights off (DD), course hatched bars indicated subjective day (DD), and fine hatched bars indicate subjective night (DD). Means marked with * are significantly different from highest expression value. Representative western blots indicating 40 kD immunoreactive protein are shown to the right.

Pinealectomy did not abolish this rhythm; however, the amplitude of the rhythm was decreased, and the period appeared to lengthen in DD (Fig. 18B). Pinealectomy also consistently increased the overall levels of protein expression this tissue.

MEL_{1C} protein levels also exhibited a daily rhythm in retina under LD conditions. This rhythm was approximately 180° out of phase with the rhythm observed in diencephalon, such that protein peaked at night and was low during the day (Fig. 19A). This rhythm was, however, only maintained in LD in sham operated animals. In DD or in pinealectomized animals, the rhythm was abolished (Fig 19B).

Discussion

The present study shows that, as with melatonin receptor binding and mRNA expression (Reppert et al., 1995; Reppert, 1997; Cassone, 1998), melatonin receptor protein is regulated by the clock and is differentially expressed in the chick. The diurnal and circadian rhythm we observe in MEL_{1C} receptor protein within diencephalon corroborates previous studies in which IMEL binding was found to be higher during the day than during the night in many brain structures of the chick (Brooks and Cassone, 1992) and house sparrow (Lu and Cassone, 1993). Scatchard plots from these IMEL binding studies reveal that changes in B_{max}, but not binding affinity (K_D), occur throughout the day. Thus, the kinetic evidence for diurnal rhythms of receptor density within these tissues is supported by a similar circadian profile of receptor protein expression demonstrated in the current study.

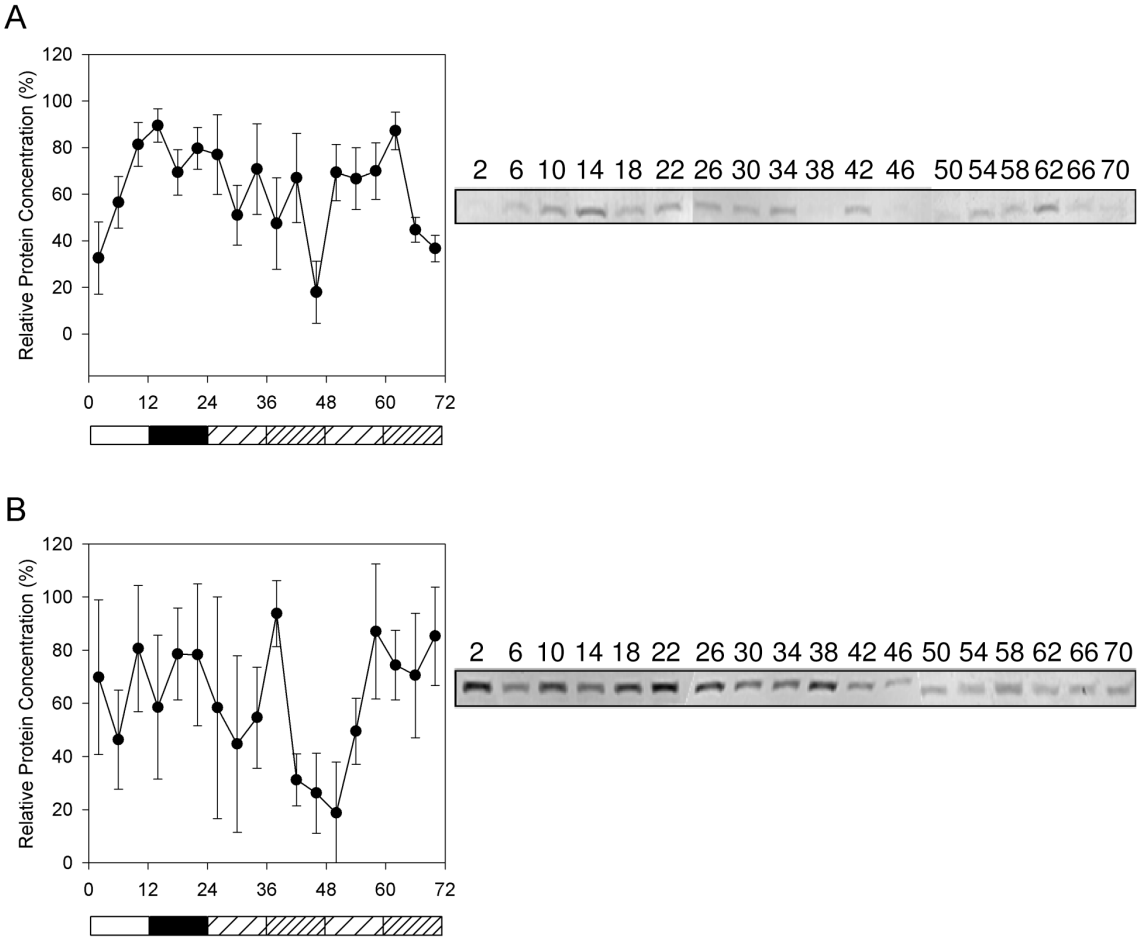

Figure 19. Mel_{1C} receptor protein in retina. Relative quantitative levels of Mel_{1C} protein are plotted for one day in LD, followed by two days in DD in sham (**A**) or pinealectomized (**B**) chickens. The abscissa indicates hours after onset of lights during the first cycle. Open bars indicate lights on (LD), black bars indicate lights off (DD), course hatched bars indicated subjective day (DD), and fine hatched bars indicate subjective night (DD). Means marked with * are significantly different from highest expression value. Representative western blots indicating 40 kD immunoreactive protein are shown to the right.

Surgical removal of the pineal gland, which abolishes detectable melatonin levels in chick brain and plasma (Pelham, 1975) increases MEL_{1C} concentration in diencephalon. Thus, circulating melatonin may directly regulate its receptor at the protein level. Such regulation of a receptor by its ligand has been reported for many other types of G protein-coupled receptors (Dohlman et al., 1991). In agreement with the increase in protein expression shown here, pinealectomy has been shown to increase overall levels of IMEL binding in chick brain (Yuan and Pang, 1992) and kidney (George et al., 1998), house sparrow brain (Lu and Cassone, 1993), rat pituitary pars tuberalis (PT) (Gauer et al., 1992a) and rat hypothalamic suprachiasmatic nucleus (SCN) (Gauer et al., 1992b). Similar effects of pinealectomy have been reported on tissues from animals maintained in constant light conditions, including rat PT (Song et al., 1996) and SCN (Gauer et al., 1992a), and guinea pig spleen (Gauer et al., 1992b). Direct down regulation of MEL_{1C} receptor density by melatonin can at least partially account for the observations noted in these binding studies. These data argue for a mechanism of receptor internalization rather than desensitization (the two most commonly invoked models), since both protein levels and IMEL binding density (B_{max}) are affected, while K_D remains constant over time and in response to pinealectomy or lighting conditions.

The fact that pinealectomy does not abolish the rhythm of MEL_{1C} protein in diencephalon suggests that rhythmic factors other than the circadian secretion of melatonin contribute to the regulation of this receptor within this tissue. This observation is consistent with the published effects of pinealectomy on IMEL binding rhythms in some species but not with others. For example, in house sparrows, pinealectomy

increases IMEL binding and attenuates binding rhythms gradually, eventually damping to arrhythmicity over an extended period (Lu and Cassone, 1993). It is unknown if a similar damping to complete arrhythmia might occur in chickens over a longer period of sampling. In the goldfish brain, pinealectomy abolishes the IMEL binding rhythm (as does constant light) (Iigo et al., 1995), while binding in the Siberian hamster is unaffected by either endogenous or exogenous sources of melatonin (Duncan et al., 1993). Even within a species, there may be distinct, tissue specific roles for melatonin, as melatonin binding rhythms are reported to be differentially regulated in the rat PT and SCN (Gauer et al., 1994) and in the chick diencephalon and retina as reported here.

Our study demonstrates that a nocturnal rise in MEL_{1C} protein occurs in the chick retina, and is thus antiphasic to the rhythm in brain. These data contradict findings of another study which reports a nocturnal rhythm in MEL_{1A} and MEL_{1B} protein levels and a diurnal rhythm in chick retinal MEL_{1C} protein (Rada and Wiechmann, 2006). This is perplexing, since both studies utilize similar methods of quantitation. While the reason for this discrepancy is unknown, it may result from subtle differences in tissue processing or extraction protocols. We also find that the MEL_{1C} protein rhythm is antiphasic to the rhythm of mRNA rhythm in LD. However, mRNA regulation appears to be complex, as this rhythm is observed to undergo a phase inversion in DD (Natesan and Cassone, 2002).

In conclusion, this study demonstrates that melatonin receptor protein, like mRNA, is regulated by the clock in a tissue specific manner. Further, we show that diencephalic rhythms of receptor levels are reinforced, but not driven, by rhythms in

ligand abundance. Overall, the present data suggest a complex dynamic of post-translational receptor regulation determines the overall binding pattern of melatonin, and, presumably, physiological sensitivity to melatonin.

APPENDIX B

RNAi METHODS IN CHICKEN PINEALOCYTES AND DIENCEPHALIC ASTROCYTES

Extensive work has been done in our laboratory to achieve genetic knockdown of selected genes in pinealocytes and other chicken cell lines, including astrocytes and embryonic fibroblasts. We have attempted to manipulate RNAi pathways in these cells using an assortment of molecular constructs, including morpholinos, chemically and endogenously synthesized siRNA oligos, and plasmid-based shRNA molecules. We have also used a variety of eukaryotic gene transfer techniques including electroporation, chemical transfection, and viral transduction. In our chicken cell lines of interest, we have had limited success with shRNA mediated RNAi using chemical and viral transfer, and we present some of this work here.

Optimization of Transfection Efficiency

In order to optimize transfection efficiency for vector mediated RNAi expreriments, we transfected two chicken cell types with an EmGFP expression plasmid driven by a CMV promoter (pLenti6.2-GW/EmGFP Control Vector, Invitrogen), using a variety of different transfection reagents and protocols. Though this construct had only been tested for use in mammalian cells, use of the CMV promoter has been validated in chicken cells (Harvey et al., 2002). Therefore, we found this expression vector suitable for direct visualization of transfection efficiency in our chosen cell lines.

Ultrapure transfection grade EmGFP vector was obtained by propagating in Stbl3 cells (Invitrogen) and isolating plasmid with a High-Speed Plasmid Midi Kit modified for use with endotoxin-free reagents (Qiagen). In order to test for functional EmGFP expression, HEK293FT cells (Invitrogen) were transfected with EmGFP vector alone or cotransfected with EmGFP vector plus an empty expression vector (pLenti6.2/V5-DEST Vector, Invitrogen) as a positive control, following Invitrogen's guidelines for transfection of this cell line. Twenty hours post-transfection, cells were washed and visualized in PBS using an Olympus Flurourescent Microscope equipped with a GFP filter set. Using this method, transfection efficiency was determined as the ratio of the number of fluorescent cells to total cells within randomly chosen microscopic fields of view, as shown in Fig. 20 A, B. Since greater transfection efficiency was obtained using expression vector alone (~60% vs. ~40%), this protocol was followed for subsequent transfection experiments.

Multiple transfection reagents were used to transfect the EmGFP vector into both chicken cell lines, including: a cationic liposomal lipid reagent (Lipofectamine 2000, Invitrogen); a non-liposomal lipid reagent (Effectene, Qiagen); and an activated-dendrimer reagent (Superfect, Qiagen). Pineal cultures were established as previously described (Chapter II), and plated onto 6-well polystyrene plates. Primary cultures were transfected on the second day after plating, when cells were 40-80% confluent, following the manufacturer's recommended protocols for each transfection reagent. Antibiotics and serum were not included in culture medium during transfection. Among these different formulations, the lipid-based transfection reagents yielded better

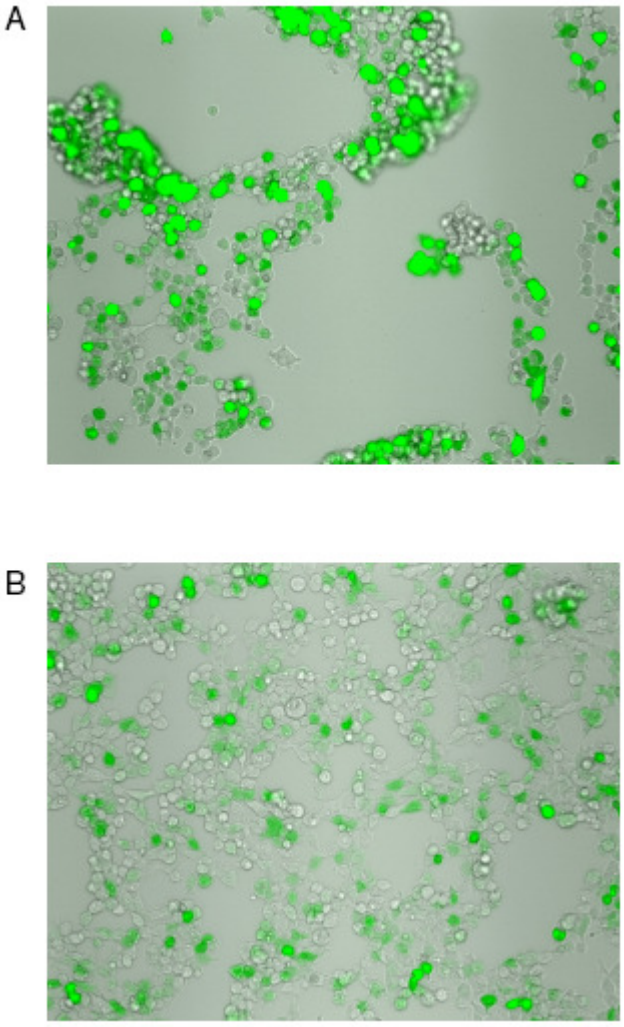

Figure 20. Visual assay for transfection efficiency using GFP fluorescence. Examples of EmGFP fluorescence in cultured HEK293FT cells are shown. Cells were transfected with pLenti6.2-GW/EmGFP plasmid alone (**A**) or co-transfected with an empty vector (**B**).

transfection efficiencies and lower toxicity than the dendrimer solution. The non-liposomal Effectene reagent plus Enhancer solution (*Qiagen*) was maximally effective at low concentrations of plasmid DNA (0.8 μg/well) and yielded moderate transfection efficiencies (30-40%). The liposomal lipid reagent worked best when supplemented with PLUS reagent (Invitrogen) and at higher concentration of plasmid DNA (4-8 μg/well), but resulted in slightly higher transfection efficiencies (≤50%). GFP fluorescence peaked between 18-24 hours, and was greatly reduced when measured 48 our 72 hours post-transfection. The overall optimal transfection efficiency was obtained using 4 μg plasmid with 20 μl Lipofectamine 2000 and 20 μl PLUS reagent (2.5 ml total volume per 10 cm^2 well). This formulation was subsequently used to transiently transfect pineal cells to screen RNAi constructs.

For the astrocyte transfections, cultures of diencephalic astrocytes were established as previously described (Peters et al., 2005). On the day before transfection, astrocytes were plated into 6-well culture plates at a density of $4x10^5$ cells/$10cm^2$ well. All transfections were performed during the third or fourth passage of culture, as these cells appear to be healthiest during this time. Serum was left in growth media during transfections, as cells cultured in serum-free media rapidly died and exhibited diminished GFP fluorescense. Because toxicity was observed after treating cells with high concentrations of Superfect for more than two hours, media was replaced after a two hour incubation with this reagent. No noticeable toxicity was observed after treatment with lipid-based transfection reagents. In contrast to pinealocytes, the dendrimer-based formulation yielded high transfection efficiencies with the GFP

A

GATGCCAATCTACGGAAACTGAATTCACGTTTGTTTGTTATTCGTGGACAGCCAGCAGA
TGTTTTCCCCAGGCTTTTTAAGGAATGGAGCATTGCAAAACTCTCTATTGAATATGATTC
TGAACCGTTTGGGAAGGAGAGAGATGCA**GCAATTAAGAAGCTGGCTAGT**GAAGCTGG
AGTGGAGGTCATCGTTCGAATTTCTCACACATTATATGACCTAGACAAAATAATAGAAT
TAAATGGAGGACAGCCACCTCTTACTTACAA**GCGATTCCAGACTCTAATTAG**TAGGAT
GGAACCACTGGAGATGCCAGTGGAGACTATAACCCCAGAGGTAATGCAGAAATGTACC
ACTCCTGTCTCTGATGACCATGATGAGAAATACGGTGTCCCGTCGCTTGAAGAGCTAGG
TTTTGACACAGATGGTCTGCCTTCTGCAGTATGGCCTGGGGGAGAAACAGAAGCTCTCA
CACGACTGGAAAGGCATCTAGAACGAAAGGCTTGGGTAGCAAACTTTGAAAGACCACG
AATGAACGCCAATTCCCTTCTGGCAAGCCC

B

GACTCCCAGTCAGGCACAGGTTCAGCAGCATCAGGCAGTGGATTGGCTTTATCTAGTTC
TTTAGGCTCTCACTCCTGTGAAACTTCTGGTGGTGGCACAGACAGTGGGAAAAACAGCA
ACTGTTTTGCCAGTAATGATTCTTCTGAAACTTCCAA**AGCAGAGACTGATCAAGAA**GC
AAAAGAAAAAGAGACACCTCATAAATCTAAATATGAGTCAGCCTGGGTGATGATGGAT
CACACACCTGAGCAA**GTTCTAATGACGTACCAAA**TGCCTAACAGAGTTAAAGAGGAA
GTTTTAAAA**GAGGATATGGAGAAGCTGA**TAGTCATGCGAAAGCAGCAGCCTTGGTTTT
CAGATAGACAAAAGAGGGAGCTTGCAGAAGTGCATACGTGGATCCGGACACAGACTGT
CCCACTACAAATCAACACTCAAGGATGTGTTACATGTGACATCAGGGAA**GCAACTTGT**
GAGTCTGCAATGGCTGATGACAATATGGAAAACAAAGGGAAACCGCTTCCAGTCTTGG
AACACTGA

Figure 21. shRNA target sequences. **A**, A partial cds for *gcry1* shows target sequences for shRNA probes designed using Invitrogen's algorithm (red underlined sequences). The probes are located at 429 and 548 base pairs after the start of the coding sequence. **B**, A partial cds for *gper3* shows target sequences for shRNA probes designed using algorithms from *Ambion* (blue underlined sequences). The probes are located at positions, 175, 269, 320, and 476 in the coding sequence.

plasmid, and were comparable to efficiencies achieved using the lipid based reagents (30-50%). A third liposomal reagent, Gen-Carrier 2 (Epoch biolabs), was also tested with the GFP plasmid in astrocytes, but resulted in no measurable fluorescence signal. Transfection efficiency using Superfect was maximized by using a ratio of 4 µg DNA to 20 µl dendrimer solution (710µl total volume per 10 cm^2 well). Up to 32 µg DNA was transfected using various ratios of DNA:dendrimer solution, but no additional increase in GFP fluorescence was observed. As with pinealocytes, the GFP fluorescence signal degraded after 24 hours post-transfection.

Design and Transient Transfection of Vector Based shRNA Antisense Probes

We designed shRNA probes targeting two different regions of the coding sequence for chicken *cry1*, and four regions of the chicken *per3* gene (Fig. 21). We chose sequences that showed the highest probability of knockdown against mammalian transcripts based on RNAi algorithms developed by Invitrogen or Ambion corps. Each oligonucleotide consisted of a palindromic target sequence separated by a short, 4-nucleotide (Invitrogen) or 9-nucleotide (Ambion) loop, to generate a sense-loop-antisense hairpin configuration (Fig. 22). Each oligonucleotide, along with its complementary strand, also contained a 4-nucleotide flanking sequence on the 5' end to facilitate directional cloning into a human U6 cassette within a pENTR/U6 entry vector (Invitrogen). Functional motifs of the human U6 promoter are highly conserved in chicken, and it has been successfully used to drive expression of shRNA in chicken cells (Dai et al., 2005).

A

gcry1 423

5′ CACCGCAATTAAGAAGCTGGCTAGTCGAAACTAGCCAGCTTCTTAATTGC 3′

gcry1 548

5′ CACCGCGATTCCAGACTCTAATTAGCGAACTAATTAGAGTCTGGAATCGC 3′

B

gper3 175

5′ CACCAGCAGAGACTGATCAAGAATTCAAGAGATTCTTGATCAGTCTCTGCT 3′

gper3 269

5′ CACCGTTCTAATGACGTACCAAATTCAAGAGATTTGGTACGTCATTAGAAC 3′

gper3 320

5′ CACCGAGGATATGGAGAAGCTGATTCAAGAGATCAGCTTCTCCATATCCTC 3′

gper3 476

5′ CACCGCAACTTGTGAGTCTGCAATTCAAGAGATTGCAGACTCACAAGTTGC 3′

Figure 22. shRNA probe sequences. Palindromic sequences designed using Invitrogen's RNAi designer utility (**A**) or Ambion's pSilencer design tool (**B**) are shown. The probe number indicates the position targeted in the gene coding sequence. Blue indicates the cloning site for a pENTR/U6 RNAi entry vector (Invitrogen), green indicates the sense sequence, red indicates the antisense sequence, and black indicates the hairpin loop sequence.

Single-stranded oligonucleotides were synthesized by *Integrated DNA Technologies*, and the complementary strands were annealed and subcloned into the pENTR/U6 vector following the standard user's protocol from Invitrogen. Positive transformants were isolated, and the entry construct was sequenced to ensure correct orientation and sequence of the double-stranded oligonucleotide. A functional shRNA construct targeting *lacZ* (Invitrogen) was also generated to use as a negative control. Transfection grade pENTR/U6^{shRNA} plasmids were then isolated for each construct using endotoxin free isolation procedures (Qiagen) as before.

For the first RNAi screening experiment, astrocyte cultures were transfected with pENTR/U6 plasmid containing the cry1-423, cry1-548, or lacZ shRNA probes (0.5 or 2 μg DNA/well) using lipofectamine 2000 transfection reagent, following the recommended protocol from Invitrogen. Mock transfected cells received corresponding concentrations of carrier solution only. Cells were incubated with DNA:liposmal complexes overnight in media containing serum before washing and replenishing normal growth serum. Cells were harvested 48 hours post-transfection and total RNA was extracted using an RNeasy kit (Qiagen). *Cry1* mRNA levels were quantified following reverse transcription using real time PCR and normalizing to cyclophilin expression, as described previously (Chapters II, III, IV). Due to poor quality of some samples transfected with cry1-548^{shRNA}, this portion of the experiment was repeated with a separate lacZ negative control (Fig. 23 B).

Cry1 mRNA levels were higher in astrocytes transfected with cry1-423^{shRNA} compared to either negative control (Fig. 23 A). However, *cry1* mRNA was also

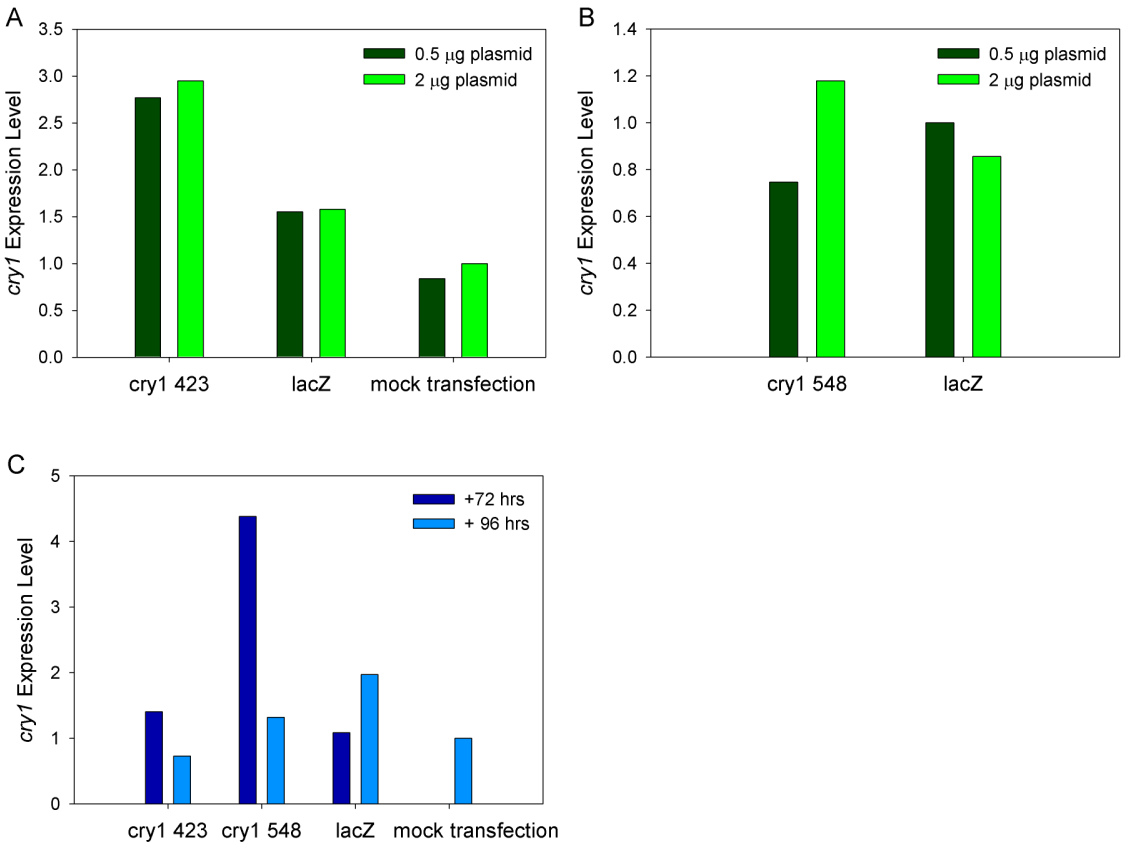

Figure 23. Transient transfection of astrocytes with cry1^{shRNA}. **A**, Chick diencephalic astrocytes were transfected with 0.5 or 2 µg plasmid containing cry1-423^{shRNA} or lacZ^{shRNA} per well of culture dish. Mock transfected cells received only carrier solution for corresponding concentrations of transfected DNA. *Cry1* mRNA levels are shown 48 hours post-transfection. **B**, Astrocytes were transfected with the same concentrations of plasmid containing cry1-548^{shRNA} or lacZ^{shRNA}. *Cry1* mRNA levels were measured 48 hours post-transfection. **C**, Astrocytes were transfected with 0.5 µg of the indicated constructs, and *cry1* expression was measured 72 or 96 hours post-transfection.

elevated in cells transfected with lacZ^{shRNA} compared to mock transfected cells, suggesting that transfection of astrocytes with DNA may elicit a non-specific increase in target gene expression in these cells. Transfection of astrocytes with the higher concentration of cry1-548^{shRNA} also increased *cry1* mRNA, though a lower concentration of plasmid resulted in a modest (~20%) decrease in the target transcript levels relative to the lacZ^{shRNA} control (Fig. 23 B).

Because of this modest preliminary result, the RNAi experiment was repeated using the low concentrations of each shRNA probe, and *cry1* mRNA was measured from RNA harvested 72 and 96 hours after cells were transfected. RNA was harvested from mock transfected cells 96 hours later only. After 72 hours, *cry1* mRNA was again elevated in cells transfected with cry1-423^{shRNA} and cry1-548^{shRNA} compared with the lacZ^{shRNA} control. After 96 hours, *cry1* levels were reduced in experimental shRNA samples compared with cells that received the lacZ^{shRNA} control, but were not appreciably different from those of mock transfected cells. Because of these negative results, screening of these shRNA probes was discontinued in chick astrocytes.

For the next RNAi experiment, pineal cultures were established and maintained in a LD cycle, then transfected the following day with one of each per3^{shRNA} (Fig. 22 B) or lacZ^{shRNA}. We followed the same protocol used to transfect the GFP plasmid, as described above. Mock transfected cells were incubated with carrier only. Cultures were maintained for 22 or 46 hours before harvesting RNA for *per3* quantitation. After 22 hours, *per3* mRNA levels were reduced in all four cultures that were transfected with per3^{shRNA} plasmids, relative to both lacZ^{shRNA} and mock control cultures (33% and 39%

maximal decrease, respectively; Fig. 24 A). After 46 hours, no decrease was observed in *per3* expression, which was in fact elevated in all transfected cultures.

Subsequently, pineal cultures were co-transfected with varying concentrations of per3^{shRNA} or lacZ^{shRNA} as shown in Fig. 24 B, and RNA was harvested 22 hours post-transfection. Because non-specific changes in mRNA levels were suspected to occur in transfected cultures, *per3* mRNA levels were independently normalized to both *cyclophilin* and *β-actin*. When normalizing to *β-actin*, *per3* levels were shown to decrease in cultures transfected with a cocktail of all four per3^{shRNA} plasmids. However, no such decrease was observed when *cylophilin* was used as an endogenous control gene. This result suggested that the transfections may have had non-specific effects on control gene transcript levels.

To confirm whether the per3^{shRNA} cocktail could reproducibly knockdown *per3* expression in pineal cultures, we repeated the most successful result by co-transfecting all four per3^{shRNA} plasmids (1 μg/well each), and normalized *per3* expression to *β-actin*. To achieve statistical power, we performed 6 biological replicates of each sample. In this experiment, *per3* mRNA levels were significantly higher in cells transfected with per3^{shRNA} probes compared to mock transfected controls ($p = 0.024$, ANOVA; Holm-Sidak *post hoc*; Fig. 24 C).

Viral Transduction of Vector Based shRNA Antisense Probes

Lentiviral expression vectors were generated by performing LR recombination between the pENTR/U6 cry1^{shRNA} entry clones and a lentiviral expression destination

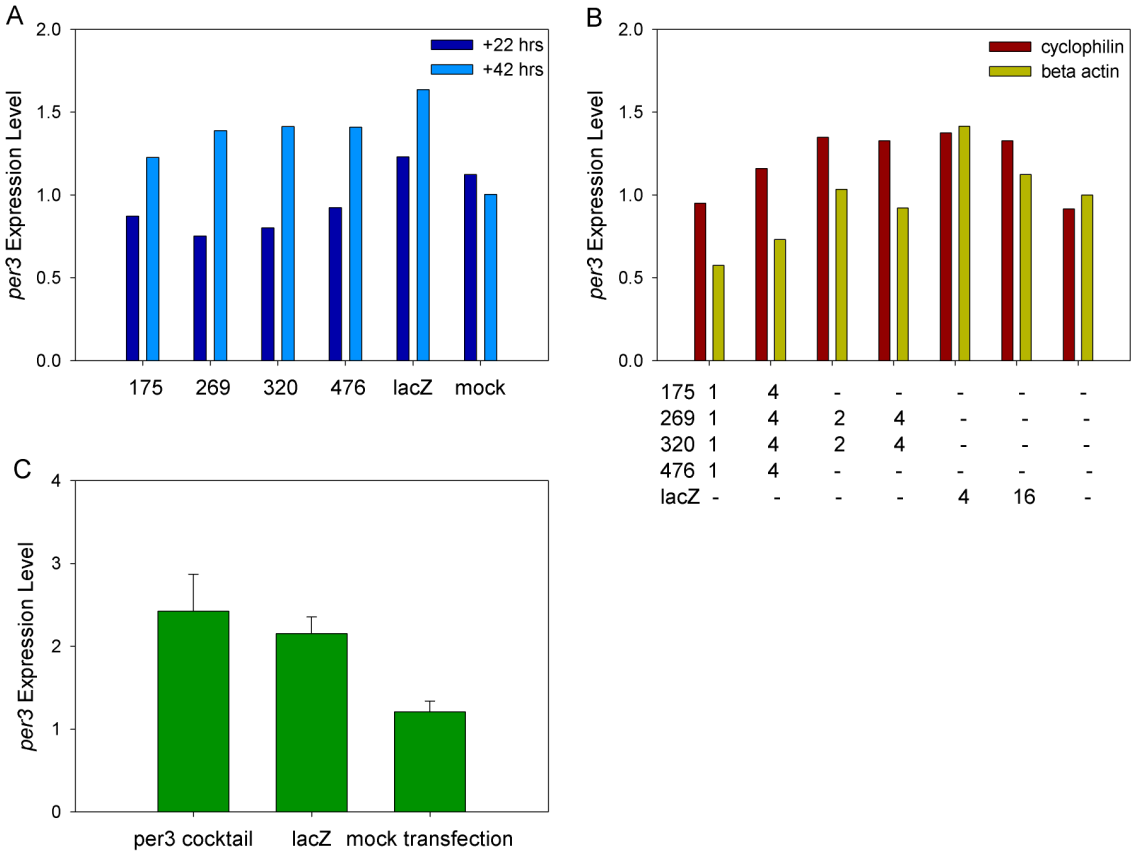

Figure 24. Transient transfection of pinealocytes with per3^{shRNA}. **A**, Chick pinealocyte cultures were transfected with 4 µg plasmid/well containing one of four per3^{shRNA} sequences or lacZ^{shRNA}. Mock transfected cells received only carrier solution for corresponding concentrations of transfected DNA. *Per3* mRNA levels were measured 22 and 42 hours post-transfection. **B**, Pinealocytes were co-transfected with varying concentrations of multiple per3^{shRNA} constructs (in µg/well) or were transfected with lacZ^{shRNA} alone, as indicated below the graph. *Per3* mRNA levels were measured 22 hours post-transfection, and were normalized to *cyclophilin A* and *β-actin*. **C**, N = 6. Pinealocytes were co-transfected with a cocktail containing 1 µg/well each per3^{shRNA} plasmid or with 4 µg/well lacZ^{shRNA}. *Per3* mRNA levels were measured 22 hours post-transfection, and values were normalized to *β-actin*. Mock transfected wells received carrier only.

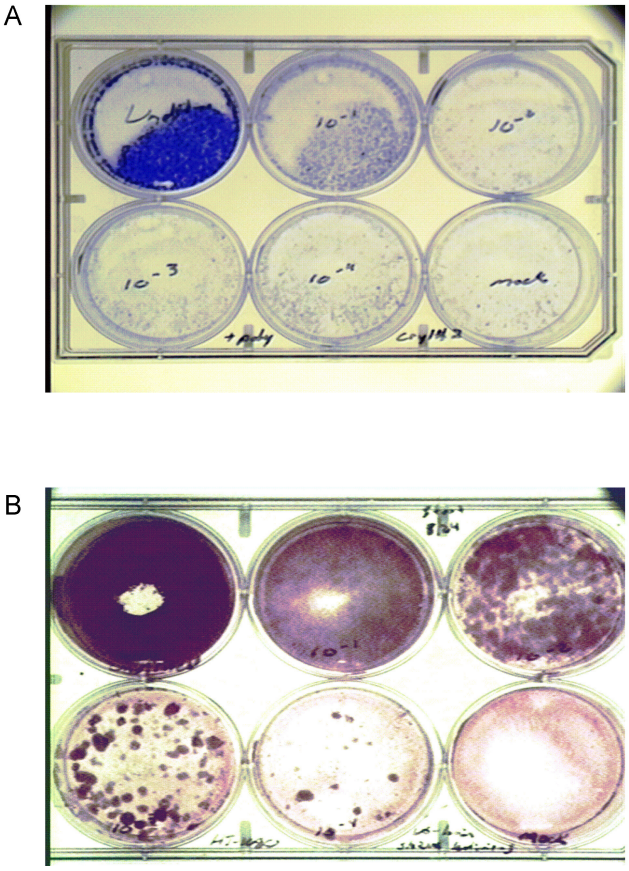

Figure 25. Titering VSV-G lentivirus. Examples of cultures used to titer lentiviral stocks are shown. Cultures of chicken pineal (**A**) or human fibrosarcoma (HT-1080) (**B**) cells were maintained under blasticidin selection (2 and 4 µg/ml, respectively) for 10-14 days and then stained with crystal violet.

vector (pLenti6/BLOCK-iT DEST) using the *Gateway* method from Invitrogen's Lentiviral RNAi Expression System. Positive clones selected for ampicillin resistance and chloramphenicol sensitivity were isolated and propagated for production of lentiviral vectors. To produce VSV-G pseudotyped lentivirus packaged with the shRNA construct of interest, each expression clone encoding shRNA against *cry1* was cotransfected with ViraPower packaging mix into HEK293FT cells using Lipofectamine 2000 reagent (Invitrogen), as recommended in the product user's protocol. We also generated lentiviral vectors containing a pLenti6-GW/U6-lamin^{shRNA} construct provided by Invitrogen, for use as a negative control. Viral supernatant was then collected 48 and 72 hours post-transfection and cryogenically stored until use.

Lentiviral stocks were titered using both pinealocytes and HT-1080 human fibrosarcoma cells. First, kill curves were performed for each cell line to determine minimal lethal blasticidin sensitivity (pinealocytes, 2μg/ml; HT-1080 cells, 4μg/ml). Then, cultures were transduced overnight with serially diluted viral supernatants to confer blasticidin resistance. Cells were washed the next day and maintained in normal growth medium for 10-14 days, until all non-transduced cells were killed. Cells were then stained with crystal violet solution, and titer was measured by determining the number of remaining cell colonies for each dilution of viral supernatant. Because transduced pineal cultures did not yield distinct colonies (see Fig. 25 A), HT-1080 cells were used to determine lentiviral titers (Fig. 25 B; Table 5). Addition of polybrene to culture media did not consistently increase transduction in either cell type, and was therefore not used during RNAi experiments.

Table 5. Lentiviral Titers

Lentiviral stock	+/- Polybrene	Viral Titer (TU/ml)
cry1-423^{shRNA}	-	4.09 x 10^4
cry1-423^{shRNA}	+	1.17 x 10^4
cry1-548^{shRNA}	-	7.63 x 10^3
cry1-548^{shRNA}	+	1.17 x 10^4
hlamin^{shRNA}	-	5.6 x 10^3
hlamin^{shRNA}	+	2 x 10^3

Titers of lentivirus stocks used for RNAi screening are listed. HT-1080 cells were used as the titering cell line in the presence or absence of hexadimethrine bromide (polybrene). TU = transducing units.

Titered lentiviral stocks were used to transduce astrocytes with cry1-423^{shRNA}, cry1-548^{shRNA}, or hlamin^{shRNA} (negative control). Cells were incubated with 10-fold serial dilutions (10^{-1}-10^{-4}) of viral supernatant after diluting volumes to insure equivalent multiplicity of infection (MOI) during transduction. 72 hours post-transduction, cells were harvested into Trizol reagent. Total RNA was extracted, and *cry1* mRNA levels were assayed using quantitative real time RT-PCR. A relative decrease in *cry1* mRNA levels was only observed in cells transduced with undiluted cry1-548^{shRNA} viral supernatant (Fig. 26 B). *Cry1* levels were increased in cells transduced with a 10^{-1} dilution of the same viral stock, relative to hlamin^{shRNA} control. A similar result occurred when transducing cells with cry1-423^{shRNA}, for most dilutions of the viral supernatant, (Fig. 26 A).

In order to determine if *cry1* mRNA could be knocked down in pinealocytes, the experiment was repeated by transducing pineal cultures with undiluted lentiviral stocks for each cry1^{shRNA} construct. Cultures were maintained in an LD, then transduced on

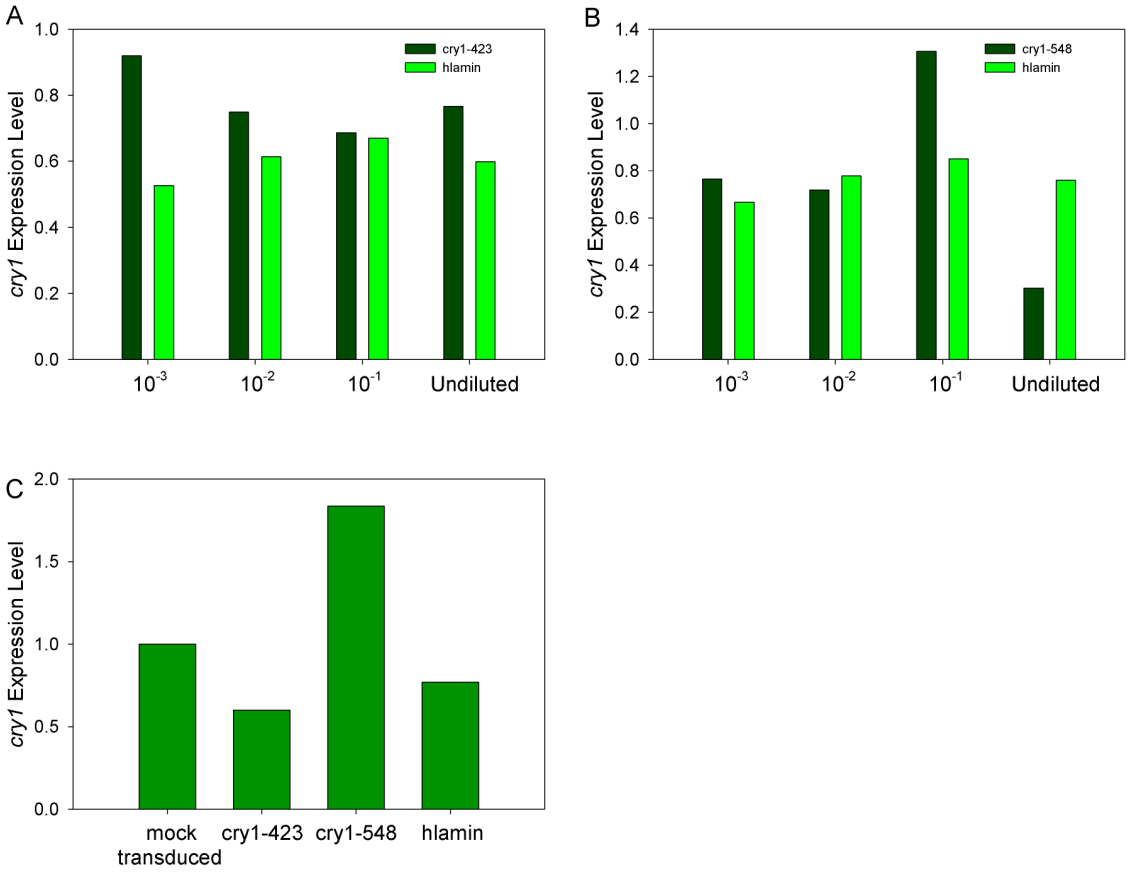

Figure 26. Lentiviral transduction of astrocyte and pineal cultures with cry1^{shRNA}. Chick astrocyte cultures were transduced with serial dilutions of supernatant containing lentivirus packaged hlamin^{shRNA} and cry1-423^{shRNA} (**A**) or cry1-548^{shRNA} (**B**). *Cry1* mRNA levels were measured 72 hours post-transduction. **C**, Pinealocytes were maintained in normal growth medium or were transduced with undiluted lentiviral supernatant containing cry1-423^{shRNA}, cry1-548^{shRNA}, or hlamin^{shRNA}.

day four. RNA has harvested 72 hours later at ZT6, a time when *cry1* mRNA is known to peak in pinealocytes (Chapter II). *Cry1* mRNA levels were reduced by 40% in cells transduced with lentivirus containing cry1-423^{shRNA} relative to mock transduced cells (Fig. 26 C). However, this decrease was <20% compared to cells transduced with hlamin^{shRNA} lentivirus. In contrast to astrocytes, c*ry1* levels were elevated in pineal cells transduced with cry1-548^{shRNA}.

Conclusions

We have not been able to reproducibly knockdown expression of different target genes in either chick pinealocytes or astrocytes. However, we have been reasonably successful in developing multiple methods of gene transfer into these two model cell types. Transient transfection experiments will be a useful method to screen for functional vector based RNAi probes such as shRNA or miRNA. Viral mediated RNAi transduction may prove useful for carrying out genetic knockdown experiments *in vivo*, or in developing stable RNAi expressing cell lines. Currently, work is underway in our laboratory to continue screening RNAi constructs and develop selection protocols to enrich transgenic cell populations in model systems.

APPENDIX C

SUPPLEMENTAL DATA

Supplemental Table 1. Primer Sequences

qPCR Primer	Primer Sequence
Bmal1-F	TTCCCACAGCTTGCAGCTT
Bmal1-R	TTTTGGGCCGCCTTCTC
Cry1-F	CCGGGAAACGCCCAAA
Cry1-R	TGCTCTGCCGCTGGACTT
Cyclophilin-F	GCAAGCAGATCACCATTTCCA
Cyclophilin-R	CGGAATGTCAGGCGTTAAGAC
Cystatin C-F	GAACGACGAGGGCTTGCA
Cystatin C-R	TTATCGTTGCTGGCCCTGTT
HIOMT-F	TGCAGTCAGGACGACCTCTATCT
HIOMT-R	TCCATCCCCATGATGCTTGT
NF1X-F	TGATACCGCCGCCATGTAC
NF1X-R	GCCTCGATGAAGGGATGGA
Per3-F	CAGAATGGAAACGATCAGCCTAT
Per3-R	TCGGGAGAAAACAGGAAGCA
Purpurin-F	TGCTGACATGGCTGCTCAGT
Purpurin-R	CCCTGGTACGTCATGTACATCTT

Supplemental Table 2. Rhythmic Transcripts (t-test analysis)

Clone ID (LD)	ID # (LD)
1609082A aldolase C	cp6394
2',5'-oligo adenylate synthetase A [Gallus gallus]	cp3331
A Chain A, Crystal Structure Of Aluminum-Bound Ovotransferrin At 2.15	cp7685
acetylserotonin O-methyltransferase [Gallus gallus]	cp114; 1553*; 2636*; 3725*; 4873; 5913*; 6149*; 6442; 6496*; 8043*
acyl-Coenzyme A dehydrogenase, long chain [Gallus gallus]	cp5; cp9
ADAM metallopeptidase domain 33 [Gallus gallus]	cp6178
AF199487_1 beta-actin [Anolis carolinensis]	cp156
AF202934_1 myeloid ecotropic viral insertion site-2a protein [Gallus gallus]	cp4705
AF355752_1 reverse transcriptase [Chelonia mydas]	cp1255
AF368030_1 actin [Heliothis virescens]	cp145
AF387865_1 heat shock protein 108 [Gallus gallus]	cp6154
apolipoprotein A-I	cp1249
apolipoprotein A-I [Gallus gallus]	cp340
B lymphocyte induced maturation protein 1 [Takifugu rubripes]	cp4616*

beta actin [Pagrus pagrus]	cp1630
CD74 antigen (invariant polypeptide of major histocompatibility	cp383
CG15021-PA [Drosophila melanogaster]	cp2488
chaperonin containing TCP1, subunit 7 [Gallus gallus]	cp5424
chemokine (C-X-C motif) ligand 14 [Gallus gallus]	cp905
Churchill protein [Gallus gallus]	cp497
Clock 1.1Kb gel pcr	cp8080
clusterin [Gallus gallus]	cp2120
cold inducible RNA binding protein [Gallus gallus]	cp3710
connexin 43 [Gallus gallus]	cp3286
cystatin C [Gallus gallus]	cp13; 147; 3113*; 4568; 7729
cytochrome c oxidase subunit III [Podiceps cristatus]	cp244
cytochrome oxidase subunit I [Gallus gallus]	cp2026
cytochrome oxidase subunit I [Melanoplus marshalli]	cp1974
cytochrome oxidase subunit II [Gallus gallus]	cp1356; 3859
cytochrome oxidase subunit III [Nycticryphes semicollaris]	cp2169
D4 (Per3)	cp8068; 8070
D7 (Cry1)	cp8069
DDX54 protein [Homo sapiens]	cp3752
EF2_CHICK Elongation factor 2 (EF-2)	cp154
ferritin [Coturnix japonica]	cp1156; 625; 772
fibroblast growth factor receptor 1 [Gallus gallus]	cp1204
gammaA-like protocadherin precursor [Gallus gallus]	cp6766
glyceraldehyde-3-phosphate dehydrogenase	cp338
guanine nucleotide binding protein (G protein), beta polypeptide	cp778
hCG2042714 [Homo sapiens]	cp7239
high-mobility group box 1 [Gallus gallus]	cp776
hypothetical protein [Gallus gallus]	cp1164; 1594; 5490
Hypothetical protein CBG17156 [Caenorhabditis briggsae]	cp2401
hypothetical protein DaciDRAFT_2108 [Delftia acidovorans SPH-1]	cp53
hypothetical protein DDBDRAFT_0189484 [Dictyostelium	cp58
hypothetical protein LOC310926 [Rattus norvegicus]	cp150
hypothetical protein LOC379066 [Xenopus laevis]	cp436
hypothetical protein LOC419902 [Gallus gallus]	cp3847
hypothetical protein LOC423668 [Gallus gallus]	cp872
hypothetical protein XP_429509 [Gallus gallus]	cp6715
I Chain I, The Plasmodium Falciparum Cysteine Protease Falcipain-2	cp57
Ig light chain precursor	cp1659
Im:6892314 protein [Danio rerio]	cp3838
immunoglobulin lambda-chain	cp448
integrin beta 1 binding protein 3 [Gallus gallus]	cp1308
invariant chain [Gallus gallus]	cp1547
Jumonji, AT rich interactive domain 1B (RBP2-like) [Gallus gallus]	cp6355
leukotriene A4 hydrolase [Gallus gallus]	cp627
matrix Gla protein [Gallus gallus]	cp344
matrix metalloproteinase 2 [Gallus gallus]	cp629
MHC class I [Gallus gallus]	cp6463
mitochondrial creatine kinase [Gallus gallus]	cp7839

myosin light chain kinase [Gallus gallus]	cp1888
NAD-dependent deacetylase SIRT2 [Gallus gallus]	cp634
NAT	cp8076
NK-lysin [Gallus gallus]	cp43
no chromat	cp100*; 121*; 1250; 1273; 1322; 1442; 1445; 1450; 1478; 1496; 170*; 194; 2; 2114; 290*; 386; 482; 6434; 6554; 6590; 6616*; 674; 6859; 7063; 7090*; 7102; 7650*; 7652; 98*
no hit	cp1012; 1013; 105; 106*; 1063; 1065; 108; 112; 1203; 1206; 1297; 1298; 1332; 1350; 1378; 1404; 146; 15; 1540; 1544; 1586; 1645; 1649; 1702; 1738*; 1755; 1782; 1784; 1795; 1797*; 1815; 1868*; 1900; 1918*; 1921; 1954; 1959; 196; 1973; 200; 202; 203; 2047; 2069; 2071; 2117; 2129*; 2153; 2159*; 2161*; 226; 2269; 2308; 2309; 2310; 2336; 2345; 2351; 2358*; 2363; 2374; 2394; 2405; 241; 2418; 2423*; 246; 250; 2501; 2533*; 2539; 2545; 2552; 2588; 2624*; 2642; 2656*; 2701; 2713; 2776*; 2838; 2840; 2868; 2881; 2896; 2901; 291; 2924; 2961; 297; 3; 3081; 317*; 3205; 3355; 34; 3598; 365; 3716; 3775; 387; 3906; 391; 3918; 392; 396*; 4; 440; 444; 447; 4588*; 4653; 4694; 4717*; 472; 473; 4796; 483; 490; 50; 5140*; 5180*; 52; 5564; 56; 566*; 579; 5812*; 5887*; 5895*; 59; 5950*; 598*; 6128; 6157; 6205; 626; 630; 6309; 6493; 6504; 6517; 6628; 6648; 6652; 6676*; 6693; 677*; 6816; 69; 691*; 6987; 7; 7241; 7243; 7266*; 7280*; 7342; 7344; 7431; 7435; 747; 7519; 7526; 7531; 7536; 7565; 761; 7720; 7722; 7767; 7773; 7788; 779; 7815; 7866*; 7871; 7905; 7957; 7962; 7974; 800; 826; 841; 868; 911*
nuclear factor I-X protein [Gallus gallus]	cp4545*
nucleophosmin 1 [Gallus gallus]	cp536
ORAI calcium release-activated calcium modulator 2 [Gallus gallus]	cp342
pherophorin-dz1 protein [Volvox carteri f. nagariensis]	cp827
polymerase (DNA directed), delta 1, catalytic subunit [Xenopus	cp884
PRB4M_HUMAN Basic salivary proline-rich protein 4 allele M (Salivary	cp5846*
predicted protein [Nematostella vectensis]	cp2659; 3727
PREDICTED: hypothetical protein [Danio rerio]	cp1313
PREDICTED: hypothetical protein [Gallus gallus]	cp1254; 151; 2072; 2942; 3306; 435; 437; 4576*; 4635; 4663; 489; 5764*; 5988; 60; 6371; 728; 8*; 949
PREDICTED: hypothetical protein [Pan troglodytes]	cp148
PREDICTED: hypothetical protein, partial [Strongylocentrotus	cp7238
PREDICTED: similar to 14-3-3 protein gamma subtype; 14-3-3 gamma	cp10
PREDICTED: similar to 16.7Kd protein [Equus caballus]	cp587
PREDICTED: similar to 60S ribosomal protein L7a [Rattus norvegicus]	cp2846
PREDICTED: similar to Aromatic-L-amino-acid decarboxylase (AADC)	cp492

PREDICTED: similar to bactericidal/permeability-increasing	cp152
PREDICTED: similar to Band 4.1-like protein 3 (4.1B)	cp636
PREDICTED: similar to beta-tubulin cofactor E [Gallus gallus]	cp12
PREDICTED: similar to bromodomain containing protein 3 [Gallus	cp1201
PREDICTED: similar to BTB/POZ domain containing protein 6 (Lens BTB	cp2067
PREDICTED: similar to Calponin 3, acidic [Gallus gallus]	cp1158
PREDICTED: similar to carbonic anhydrase III [Gallus gallus]	cp7771
PREDICTED: similar to Carboxypeptidase E precursor (CPE)	cp341
PREDICTED: similar to cathepsin L [Gallus gallus]	cp3834
PREDICTED: similar to Chromosome 18 open reading frame 8 [Gallus	cp699
PREDICTED: similar to Chromosome 2 open reading frame 3 [Gallus	cp1683*
PREDICTED: similar to Crm, cramped-like [Gallus gallus]	cp346
PREDICTED: similar to Ddhd2 protein [Gallus gallus]	cp695
PREDICTED: similar to deleted in malignant brain tumors 1 isoform b	cp2494
PREDICTED: similar to delta-like 1-like protein [Gallus gallus]	cp2022
PREDICTED: similar to delta-sarcoglycan [Gallus gallus]	cp235
PREDICTED: similar to Diacylglycerol O-acyltransferase homolog 2	cp6237
PREDICTED: similar to Dolichyl-diphosphooligosaccharide--protein	cp4549
PREDICTED: similar to early response to neural induction ERNI	cp487
PREDICTED: similar to ectonucleotide	cp2693
PREDICTED: similar to epsilon isoform of 14-3-3 protein	cp8014
PREDICTED: similar to FLJ00258 protein [Gallus gallus]	cp922
PREDICTED: similar to heat shock protein [Monodelphis domestica]	cp1245
PREDICTED: similar to heat shock protein 8 isoform 1 [Apis	cp2021
PREDICTED: similar to hippocalcin isoform 2 [Gallus gallus]	cp7881
PREDICTED: similar to IlvB (bacterial acetolactate synthase)-like,	cp6640*
PREDICTED: similar to kelch-like protein C3IP1 [Ornithorhynchus	cp155
PREDICTED: similar to KIAA1520 splice [Gallus gallus]	cp825
PREDICTED: similar to LOC446973 protein [Gallus gallus]	cp743
PREDICTED: similar to LOC495018 protein	cp1161
PREDICTED: similar to metalloprotease-disintegrin [Gallus gallus]	cp289
PREDICTED: similar to Methionine adenosyltransferase II, beta	cp6520
PREDICTED: similar to MGC108301 protein [Gallus gallus]	cp252*
PREDICTED: similar to MMAC1 [Pan troglodytes]	cp682
PREDICTED: similar to mucin 17 [Rattus norvegicus]	cp6018
PREDICTED: similar to natural killer tumor recognition protein	cp268
PREDICTED: similar to Netrin-G2a [Gallus gallus]	cp751
PREDICTED: similar to P25 protein [Pan troglodytes]	cp102
PREDICTED: similar to PACT [Gallus gallus]	cp292; 298
PREDICTED: similar to Pcmt1-prov protein [Gallus gallus]	cp6242
PREDICTED: similar to phospholipid scramblase PLSCR isoform 2	cp1060; 1064
PREDICTED: similar to PI-3-kinase-related kinase SMG-1 [Gallus	cp7781
PREDICTED: similar to Pla2g3 protein [Monodelphis domestica]	cp7183
PREDICTED: similar to prostacyclin-stimulating factor;	cp51
PREDICTED: similar to Proteasome subunit alpha type 1 (Proteasome	cp719
PREDICTED: similar to Purpurin [Monodelphis domestica]	cp2911*
PREDICTED: similar to putative DNA dependent ATPase and helicase	cp204*
PREDICTED: similar to QN1 orf [Gallus gallus]	cp293

PREDICTED: similar to RAB30 [Monodelphis domestica]	cp914
PREDICTED: similar to rapamycin insensitive companion of mTOR; rictor	cp2658
PREDICTED: similar to REX1, RNA exonuclease 1 homolog (S.	cp320
PREDICTED: similar to ribosomal protein L18 [Equus caballus]	cp201
PREDICTED: similar to ribosomal protein S19 [Pan troglodytes]	cp339
PREDICTED: similar to ribosomal protein S7 isoform 6 [Gallus	cp242
PREDICTED: similar to Sorting and assembly machinery component 50	cp680
PREDICTED: similar to synaptotagmin XV-a [Monodelphis domestica]	cp11
PREDICTED: similar to TCF7L2 [Gallus gallus]	cp101; 107
PREDICTED: similar to TECT2 [Macaca mulatta]	cp7796
PREDICTED: similar to Tetratricopeptide repeat domain 25 [Danio	cp964
PREDICTED: similar to thioredoxin-like [Gallus gallus]	cp1010
PREDICTED: similar to transducin gamma subunit [Monodelphis	cp655
PREDICTED: similar to tumor protein p53 binding protein, 2 [Gallus	cp247
PREDICTED: similar to UDP-GalNAc:betaGlcNAc beta	cp7769
PREDICTED: similar to uKATP-1 [Gallus gallus]	cp1685
PREDICTED: similar to Uridine phosphorylase 1 [Gallus gallus]	cp1024
progestin and adipoQ receptor family member IX [Homo sapiens]	cp2135*
proline-rich protein 15, isoform CRA_a [Rattus norvegicus]	cp592*
protein kinase, cAMP-dependent, regulatory, type I, alpha (tissue	cp248
protocadherin gamma subfamily C, 3 [Gallus gallus]	cp1153
purpurin [Gallus gallus]	cp1559*; 2271*; 2612*
putative enzyme [Shigella flexneri 5 str. 8401]	cp564
R3 (BMal1)	cp8074*
rCG40478, isoform CRA_j [Rattus norvegicus]	cp438
retinol binding protein 3, interstitial [Gallus gallus]	cp49
ribosomal protein S3A, isoform CRA_g [Homo sapiens]	cp54
ribosomal protein S4, X-linked [Gallus gallus]	cp353
secreted protein, acidic, cysteine-rich (osteonectin) [Gallus	cp1067
sorting nexin 6 [Gallus gallus]	cp6298
Syntenin	cp1014
tec protein tyrosine kinase [Gallus gallus]	cp1258
TR5H_CHICK Tryptophan 5-monooxygenase	cp3412*; 425*; 5106; 5886*; 600*; 6090; 643*; 723: 736*
transthyretin [Gallus gallus]	cp1; 1113; 149; 236; 5824; 628; 632; 954
tumor differentially expressed 2 [Gallus gallus]	cp97
ubiquitin [Oreochromis mossambicus]	cp2691
Unknown (protein for IMAGE:8415934) [Bos taurus]	cp249
Unknown (protein for MGC:166416) [Bos taurus]	cp7961
unknown [Schistosoma japonicum]	cp6187
unnamed protein product [Mus musculus]	cp295
unnamed protein product [Tetraodon nigroviridis]	cp1089*
Y-Box binding protein	cp484
Ymf77 [Tetrahymena paravorax]	cp296

Clone ID (DD)	ID # (DD)
2',3'-cyclic nucleotide 3' phosphodiesterase [Gallus gallus]	cp1155
acetylserotonin O-methyltransferase [Gallus gallus]	cp8043
acyl-Coenzyme A dehydrogenase, long chain [Gallus gallus]	cp5
adenosine deaminase [Gallus gallus]	cp3343
AF110987_1 proline-rich protein 3 [Arabidopsis thaliana]	cp2684
AF368030_1 actin [Heliothis virescens]	cp145
apolipoprotein A-I	cp1249; 2218
apolipoprotein A-I [Gallus gallus]	cp3251; 340*; 3706; 5903
arylalkylamine N-acetyltransferase [Gallus gallus]	cp855
ATP6_10016 ATP synthase F0 subunit 6 [Gallus gallus]	cp7725
BUD13 homolog [Gallus gallus]	cp286
capping protein (actin filament) muscle Z-line, alpha 2 [Gallus	cp6270
CDC-like kinase 3 [Gallus gallus]	cp3356
chromosome 3 open reading frame 9 [Gallus gallus]	cp6216
CIC2_RABIT Dihydropyridine-sensitive L-type	cp1803
claudin 3 [Gallus gallus]	cp4553
Clock (full)	cp8083
clusterin [Gallus gallus]	cp2120
coatomer protein complex, subunit gamma [Gallus gallus]	cp7237
cognin/prolyl-4-hydroxylase/protein disulfide isomerase [Gallus	cp55
COX1_15261 cytochrome c oxidase subunit I [Talpa europaea]	cp1077
CSPG5_CHICK Chondroitin sulfate proteoglycan 5 precursor (Acidic leucine-rich	cp3663
cystatin C [Gallus gallus]	cp13; 147
cytochrome c oxidase subunit III [Podiceps cristatus]	cp244
DB7	cp8065
dCMP deaminase [Gallus gallus]	cp5056
DDX54 protein [Homo sapiens]	cp3752
DEAD (Asp-Glu-Ala-Asp) box polypeptide 5 [Gallus gallus]	cp1595
DnaJ (Hsp40) homolog, subfamily C, member 3 [Gallus gallus]	cp3125
eukaryotic translation elongation factor 2 [Gallus gallus]	cp6767
ferritin [Coturnix japonica]	cp1156
gammaA-like protocadherin precursor [Gallus gallus]	cp6766*
glutathione S-transferase A3 [Gallus gallus]	cp7778
glycine dehydrogenase (decarboxylating) [Gallus gallus]	cp47
gtpase_rho [Aedes aegypti]	cp153
gustatory receptor candidate 19 [Tribolium castaneum]	cp1231
hCG2042714 [Homo sapiens]	cp7239*
hypothetical protein [Gallus gallus]	cp279; 539; 5490
hypothetical protein [Yarrowia lipolytica]	cp7578*
hypothetical protein BURPS1710b_A0534 [Burkholderia pseudomallei	cp1437
hypothetical protein DaciDRAFT_2108 [Delftia acidovorans SPH-1]	cp53*
hypothetical protein DDBDRAFT_0189484 [Dictyostelium	cp58
hypothetical protein EhV364 [Emiliania huxleyi virus 86]	cp6457*
hypothetical protein LOC310926 [Rattus norvegicus]	cp150
hypothetical protein Mflv_4674 [Mycobacterium gilvum PYR-GCK]	cp189
hypothetical protein Strop_1450 [Salinispora tropica CNB-440]	cp1331

I Chain I, The Plasmodium Falciparum Cysteine Protease Falcipain-2	cp57
immunoglobulin lambda-chain	cp448
JC1348 hypothetical 18K protein - goldfish mitochondrion	cp7576
karyopherin (importin) beta 1 [Danio rerio]	cp1328
matrix Gla protein [Gallus gallus]	cp344
mitochondrial creatine kinase [Gallus gallus]	cp1392; 7839
NADH dehydrogenase (ubiquinone) flavoprotein 1, 51kDa [Gallus	cp6401
NADH dehydrogenase subunit 4 [Gallus gallus]	cp282
ND4_10016 NADH dehydrogenase subunit 4 [Gallus gallus]	cp2258
NK-lysin [Gallus gallus]	cp37; 43
no chromat	cp100; 1034; 1445; 1458; 1466; 1849; 2; 25; 290; 4298; 458; 6616*; 6858; 6863; 6889; 6903; 697*; 7049; 7051; 7055; 7063; 7090; 7099; 7101; 7650; 98
no hit	cp1012; 106; 1063; 1065; 108; 1203; 146; 15*; 1537; 1645; 1649; 1686; 17; 1711*; 1713*; 1783; 1797; 1807; 1959*; 1977; 1979; 1988; 202; 203; 2069; 2088*; 2129; 2146; 2309; 2405; 2406; 2407; 246; 250; 2504; 2513; 2539; 2540; 2558; 2621; 2624; 2656; 2683; 2696; 273; 2749; 2797; 2838; 2851; 2879; 2881; 2896; 2921; 2933; 2961; 3; 3079; 3081; 3285; 348; 3716; 4; 4230*; 4243; 4379; 443; 4531; 4688; 4699; 470; 4717; 490; 50; 5197; 52*; 532; 535; 5380; 553; 56*; 577; 5812; 583; 586; 598; 6128; 6172*; 6191; 6193; 6231; 6417; 6472; 6628; 6664; 6669; 679; 69; 691; 6977; 6987; 7; 7195; 7241; 7243; 7245; 7266; 7280; 729; 7329; 7367; 7375*; 7431*; 7435; 7437; 7484; 7503; 758; 7584; 7615; 7640; 7740; 7768; 7779*; 779; 7815; 7822; 7878; 7892; 7960; 7962; 7976*; 8005; 8013; 816; 826; 885; 960
nuclear factor I-X protein [Gallus gallus]	cp4545
ORAI calcium release-activated calcium modulator 2 [Gallus gallus]	cp342
peptidyl arginine deiminase, type III [Gallus gallus]	cp7743
pherophorin-dz1 protein [Volvox carteri f. nagariensis]	cp827
platelet-derived growth factor beta polypeptide [Gallus gallus]	cp7956
predicted adhesin [Escherichia coli K12]	cp5419
PREDICTED: hypothetical protein [Gallus gallus]	cp1261*; 151; 2027; 245; 380; 489; 5554; 567*; 5764; 60; 668; 8
PREDICTED: hypothetical protein [Pan troglodytes]	cp148
PREDICTED: hypothetical protein [Rattus norvegicus]	cp969
PREDICTED: hypothetical protein, partial [Strongylocentrotus	cp7238
PREDICTED: similar to bactericidal/permeability-increasing	cp152
PREDICTED: similar to carbonic anhydrase III [Gallus gallus]	cp7771
PREDICTED: similar to Centaurin, beta 5 [Gallus gallus]	cp780
PREDICTED: similar to CG13731-PA [Homo sapiens]	cp2577
PREDICTED: similar to Chromosome 2 open reading frame 3 [Gallus	cp3424
PREDICTED: similar to Crm, cramped-like [Gallus gallus]	cp346

PREDICTED: similar to delta-like 1-like protein [Gallus gallus]	cp2022
PREDICTED: similar to echinoderm microtubule associated protein	cp2085*
PREDICTED: similar to ectonucleotide	cp2693
PREDICTED: similar to epsilon isoform of 14-3-3 protein	cp8014
PREDICTED: similar to Eukaryotic translation initiation factor	cp139
PREDICTED: similar to glycine receptor alpha 3 subunit [Gallus	cp3203
PREDICTED: similar to kelch-like protein C3IP1 [Ornithorhynchus	cp155
PREDICTED: similar to KIAA1520 splice [Gallus gallus]	cp825
PREDICTED: similar to KIAA1576 protein [Gallus gallus]	cp1162*
PREDICTED: similar to LOC495018 protein	cp1161
PREDICTED: similar to LOC495018 protein [Gallus gallus]	cp6625
PREDICTED: similar to MGC108301 protein [Gallus gallus]	cp252
PREDICTED: similar to Mrps34-prov protein [Gallus gallus]	cp684*
PREDICTED: similar to natural killer cell enhancing factor isoform	cp873
PREDICTED: similar to nucleoside diphosphate kinase [Gallus gallus]	cp103
PREDICTED: similar to P25 protein [Pan troglodytes]	cp102
PREDICTED: similar to P2X7 receptor subunit [Gallus gallus]	cp5058
PREDICTED: similar to PACT [Gallus gallus]	cp298
PREDICTED: similar to Pcmt1-prov protein [Gallus gallus]	cp6242
PREDICTED: similar to Peroxisome proliferator-activated	cp6406
PREDICTED: similar to phospholipid scramblase PLSCR isoform 2	cp1064
PREDICTED: similar to prostacyclin-stimulating factor;	cp51
PREDICTED: similar to Prostaglandin F2 receptor negative regulator	cp725
PREDICTED: similar to Purpurin [Monodelphis domestica]	cp2911
PREDICTED: similar to putative DNA dependent ATPase and helicase	cp204
PREDICTED: similar to QN1 orf [Gallus gallus]	cp299
PREDICTED: similar to RAB30 [Monodelphis domestica]	cp920
PREDICTED: similar to retinal fascin [Monodelphis domestica]	cp237
PREDICTED: similar to ribosomal protein L18 [Equus caballus]	cp201
PREDICTED: similar to Ribosomal protein S6 [Pan troglodytes]	cp7916
PREDICTED: similar to RNA polymerase-associated protein RTF1	cp1593
PREDICTED: similar to Rps21-prov protein [Gallus gallus]	cp4998
PREDICTED: similar to Strawberry notch homolog 1 (Drosophila)	cp2477
PREDICTED: similar to synaptotagmin XV-a [Monodelphis domestica]	cp11
PREDICTED: similar to TCF7L2 [Gallus gallus]	cp101; 107
PREDICTED: similar to tetratricopeptide repeat domain 19 [Gallus	cp1718
PREDICTED: similar to TGF-beta inducible early protein [Gallus	cp1099
PREDICTED: similar to UDP-GalNAc:betaGlcNAc beta	cp7769
PREDICTED: similar to WD repeat and FYVE domain containing 3	cp5803
PREDICTED: similar to zinc finger protein 792 [Ornithorhynchus	cp6358
proline-rich protein 15, isoform CRA_a [Rattus norvegicus]	cp592
prostaglandin H2 D-isomerase [Gallus gallus]	cp395
protein kinase, cAMP-dependent, regulatory, type I, alpha (tissue	cp248; 4675
protocadherin gamma subfamily C, 3 [Gallus gallus]	cp1153
purpurin [Gallus gallus]	cp1559; 2271; 2612
rCG40478, isoform CRA_j [Rattus norvegicus]	cp438
rCG40478, isoform CRA_m [Rattus norvegicus]	cp442
rCG59085, isoform CRA_b [Rattus norvegicus]	cp708

multiple coagulation factor deficiency 2 [Gallus gallus]	cp921
RH71862p [Drosophila melanogaster]	cp2065
ribosomal protein S3A, isoform CRA_g [Homo sapiens]	cp54
RuvB-like 1 [Gallus gallus]	cp828
secreted frizzled-related protein 1 [Gallus gallus]	cp193
secreted protein, acidic, cysteine-rich (osteonectin) [Gallus	cp1067
similar to 40S ribosomal protein S2 [Gallus gallus]	cp6225
syndecan 3 [Gallus gallus]	cp1386
transthyretin [Gallus gallus]	cp1*; 1032; 1113; 1198; 1338*; 149; 1948; 236*; 38*; 533; 6311; 953
twinfilin-like protein [Gallus gallus]	cp1912
ubiquitin [Oreochromis mossambicus]	cp2691
ubiquitin C [Homo sapiens]	cp195
unknown [Gallus gallus]	cp7900
unnamed protein product [Homo sapiens]	cp345
unnamed protein product [Mus musculus]	cp324
unnamed protein product [Tetraodon nigroviridis]	cp1089; 2293
WAS/WASL interacting protein family, member 1 [Gallus gallus]	cp6807

* Indicates ≥ 2-fold rhythm amplitude

Supplemental Table 3. Rhythmic Transcripts (ANOVA)

Clone ID (LD)	ID # (LD)
1609082A aldolase C	cp6394
2',5'-oligo adenylate synthetase A [Gallus gallus]	cp3331
A Chain A, Crystal Structure Of Aluminum-Bound Ovotransferrin At 2.15	cp7685
acetylserotonin O-methyltransferase [Gallus gallus]	cp114; 1553*; 2636*; 3725*; 4873; 5913*; 6442; 6496*; 8043*
actin related protein 2/3 complex subunit 5 [Gallus gallus]	cp6232
AF202934_1 myeloid ecotropic viral insertion site-2a protein [Gallus gallus]	cp4705
B lymphocyte induced maturation protein 1 [Takifugu rubripes]	cp4616*
beta actin [Pagrus pagrus]	cp1630
chaperonin containing TCP1, subunit 7 [Gallus gallus]	cp5424
cold inducible RNA binding protein [Gallus gallus]	cp3710
cystatin C [Gallus gallus]	cp3113*; 4568
cytochrome c oxidase subunit III [Podiceps cristatus]	cp244
cytochrome oxidase subunit II [Gallus gallus]	cp3859
D4 (Per3)	cp8068; 8070
D7 (Cry1)	cp8069
F-box only protein 22 [Gallus gallus]	cp1107*
hypothetical protein [Gallus gallus]	cp1164; 5490
hypothetical protein DDBDRAFT_0189484 [Dictyostelium	cp58
hypothetical protein LOC379066 [Xenopus laevis]	cp436

hypothetical protein LOC419902 [Gallus gallus]	cp3847
hypothetical protein M446DRAFT_3515 [Methylobacterium sp. 4-46]	cp2611*
hypothetical protein XP_429509 [Gallus gallus]	cp6715
invariant chain [Gallus gallus]	cp1547
no chromat	cp100*; 121*; 1250; 1273*; 1442; 1478; 1496; 1506; 170*; 290*; 386; 6554; 6616*; 7090*; 7102; 7225*; 7650*; 7652
no hit	cp112; 1332; 1378; 1645; 1702; 1728; 1738*; 1787*; 1797*; 1807; 1918*; 1968; 2129*; 2149*; 2245; 226; 2358*; 2363; 2423*; 246; 2624*; 2656*; 2701; 2729; 2901; 2961; 317*; 3192; 3355; 34; 3598; 3716; 3775; 3906; 3918; 440; 4588*; 4653; 4717*; 4796; 490; 5140*; 5180*; 5564; 5565; 56; 5812*; 5887*; 5895*; 5950*; 598*; 606; 6159; 6197; 626; 630; 6392*; 6412*; 6504; 6628; 6652; 6676*; 678; 6816; 69*; 691*; 6948; 7266*; 7280; 7519; 7866*; 903*; 911*
nuclear factor I-X protein [Gallus gallus]	cp4545*
PRB4M_HUMAN Basic salivary proline-rich protein 4 allele M (Salivary	cp5846*
predicted protein [Nematostella vectensis]	cp2659
PREDICTED: hypothetical protein [Danio rerio]	cp1313
PREDICTED: hypothetical protein [Gallus gallus]	cp1052; 1254; 1261; 4576*; 5764*
PREDICTED: similar to 14-3-3 protein gamma subtype; 14-3-3 gamma	cp10
PREDICTED: similar to 60S ribosomal protein L7a [Rattus norvegicus]	cp2846
PREDICTED: similar to beta-tubulin cofactor E [Gallus gallus]	cp12
PREDICTED: similar to Calponin 3, acidic [Gallus gallus]	cp1158
PREDICTED: similar to Ddhd2 protein [Gallus gallus]	cp695
PREDICTED: similar to Dolichyl-diphosphooligosaccharide--protein	cp4549
PREDICTED: similar to early response to neural induction ERNI	cp487
PREDICTED: similar to hippocalcin isoform 2 [Gallus gallus]	cp7881
PREDICTED: similar to IlvB (bacterial acetolactate synthase)-like,	cp6640*
PREDICTED: similar to KIAA1607 protein, partial [Ornithorhynchus	cp6267*
PREDICTED: similar to LOC129293 protein [Bos taurus]	cp2717*
PREDICTED: similar to LOC446973 protein [Gallus gallus]	cp743
PREDICTED: similar to MGC108301 protein [Gallus gallus]	cp252*
PREDICTED: similar to mucin 17 [Rattus norvegicus]	cp6018
PREDICTED: similar to natural killer cell enhancing factor isoform	cp867*
PREDICTED: similar to Pcmt1-prov protein [Gallus gallus]	cp6242
PREDICTED: similar to phospholipid scramblase PLSCR isoform 2	cp1060
PREDICTED: similar to PI-3-kinase-related kinase SMG-1 [Gallus	cp7781
PREDICTED: similar to Pla2g3 protein [Monodelphis domestica]	cp6212*; 7183
PREDICTED: similar to P-Rex1 protein [Gallus gallus]	cp1641
PREDICTED: similar to Purpurin [Monodelphis domestica]	cp2911*
PREDICTED: similar to putative DNA dependent ATPase and helicase	cp204*
PREDICTED: similar to RAB30 [Monodelphis domestica]	cp914
PREDICTED: similar to ribosomal protein S7 isoform 6 [Gallus	cp242
PREDICTED: similar to thioredoxin-like [Gallus gallus]	cp1010
progestin and adipoQ receptor family member IX [Homo sapiens]	cp2135*

proline-rich protein 15, isoform CRA_a [Rattus norvegicus]	cp592*
protein kinase, cAMP-dependent, regulatory, type I, alpha (tissue	cp248
purpurin [Gallus gallus]	cp1559*; 2271*; 2612*
R3 (BMal1)	cp8074*
rCG40478, isoform CRA_j [Rattus norvegicus]	cp438
ribosomal protein S3A, isoform CRA_g [Homo sapiens]	cp54
ribosomal protein S4, X-linked [Gallus gallus]	cp353
stathmin-like 2 [Gallus gallus]	cp1103*
tec protein tyrosine kinase [Gallus gallus]	cp1258
Tim	cp8079
TR5H_CHICK Tryptophan 5-monooxygenase	cp3412*; 425*; 5106; 5886*; 600*; 6090; 643*; 736*
transthyretin [Gallus gallus]	cp503; 5824; 628; 632; 953*
unnamed protein product [Tetraodon nigroviridis]	cp1089*

Clone ID (DD)	**ID # (DD)**
2',3'-cyclic nucleotide 3' phosphodiesterase [Gallus gallus]	cp1155
acetylserotonin O-methyltransferase [Gallus gallus]	cp1553; 1557; 5913
Actin R2	cp8067*
AF110987_1 proline-rich protein 3 [Arabidopsis thaliana]	cp2684
AF403117_1 adenosine deaminase [Gallus gallus]	cp6165
apolipoprotein A-I [Gallus gallus]	cp3706
BUD13 homolog [Gallus gallus]	cp286
capping protein (actin filament) muscle Z-line, alpha 2 [Gallus	cp6270
claudin 3 [Gallus gallus]	cp4553
Clock (full)	cp8083
coagulation factor XIII, A1 polypeptide [Gallus gallus]	cp6293*
cytochrome oxidase subunit 1 [Equus caballus]	cp1118*
cytochrome P450	cp1122*
EPHB3_CHICK Ephrin type-B receptor 3 (Tyrosine-protein kinase receptor CEK10)	cp347
gammaA-like protocadherin precursor [Gallus gallus]	cp6766*
hypothetical protein [Yarrowia lipolytica]	cp7578*
hypothetical protein DaciDRAFT_2108 [Delftia acidovorans SPH-1]	cp2495*
hypothetical protein Strop_1450 [Salinispora tropica CNB-440]	cp1331
immunoglobulin lambda-chain	cp448
JC1348 hypothetical 18K protein - goldfish mitochondrion	cp7576
karyopherin (importin) beta 1 [Danio rerio]	cp1328
mitochondrial creatine kinase [Gallus gallus]	cp7839
no chromat	cp1034; 1454*; 1458; 1849; 6863; 6903; 7051; 7063; 7099; 7101; 7650
no hit	cp1284*; 15*; 1645; 1680*; 17; 1728*; 1854*; 1993; 2029; 2121; 2146; 2172; 2242*; 2296; 2416*; 2446; 2540; 2552; 2624; 2656; 2696; 2749; 2869; 2933; 2961; 397; 4717; 535; 5812; 598; 6155*; 6288; 6393*; 69; 6977; 6987; 7002; 7241; 7245; 7367; 7437; 7905; 837

nuclear factor I-X protein [Gallus gallus]	cp4545
PREDICTED: hypothetical protein [Gallus gallus]	cp4378*; 489; 5764
PREDICTED: similar to Ddhd2 protein [Gallus gallus]	cp695
PREDICTED: similar to High density lipoprotein (HDL) binding protein	cp6271
PREDICTED: similar to isoleucyl-tRNA synthetase [Gallus gallus]	cp210
PREDICTED: similar to KIAA1018 protein [Gallus gallus]	cp267
PREDICTED: similar to L-3-hydroxyacyl-Coenzyme A dehydrogenase	cp6265
PREDICTED: similar to mucin 17 [Rattus norvegicus]	cp6018*
PREDICTED: similar to Pddc1 protein isoform 2 [Gallus gallus]	cp356
PREDICTED: similar to retinal fascin [Monodelphis domestica]	cp237
PREDICTED: similar to Rps21-prov protein [Gallus gallus]	cp4998
PREDICTED: similar to WD repeat and FYVE domain containing 3	cp5803
prostaglandin H2 D-isomerase [Gallus gallus]	cp6344*
protein disulfide isomerase-associated 3 precursor [Gallus gallus]	cp4311
purpurin [Gallus gallus]	cp1559; 2271; 2612
secreted protein, acidic, cysteine-rich (osteonectin) [Gallus	cp1067
sirtuin [Gallus gallus]	cp1889
syndecan 3 [Gallus gallus]	cp1386
transthyretin [Gallus gallus]	cp1338*; 2473; 4617*; 953
twinfilin-like protein [Gallus gallus]	cp1912
ubiquitin-conjugating enzyme E2G 1 (UBC7 homolog, yeast), isoform	cp4317
unnamed protein product [Gallus gallus]	cp2596
unnamed protein product [Tetraodon nigroviridis]	cp1089

* Indicates ≥ 2-fold rhythm amplitude

Supplemental Table 4. Functional Clustering

Clone ID (LD)	Functional Cluster
1609082A aldolase C	R
2',5'-oligo adenylate synthetase A [Gallus gallus]	A
A Chain A, Crystal Structure Of Aluminum-Bound Ovotransferrin At 2.15	H
acetylserotonin O-methyltransferase [Gallus gallus]	C
acyl-Coenzyme A dehydrogenase, long chain [Gallus gallus]	A
ADAM metallopeptidase domain 33 [Gallus gallus]	R
AF199487_1 beta-actin [Anolis carolinensis]	I
AF202934_1 myeloid ecotropic viral insertion site-2a protein [Gallus gallus]	E
AF355752_1 reverse transcriptase [Chelonia mydas]	T
AF368030_1 actin [Heliothis virescens]	I
AF387865_1 heat shock protein 108 [Gallus gallus]	P
apolipoprotein A-I	H
apolipoprotein A-I [Gallus gallus]	H
ATP-binding cassette, sub-family B,	H
B lymphocyte induced maturation protein 1 [Takifugu rubripes]	B
beta actin [Pagrus pagrus]	I

CD74 antigen (invariant polypeptide of major histocompatibility	P
CG15021-PA [Drosophila melanogaster]	U
chaperonin containing TCP1, subunit 7 [Gallus gallus]	P
chemokine (C-X-C motif) ligand 14 [Gallus gallus]	P
Churchill protein [Gallus gallus]	B
clusterin [Gallus gallus]	B
cold inducible RNA binding protein [Gallus gallus]	P
connexin 43 [Gallus gallus]	K
cystatin C [Gallus gallus]	R
cytochrome c oxidase subunit III [Podiceps cristatus]	A
cytochrome oxidase subunit I [Gallus gallus]	A
cytochrome oxidase subunit I [Melanoplus marshalli]	A
cytochrome oxidase subunit II [Gallus gallus]	A
cytochrome oxidase subunit III [Nycticryphes semicollaris]	A
DDX54 protein [Homo sapiens]	L
eukaryotic translation elongation factor 2 [Gallus gallus]	O
ferritin [Coturnix japonica]	T
fibroblast growth factor receptor 1 [Gallus gallus]	F
g BMal1	M
g Clock 1.1Kb gel pcr	M
g Cry1	M
g Per3	M
glyceraldehyde-3-phosphate dehydrogenase	A
guanine nucleotide binding protein (G protein), beta polypeptide	S
hCG2042714 [Homo sapiens]	U
high-mobility group box 1 [Gallus gallus]	F
hypothetical protein [Gallus gallus] cp1164	U
hypothetical protein [Gallus gallus] cp1594	U
Hypothetical protein CBG17156 [Caenorhabditis briggsae]	U
hypothetical protein DaciDRAFT_2108 [Delftia acidovorans SPH-1]	U
hypothetical protein DDBDRAFT_0189484 [Dictyostelium	U
hypothetical protein LOC310926 [Rattus norvegicus]	U
hypothetical protein LOC379066 [Xenopus laevis]	U
hypothetical protein LOC419902 [Gallus gallus]	U
hypothetical protein LOC423668 [Gallus gallus]	F
hypothetical protein Strop_1450 [Salinispora tropica CNB-440]	U
I Chain I, The Plasmodium Falciparum Cysteine Protease Falcipain-2	R
Ig light chain precursor	P
Im:6892314 protein [Danio rerio]	R
immunoglobulin lambda-chain	P
integrin beta 1 binding protein 3 [Gallus gallus]	A
invariant chain [Gallus gallus]	P
Jumonji, AT rich interactive domain 1B (RBP2-like) [Gallus gallus]	Q
leukotriene A4 hydrolase [Gallus gallus]	U
matrix Gla protein [Gallus gallus]	P
matrix metalloproteinase 2 [Gallus gallus]	U
MHC class I [Gallus gallus]	P
mitochondrial creatine kinase [Gallus gallus]	J

myosin light chain kinase [Gallus gallus]	I
NAD-dependent deacetylase SIRT2 [Gallus gallus]	U
NAT	C
NK-lysin [Gallus gallus]	P
nuclear factor I-X protein [Gallus gallus]	Q
nucleophosmin 1 [Gallus gallus]	T
ORAI calcium release-activated calcium modulator 2 [Gallus gallus]	J
pherophorin-dz1 protein [Volvox carteri f. nagariensis]	U
polymerase (DNA directed), delta 1, catalytic subunit [Xenopus	T
predicted protein [Nematostella vectensis] cp2659	U
predicted protein [Nematostella vectensis] cp3727	U
PREDICTED: hypothetical protein [Danio rerio] cp1313	U
PREDICTED: hypothetical protein [Gallus gallus] cp1254	U
PREDICTED: hypothetical protein [Gallus gallus] cp151	U
PREDICTED: hypothetical protein [Gallus gallus] cp2072	U
PREDICTED: hypothetical protein [Gallus gallus] cp2942	U
PREDICTED: hypothetical protein [Gallus gallus] cp3306	U
PREDICTED: hypothetical protein [Gallus gallus] cp435	U
PREDICTED: hypothetical protein [Gallus gallus] cp437	U
PREDICTED: hypothetical protein [Gallus gallus] cp4576	U
PREDICTED: hypothetical protein [Gallus gallus] cp4635	U
PREDICTED: hypothetical protein [Gallus gallus] cp4663	U
PREDICTED: hypothetical protein [Gallus gallus] cp489; cp949	U
PREDICTED: hypothetical protein [Gallus gallus] cp5764	U
PREDICTED: hypothetical protein [Gallus gallus] cp5988	U
PREDICTED: hypothetical protein [Gallus gallus] cp60	U
PREDICTED: hypothetical protein [Gallus gallus] cp6371	U
PREDICTED: hypothetical protein [Gallus gallus] cp728	U
PREDICTED: hypothetical protein [Gallus gallus] cp8	U
PREDICTED: hypothetical protein [Pan troglodytes] cp148	U
PREDICTED: hypothetical protein, partial [Strongylocentrotus	U
PREDICTED: similar to 14-3-3 protein gamma subtype; 14-3-3 gamma	J
PREDICTED: similar to 16.7Kd protein [Equus caballus]	U
PREDICTED: similar to 60S ribosomal protein L7a [Rattus norvegicus]	O
PREDICTED: similar to Aromatic-L-amino-acid decarboxylase (AADC)	C
PREDICTED: similar to bactericidal/permeability-increasing	P
PREDICTED: similar to Band 4.1-like protein 3 (4.1B)	U
PREDICTED: similar to beta-tubulin cofactor E [Gallus gallus]	I
PREDICTED: similar to bromodomain containing protein 3 [Gallus	T
PREDICTED: similar to BTB/POZ domain containing protein 6 (Lens BTB	T
PREDICTED: similar to Calponin 3, acidic [Gallus gallus]	I
PREDICTED: similar to carbonic anhydrase III [Gallus gallus]	H
PREDICTED: similar to Carboxypeptidase E precursor (CPE)	R
PREDICTED: similar to cathepsin L [Gallus gallus]	R
PREDICTED: similar to Chromosome 18 open reading frame 8 [Gallus	E
PREDICTED: similar to Chromosome 2 open reading frame 3 [Gallus	U
PREDICTED: similar to Crm, cramped-like [Gallus gallus]	T
PREDICTED: similar to Ddhd2 protein [Gallus gallus]	J

PREDICTED: similar to deleted in malignant brain tumors 1 isoform b	S
PREDICTED: similar to delta-like 1-like protein [Gallus gallus]	U
PREDICTED: similar to delta-sarcoglycan [Gallus gallus]	I
PREDICTED: similar to Diacylglycerol O-acyltransferase homolog 2	A
PREDICTED: similar to Dolichyl-diphosphooligosaccharide--protein	R
PREDICTED: similar to early response to neural induction ERNI	D
PREDICTED: similar to ectonucleotide	J
PREDICTED: similar to FLJ00258 protein [Gallus gallus]	U
PREDICTED: similar to heat shock protein [Monodelphis domestica]	P
PREDICTED: similar to heat shock protein 8 isoform 1 [Apis	P
PREDICTED: similar to hippocalcin isoform 2 [Gallus gallus]	J
PREDICTED: similar to IlvB (bacterial acetolactate synthase)-like,	A
PREDICTED: similar to kelch-like protein C3IP1 [Ornithorhynchus	U
PREDICTED: similar to LOC446973 protein [Gallus gallus]	U
PREDICTED: similar to LOC495018 protein	H
PREDICTED: similar to metalloprotease-disintegrin [Gallus gallus]	U
PREDICTED: similar to Methionine adenosyltransferase II, beta	A
PREDICTED: similar to MGC108301 protein [Gallus gallus]	H
PREDICTED: similar to MMAC1 [Pan troglodytes]	G
PREDICTED: similar to mucin 17 [Rattus norvegicus]	J
PREDICTED: similar to natural killer tumor recognition protein	P
PREDICTED: similar to Netrin-G2a [Gallus gallus]	Q
PREDICTED: similar to P25 protein [Pan troglodytes]	D
PREDICTED: similar to PACT [Gallus gallus]	P
PREDICTED: similar to Pcmt1-prov protein [Gallus gallus]	R
PREDICTED: similar to phospholipid scramblase PLSCR isoform 2	J
PREDICTED: similar to PI-3-kinase-related kinase SMG-1 [Gallus	J
PREDICTED: similar to Pla2g3 protein [Monodelphis domestica]	A
PREDICTED: similar to prostacyclin-stimulating factor;	F
PREDICTED: similar to Proteasome subunit alpha type 1 (Proteasome	R
PREDICTED: similar to putative DNA dependent ATPase and helicase	T
PREDICTED: similar to QN1 orf [Gallus gallus]	G
PREDICTED: similar to RAB30 [Monodelphis domestica]	E
PREDICTED: similar to rapamycin insensitive companion of mTOR; rictor	U
PREDICTED: similar to REX1, RNA exonuclease 1 homolog (S.	L
PREDICTED: similar to ribosomal protein L18 [Equus caballus]	O
PREDICTED: similar to ribosomal protein S19 [Pan troglodytes]	O
PREDICTED: similar to ribosomal protein S7 isoform 6 [Gallus	O
PREDICTED: similar to Sorting and assembly machinery component 50	U
PREDICTED: similar to synaptotagmin XV-a [Monodelphis domestica]	H
PREDICTED: similar to TCF7L2 [Gallus gallus]	Q
PREDICTED: similar to TECT2 [Macaca mulatta]	U
PREDICTED: similar to Tetratricopeptide repeat domain 25 [Danio	U
PREDICTED: similar to thioredoxin-like [Gallus gallus]	J
PREDICTED: similar to transducin gamma subunit [Monodelphis	N
PREDICTED: similar to tumor protein p53 binding protein, 2 [Gallus	G
PREDICTED: similar to uKATP-1 [Gallus gallus]	H
PREDICTED: similar to Uridine phosphorylase 1 [Gallus gallus]	A

progestin and adipoQ receptor family member IX [Homo sapiens]	S
proline-rich protein 15, isoform CRA_a [Rattus norvegicus]	U
protein kinase, cAMP-dependent, regulatory, type I, alpha (tissue	J
protocadherin gamma subfamily C, 3 [Gallus gallus]	K
purpurin [Gallus gallus]	N
putative enzyme [Shigella flexneri 5 str. 8401]	U
rCG40478, isoform CRA_j [Rattus norvegicus]	O
retinol binding protein 3, interstitial [Gallus gallus]	N
ribosomal protein S3A, isoform CRA_g [Homo sapiens]	O
ribosomal protein S4, X-linked [Gallus gallus]	O
secreted protein, acidic, cysteine-rich (osteonectin) [Gallus	G
sorting nexin 6 [Gallus gallus]	H
syntenin	I
tec protein tyrosine kinase [Gallus gallus]	J
TR5H_CHICK Tryptophan 5-monooxygenase	C
transthyretin [Gallus gallus]	H
tumor differentially expressed 2 [Gallus gallus]	U
ubiquitin [Oreochromis mossambicus]	R
Unknown (protein for IMAGE:8415934) [Bos taurus]	U
Unknown (protein for MGC:166416) [Bos taurus]	U
unknown [Schistosoma japonicum]	U
unnamed protein product [Mus musculus] cp295	U
unnamed protein product [Tetraodon nigroviridis] cp1089	U
Y-Box binding protein	Q
Ymf77 [Tetrahymena paravorax]	U

Clone ID	**Functional Cluster**
2',3'-cyclic nucleotide 3' phosphodiesterase [Gallus gallus]	R
acetylserotonin O-methyltransferase [Gallus gallus]	C
acyl-Coenzyme A dehydrogenase, long chain [Gallus gallus]	A
adenosine deaminase [Gallus gallus]	H
AF110987_1 proline-rich protein 3 [Arabidopsis thaliana]	U
AF368030_1 actin [Heliothis virescens]	I
apolipoprotein A-I	H
apolipoprotein A-I [Gallus gallus]	H
arylalkylamine N-acetyltransferase [Gallus gallus]	C
ATP6_10016 ATP synthase F0 subunit 6 [Gallus gallus]	A
BUD13 homolog [Gallus gallus]	U
capping protein (actin filament) muscle Z-line, alpha 2 [Gallus	I
CDC-like kinase 3 [Gallus gallus]	G
chromosome 3 open reading frame 9 [Gallus gallus]	U
CIC2_RABIT Dihydropyridine-sensitive L-type	H
claudin 3 [Gallus gallus]	K
clusterin [Gallus gallus]	B
coatomer protein complex, subunit gamma [Gallus gallus]	H
cognin/prolyl-4-hydroxylase/protein disulfide isomerase [Gallus	R
COX1_15261 cytochrome c oxidase subunit I [Talpa europaea]	A
CSPG5_CHICK Chondroitin sulfate proteoglycan 5 precursor (Acidic leucine-rich	K

cystatin C [Gallus gallus]	R
cytochrome c oxidase subunit III [Podiceps cristatus]	A
DB7	U
dCMP deaminase [Gallus gallus]	R
DDX54 protein [Homo sapiens]	L
DEAD (Asp-Glu-Ala-Asp) box polypeptide 5 [Gallus gallus]	O
DnaJ (Hsp40) homolog, subfamily C, member 3 [Gallus gallus]	P
eukaryotic translation elongation factor 2 [Gallus gallus]	O
ferritin [Coturnix japonica]	T
g Clock (full)	M
glutathione S-transferase A3 [Gallus gallus]	A
glycine dehydrogenase (decarboxylating) [Gallus gallus]	A
gtpase_rho [Aedes aegypti]	J
gustatory receptor candidate 19 [Tribolium castaneum]	U
hCG2042714 [Homo sapiens]	U
hypothetical protein [Gallus gallus] cp279	U
hypothetical protein [Gallus gallus] cp539	U
hypothetical protein [Gallus gallus] cp5490	U
hypothetical protein BURPS1710b_A0534 [Burkholderia pseudomallei	U
hypothetical protein DaciDRAFT_2108 [Delftia acidovorans SPH-1]	U
hypothetical protein DDBDRAFT_0189484 [Dictyostelium	U
hypothetical protein EhV364 [Emiliania huxleyi virus 86]	U
hypothetical protein LOC310926 [Rattus norvegicus]	U
hypothetical protein Mflv_4674 [Mycobacterium gilvum PYR-GCK]	U
hypothetical protein Strop_1450 [Salinispora tropica CNB-440]	U
I Chain I, The Plasmodium Falciparum Cysteine Protease Falcipain-2	R
immunoglobulin lambda-chain	P
JC1348 hypothetical 18K protein - goldfish mitochondrion	U
karyopherin (importin) beta 1 [Danio rerio]	H
matrix Gla protein [Gallus gallus]	P
mitochondrial creatine kinase [Gallus gallus]	J
multiple coagulation factor deficiency 2 [Gallus gallus]	F
NADH dehydrogenase (ubiquinone) flavoprotein 1, 51kDa [Gallus	A
NADH dehydrogenase subunit 4 [Gallus gallus]	A
ND4_10016 NADH dehydrogenase subunit 4 [Gallus gallus]	A
NK-lysin [Gallus gallus]	P
nuclear factor I-X protein [Gallus gallus]	Q
ORAI calcium release-activated calcium modulator 2 [Gallus gallus]	J
peptidyl arginine deiminase, type III [Gallus gallus]	R
pherophorin-dz1 protein [Volvox carteri f. nagariensis]	U
platelet-derived growth factor beta polypeptide [Gallus gallus]	F
predicted adhesin [Escherichia coli K12]	K
PREDICTED: hypothetical protein [Gallus gallus] cp1261	U
PREDICTED: hypothetical protein [Gallus gallus] cp151	U
PREDICTED: hypothetical protein [Gallus gallus] cp2027	U
PREDICTED: hypothetical protein [Gallus gallus] cp245	U
PREDICTED: hypothetical protein [Gallus gallus] cp380	U
PREDICTED: hypothetical protein [Gallus gallus] cp489	G

PREDICTED: hypothetical protein [Gallus gallus] cp5554	U
PREDICTED: hypothetical protein [Gallus gallus] cp567	U
PREDICTED: hypothetical protein [Gallus gallus] cp5764	U
PREDICTED: hypothetical protein [Gallus gallus] cp60	U
PREDICTED: hypothetical protein [Gallus gallus] cp668	U
PREDICTED: hypothetical protein [Gallus gallus] cp8	U
PREDICTED: hypothetical protein [Pan troglodytes] cp148	U
PREDICTED: hypothetical protein [Rattus norvegicus] cp969	U
PREDICTED: hypothetical protein, partial [Strongylocentrotus	U
PREDICTED: similar to 14-3-3 protein gamma subtype; 14-3-3 gamma	J
PREDICTED: similar to bactericidal/permeability-increasing	P
PREDICTED: similar to carbonic anhydrase III [Gallus gallus]	H
PREDICTED: similar to Centaurin, beta 5 [Gallus gallus]	H
PREDICTED: similar to CG13731-PA [Homo sapiens]	U
PREDICTED: similar to Chromosome 2 open reading frame 3 [Gallus	U
PREDICTED: similar to Crm, cramped-like [Gallus gallus]	T
PREDICTED: similar to delta-like 1-like protein [Gallus gallus]	U
PREDICTED: similar to echinoderm microtubule associated protein	I
PREDICTED: similar to ectonucleotide	J
PREDICTED: similar to Eukaryotic translation initiation factor	O
PREDICTED: similar to glycine receptor alpha 3 subunit [Gallus	S
PREDICTED: similar to kelch-like protein C3IP1 [Ornithorhynchus	U
PREDICTED: similar to KIAA1520 splice [Gallus gallus]	H
PREDICTED: similar to KIAA1576 protein [Gallus gallus]	A
PREDICTED: similar to LOC495018 protein	H
PREDICTED: similar to LOC495018 protein [Gallus gallus]	H
PREDICTED: similar to MGC108301 protein [Gallus gallus]	H
PREDICTED: similar to Mrps34-prov protein [Gallus gallus]	O
PREDICTED: similar to natural killer cell enhancing factor isoform	A
PREDICTED: similar to nucleoside diphosphate kinase [Gallus gallus]	J
PREDICTED: similar to P25 protein [Pan troglodytes]	D
PREDICTED: similar to P2X7 receptor subunit [Gallus gallus]	S
PREDICTED: similar to PACT [Gallus gallus]	P
PREDICTED: similar to Pcmt1-prov protein [Gallus gallus]	R
PREDICTED: similar to Peroxisome proliferator-activated	Q
PREDICTED: similar to phospholipid scramblase PLSCR isoform 2	J
PREDICTED: similar to prostacyclin-stimulating factor;	F
PREDICTED: similar to Prostaglandin F2 receptor negative regulator	O
PREDICTED: similar to putative DNA dependent ATPase and helicase	T
PREDICTED: similar to QN1 orf [Gallus gallus]	G
PREDICTED: similar to RAB30 [Monodelphis domestica]	E
PREDICTED: similar to retinal fascin [Monodelphis domestica]	N
PREDICTED: similar to ribosomal protein L18 [Equus caballus]	O
PREDICTED: similar to Ribosomal protein S6 [Pan troglodytes]	O
PREDICTED: similar to RNA polymerase-associated protein RTF1	Q
PREDICTED: similar to Rps21-prov protein [Gallus gallus]	O
PREDICTED: similar to Strawberry notch homolog 1 (Drosophila)	T
PREDICTED: similar to synaptotagmin XV-a [Monodelphis domestica]	H

PREDICTED: similar to TCF7L2 [Gallus gallus]	Q
PREDICTED: similar to tetratricopeptide repeat domain 19 [Gallus	U
PREDICTED: similar to TGF-beta inducible early protein [Gallus	F
PREDICTED: similar to WD repeat and FYVE domain containing 3	U
PREDICTED: similar to zinc finger protein 792 [Ornithorhynchus	T
proline-rich protein 15, isoform CRA_a [Rattus norvegicus]	U
prostaglandin H2 D-isomerase [Gallus gallus]	A
protein kinase, cAMP-dependent, regulatory, type I, alpha (tissue	J
protocadherin gamma subfamily C, 3 [Gallus gallus]	K
purpurin [Gallus gallus]	N
rCG40478, isoform CRA_j [Rattus norvegicus]	O
rCG40478, isoform CRA_m [Rattus norvegicus]	O
rCG59085, isoform CRA_b [Rattus norvegicus]	R
RH71862p [Drosophila melanogaster]	I
ribosomal protein S3A, isoform CRA_g [Homo sapiens]	O
RuvB-like 1 [Gallus gallus]	P
secreted frizzled-related protein 1 [Gallus gallus]	J
secreted protein, acidic, cysteine-rich (osteonectin) [Gallus	G
similar to 40S ribosomal protein S2 [Gallus gallus]	O
syndecan 3 [Gallus gallus]	I
transthyretin [Gallus gallus]	H
twinfilin-like protein [Gallus gallus]	I
ubiquitin [Oreochromis mossambicus]	R
ubiquitin C [Homo sapiens]	R
Unknown (protein for MGC:166416) [Bos taurus]	U
unknown [Gallus gallus] cp7900	U
unnamed protein product [Homo sapiens] cp345	U
unnamed protein product [Mus musculus] cp324	U
unnamed protein product [Tetraodon nigroviridis] cp1089	U
unnamed protein product [Tetraodon nigroviridis] cp2293	U
unnamed protein product [Yarrowia lipolytica CLIB99] cp7578	U
WAS/WASL interacting protein family, member 1 [Gallus gallus]	I

Key: (A) Metabolism; (B) Development; (C) Melatonin Biosynthesis; (D) Neuronal Associated; (E) Disease Related; (F) Hormones/Growth Factors; (G) Cell Cycle/Cell Death; (H) Carrier Proteins/Transport/Circulation; (I) Cytoskeletal/Microtubule-Associated; (J) Cell Signaling; (K) Cell Adhesion; (L) RNA Synthesis/Stability; (M) Circadian Clock; (N) Phototransductive Elements; (O) Ribosomal Proteins/Translation; (P) Stress Response/Host Defence/Chaperone; (Q) Transcription Factors; (R) Protein Modification; (S) Receptors; (T) DNA Synthesis/Replication/Binding; (U) Miscellaneous Function

Supplemental Table 5. Light Regulated Transcripts

Clone ID Upregulated CT6	ID #
acetylserotonin O-methyltransferase [Gallus gallus]	cp114; 1553; 2636; 3725; 4873; 5913*; 6149; 6442; 8043
cystatin C [Gallus gallus]	cp805*
D7 (Cry1)	cp8069*
hCG1820686 [Homo sapiens]	cp2191
hypothetical protein [Gallus gallus]	cp5003*
no chromat	cp6434; 6616; 6618; 6822; 7063; 7090; 7650
no hit	cp1089; 1547; 1645; 1733; 1876; 1883; 2358; 2587; 2624; 2656; 2764*; 434; 4588; 530; 5812; 6384; 6393*; 6628; 6664; 6676; 69; 7280; 7776
PRB4M_HUMAN Basic salivary proline-rich protein 4 allele M (Salivary	cp5846
PREDICTED: hypothetical protein [Gallus gallus]	cp4576; 5764
PREDICTED: similar to Clathrin light chain B (Lcb) isoform 1 [Canis	cp1550*
PREDICTED: similar to IlvB (bacterial acetolactate synthase)-like,	cp6640
PREDICTED: similar to Purpurin [Monodelphis domestica]	cp2911
progestin and adipoQ receptor family member IX [Homo sapiens]	cp2135
prostaglandin H2 D-isomerase [Gallus gallus]	cp6344*
purpurin [Gallus gallus]	cp1559; 2271; 2612

Clone ID Downregulated CT6	ID #
adenosine deaminase [Gallus gallus]	cp3343
AF202934_1 myeloid ecotropic viral insertion site-2a protein [Gallus gallus]	cp4705*
chaperonin containing TCP1, subunit 7 [Gallus gallus]	cp5424
cystatin C [Gallus gallus]	cp3113*; 4568
cytochrome oxidase subunit II [Gallus gallus]	cp3859
EURL [Gallus gallus]	cp7338
hypothetical protein LOC419902 [Gallus gallus]	cp3847
no chromat	cp170
no hit	cp112; 1332; 1738; 1797*; 1918*; 2129; 2423*; 2961; 317*; 3355*; 3598; 3716; 3906; 3918; 4616; 4653; 4717; 4796; 5180; 5803; 5887*; 5895*; 5950*; 598; 691*; 7342; 7797; 8002; 911
nuclear factor I-X protein [Gallus gallus]	cp4545*
PREDICTED: hypothetical protein [Gallus gallus]	cp669
PREDICTED: similar to Dolichyl-diphosphooligosaccharide--protein	cp4549*
proline-rich protein 15, isoform CRA_a [Rattus norvegicus]	cp592
TR5H_CHICK Tryptophan 5-monooxygenase	cp3412; 425; 4837*; 5106; 5886*; 600; 6090; 736

Clone ID Upregulated CT18	**ID #**
40S ribosomal protein S27A [Pseudopleuronectes americanus]	cp7340
acetylserotonin O-methyltransferase [Gallus gallus]	cp2636; 3725; 4873; 5913; 6149; 6442; 6496; 8043
cadherin 2, type 1, N-cadherin (neuronal) [Gallus gallus]	cp283
D7 (Cry1)	cp8069
NADH dehydrogenase subunit 4 [Gallus gallus]	cp282
no chromat	cp6434
no hit	cp1089; 2093; 2358; 6676; 7280; 7473; 7582; 7717; 7776; 8061*
PRB4M_HUMAN Basic salivary proline-rich protein 4 allele M (Salivary	cp5846
predicted protein [Nematostella vectensis]	cp2659
PREDICTED: hypothetical protein [Gallus gallus]	cp6938
PREDICTED: similar to notch 2 preproprotein [Gallus gallus]	cp5836
PREDICTED: similar to ribosomal protein L35 [Pan troglodytes]	cp3159
PREDICTED: similar to zinc finger and BTB domain containing 37	cp7867
prohibitin 2 [Gallus gallus]	cp5795
ribosomal protein S15a, isoform CRA_b [Mus musculus]	cp1635
transthyretin [Gallus gallus]	cp6763

Clone ID Downregulated CT18	**ID #**
cystatin C [Gallus gallus]	cp3113
DB7	cp8065
heat shock protein 90 [Gallus gallus]	cp4307
hypothetical protein [Gallus gallus]	cp279
Mel1A	cp8077
no chromat	cp7648; 7674
no hit	cp1918; 2370; 2423; 2495; 2751; 3341; 3358; 3729; 3906; 5803; 5887; 5950; 6094; 7316
peptidyl arginine deiminase, type III [Gallus gallus]	cp7743
Pr112 gag-pol polyprotein precursor [Avian leukosis virus]	cp4790
PREDICTED: hypothetical protein [Gallus gallus]	cp897
PREDICTED: similar to poly(A)-binding protein [Equus caballus]	cp5601
PREDICTED: similar to RNA binding/signal transduction protein Qkl-1	cp5891
PREDICTED: SUMO1/sentrin specific peptidase 6 [Gallus	cp4533
TR5H_CHICK Tryptophan 5-monooxygenase	cp3412; 5886; 6090
unnamed protein product [Tetraodon nigroviridis]	cp2293

* Indicates ≥ 2-fold change in expression

Supplemental Table 6. NE Regulated Transcripts

Clone ID Upregulated CT6	**ID #**
NADH dehydrogenase (ubiquinone) flavoprotein 1, 51kDa [Gallus	cp7765
no hit	cp1547; 2729; 2772; 8051
PREDICTED: similar to trans-Golgi protein GMx33 [Gallus gallus]	cp6345*

Clone ID Downregulated CT6	**ID #**
no chromat	cp531
no hit	cp382
PREDICTED: similar to iota-crystallin [Gallus gallus]	cp6425

Clone ID Upregulated CT18	**ID #**
no chromat	cp889
no hit	cp5038; 6169; 7763; 904
PREDICTED: similar to Ring finger protein 126 [Monodelphis	cp6480
transthyretin [Gallus gallus]	cp2201

Clone ID Downregulated CT18	**ID #**
no chromat	cp6590
no hit	cp2094; 579

* Indicates ≥ 2-fold change in expression

Supplemental Table 7. Comparative Analysis

LD, DD, Light, NE

transthyretin [Gallus gallus]

LD, DD, Light

acetylserotonin O-methyltransferase [Gallus gallus]
cystatin C [Gallus gallus]
hypothetical protein DaciDRAFT_2108 [Delftia acidovorans SPH-1]
nuclear factor I-X protein [Gallus gallus]
N-myc downstream regulated 1
PREDICTED: hypothetical protein [Gallus gallus] cp5764
proline-rich protein 15, isoform CRA_a [Rattus norvegicus]
purpurin [Gallus gallus]
unnamed protein product [Tetraodon nigroviridis] cp1089

cp1645; 1797; 2129; 2624; 2656; 2961; 3716; 4717; 5812; 598; 6616; 6628; 69; 691; 7063; 7090; 7280; 7650

LD, DD, NE

None

LD, DD

acyl-Coenzyme A dehydrogenase, long chain [Gallus gallus]
AF368030_1 actin [Heliothis virescens]
apolipoprotein A-I
apolipoprotein A-I [Gallus gallus]
clusterin [Gallus gallus]
cytochrome c oxidase subunit III [Podiceps cristatus]
cytochrome oxidase subunit I [Gallus gallus]
DDX54 protein [Homo sapiens]
eukaryotic translation elongation factor 2 [Gallus gallus]
ferritin [Coturnix japonica]
g Clock (1 full / 1 frag)
gammaA-like protocadherin precursor [Gallus gallus]
hCG2042714 [Homo sapiens]
hypothetical protein [Gallus gallus] cp1164; 5490
hypothetical protein DDBDRAFT_0189484 [Dictyostelium
hypothetical protein LOC310926 [Rattus norvegicus]
I Chain I, The Plasmodium Falciparum Cysteine Protease Falcipain-2
immunoglobulin lambda-chain
matrix Gla protein [Gallus gallus]
mitochondrial creatine kinase [Gallus gallus]
NK-lysin [Gallus gallus]
ORAI calcium release-activated calcium modulator 2 [Gallus gallus]
pherophorin-dz1 protein [Volvox carteri f. nagariensis]
PREDICTED: hypothetical protein [Gallus gallus] cp151; 60; 8
PREDICTED: hypothetical protein [Pan troglodytes] cp148
PREDICTED: similar to bactericidal/permeability-increasing
PREDICTED: similar to carbonic anhydrase III [Gallus gallus]
PREDICTED: similar to Chromosome 2 open reading frame 3 [Gallus
PREDICTED: similar to Crm, cramped-like [Gallus gallus]
PREDICTED: similar to delta-like 1-like protein [Gallus gallus]
PREDICTED: similar to ectonucleotide
PREDICTED: similar to epsilon isoform of 14-3-3 protein
PREDICTED: similar to kelch-like protein C3IP1 [Ornithorhynchus
PREDICTED: similar to KIAA1520 splice [Gallus gallus]
PREDICTED: similar to LOC495018 protein
PREDICTED: similar to P25 protein [Pan troglodytes]
PREDICTED: similar to PACT [Gallus gallus]
PREDICTED: similar to Pcmt1-prov protein [Gallus gallus]
PREDICTED: similar to phospholipid scramblase PLSCR isoform 2
PREDICTED: similar to prostacyclin-stimulating factor;
PREDICTED: similar to putative DNA dependent ATPase and helicase
PREDICTED: similar to QN1 orf [Gallus gallus]
PREDICTED: similar to RAB30 [Monodelphis domestica]
PREDICTED: similar to ribosomal protein L18 [Equus caballus]
PREDICTED: similar to synaptotagmin XV-a [Monodelphis domestica]
PREDICTED: similar to TCF7L2 [Gallus gallus]
PREDICTED: similar to UDP-GalNAc:betaGlcNAc beta

protein kinase, cAMP-dependent, regulatory, type I, alpha (tissue
protocadherin gamma subfamily C, 3 [Gallus gallus]
rCG40478, isoform CRA_j [Rattus norvegicus]
ribosomal protein S3A, isoform CRA_g [Homo sapiens]
secreted protein, acidic, cysteine-rich (osteonectin) [Gallus
ubiquitin [Oreochromis mossambicus]
unnamed protein product [Mus musculus]

cp100; 1012; 106; 1063; 1065; 108; 1203; 1445; 146; 15; 1540; 1649; 1959; 2; 202; 203; 2069; 2309; 2405; 246; 250; 2539; 2838; 2881; 2896; 290; 3; 3081; 4; 490; 50; 52; 56; 6128; 6987; 7; 7241; 7243; 7266; 7431; 7435; 779; 7815; 7962; 826; 98

LD, Light, NE

None

DD, Light, NE

None

LD, Light

AF202934_1 myeloid ecotropic viral insertion site-2a protein [Gallus gallus]
chaperonin containing TCP1, subunit 7 [Gallus gallus]
cytochrome oxidase subunit II [Gallus gallus]
g Cry1
hypothetical protein LOC419902 [Gallus gallus]
PRB4M_HUMAN Basic salivary proline-rich protein 4 allele M (Salivary
predicted protein [Nematostella vectensis] cp2659
PREDICTED: hypothetical protein [Gallus gallus] cp4576
PREDICTED: similar to Dolichyl-diphosphooligosaccharide--protein
PREDICTED: similar to IlvB (bacterial acetolactate synthase)-like,
progestin and adipoQ receptor family member IX [Homo sapiens]
TR5H_CHICK Tryptophan 5-monooxygenase

cp1332; 170; 1738; 1918; 2358; 2423; 317; 3355; 3598; 3906; 3918; 4588; 4653; 4796; 5180; 5887; 5895; 5950; 6434; 6676; 7342; 911

DD, Light

adenosine deaminase [Gallus gallus]
hypothetical protein [Gallus gallus] cp279
prostaglandin H2 D-isomerase [Gallus gallus]
DB7
NADH dehydrogenase subunit 4 [Gallus gallus]
peptidyl arginine deiminase, type III [Gallus gallus]
unnamed protein product [Tetraodon nigroviridis] cp2293
cp6664

LD, NE

invariant chain [Gallus gallus]
cp579; 6590

DD, NE

NADH dehydrogenase (ubiquinone) flavoprotein 1, 51kDa [Gallus

Light, NE

None

LD only

1609082A aldolase C
2',5'-oligo adenylate synthetase A [Gallus gallus]
A Chain A, Crystal Structure Of Aluminum-Bound Ovotransferrin At 2.15
ADAM metallopeptidase domain 33 [Gallus gallus]
AF199487_1 beta-actin [Anolis carolinensis]
AF355752_1 reverse transcriptase [Chelonia mydas]
AF387865_1 heat shock protein 108 [Gallus gallus]
B lymphocyte induced maturation protein 1 [Takifugu rubripes]
beta actin [Pagrus pagrus]
CD74 antigen (invariant polypeptide of major histocompatibility
CG15021-PA [Drosophila melanogaster]
Chemokine (C-X-C motif) ligand 14 [Gallus gallus]
Churchill protein [Gallus gallus]
cold inducible RNA binding protein [Gallus gallus]
connexin 43 [Gallus gallus]
cp_id:F1D9.26~unknown protein
cytochrome oxidase subunit I [Melanoplus marshalli]
cytochrome oxidase subunit III [Nycticryphes semicollaris]
fibroblast growth factor receptor 1 [Gallus gallus]
g BMal1
g Per3
glyceraldehyde-3-phosphate dehydrogenase
guanine nucleotide binding protein (G protein), beta polypeptide
high-mobility group box 1 [Gallus gallus]
hypothetical protein [Gallus gallus] cp1594
hypothetical protein LOC379066 [Xenopus laevis]
hypothetical protein LOC423668 [Gallus gallus]
Ig light chain precursor
Im:6892314 protein [Danio rerio]
integrin beta 1 binding protein 3 [Gallus gallus]
Jumonji, AT rich interactive domain 1B (RBP2-like) [Gallus gallus]
leukotriene A4 hydrolase [Gallus gallus]
matrix metalloproteinase 2 [Gallus gallus]
MHC class I [Gallus gallus]
myosin light chain kinase [Gallus gallus]
NAD-dependent deacetylase SIRT2 [Gallus gallus]
NAT
nucleophosmin 1 [Gallus gallus]
polymerase (DNA directed), delta 1, catalytic subunit [Xenopus

predicted protein [Nematostella vectensis] cp3727

PREDICTED: hypothetical protein [Danio rerio] cp1313; 1254; 2072 2942; 3306; 435; 437; 4635; 4663; 5988; 6371; 728
PREDICTED: similar to 16.7Kd protein [Equus caballus]
PREDICTED: similar to 60S ribosomal protein L7a [Rattus norvegicus]
PREDICTED: similar to Aromatic-L-amino-acid decarboxylase (AADC)
PREDICTED: similar to Band 4.1-like protein 3 (4.1B)
PREDICTED: similar to beta-tubulin cofactor E [Gallus gallus]
PREDICTED: similar to bromodomain containing protein 3 [Gallus
PREDICTED: similar to BTB/POZ domain containing protein 6 (Lens BTB
PREDICTED: similar to Calponin 3, acidic [Gallus gallus]
PREDICTED: similar to Carboxypeptidase E precursor (CPE)
PREDICTED: similar to cathepsin L [Gallus gallus]
PREDICTED: similar to Chromosome 18 open reading frame 8 [Gallus
PREDICTED: similar to Ddhd2 protein [Gallus gallus]
PREDICTED: similar to deleted in malignant brain tumors 1 isoform b
PREDICTED: similar to delta-sarcoglycan [Gallus gallus]
PREDICTED: similar to Diacylglycerol O-acyltransferase homolog 2
PREDICTED: similar to early response to neural induction ERNI
PREDICTED: similar to FLJ00258 protein [Gallus gallus]
PREDICTED: similar to heat shock protein [Monodelphis domestica]
PREDICTED: similar to heat shock protein 8 isoform 1 [Apis
PREDICTED: similar to hippocalcin isoform 2 [Gallus gallus]
PREDICTED: similar to LOC446973 protein [Gallus gallus]
PREDICTED: similar to metalloprotease-disintegrin [Gallus gallus]
PREDICTED: similar to Methionine adenosyltransferase II, beta
PREDICTED: similar to MMAC1 [Pan troglodytes]
PREDICTED: similar to mucin 17 [Rattus norvegicus]
PREDICTED: similar to natural killer tumor recognition protein
PREDICTED: similar to Netrin-G2a [Gallus gallus]
PREDICTED: similar to PI-3-kinase-related kinase SMG-1 [Gallus
PREDICTED: similar to Pla2g3 protein [Monodelphis domestica]
PREDICTED: similar to Proteasome subunit alpha type 1 (Proteasome
PREDICTED: similar to rapamycin insensitive companion of mTOR; rictor
PREDICTED: similar to REX1, RNA exonuclease 1 homolog (S.
PREDICTED: similar to ribosomal protein S19 [Pan troglodytes]
PREDICTED: similar to ribosomal protein S7 isoform 6 [Gallus
PREDICTED: similar to Sorting and assembly machinery component 50
PREDICTED: similar to TECT2 [Macaca mulatta]
PREDICTED: similar to Tetratricopeptide repeat domain 25 [Danio
PREDICTED: similar to thioredoxin-like [Gallus gallus]
PREDICTED: similar to transducin gamma subunit [Monodelphis
PREDICTED: similar to tumor protein p53 binding protein, 2 [Gallus
PREDICTED: similar to uKATP-1 [Gallus gallus]
PREDICTED: similar to Uridine phosphorylase 1 [Gallus gallus]
putative enzyme [Shigella flexneri 5 str. 8401]
retinol binding protein 3, interstitial [Gallus gallus]

ribosomal protein S4, X-linked [Gallus gallus]
sorting nexin 6 [Gallus gallus]
syntenin
tec protein tyrosine kinase [Homo
tumor differentially expressed 2 [Gallus gallus]
Unknown (protein for IMAGE:8415934) [Bos taurus]
Unknown (protein for MGC:166416) [Bos taurus]
unknown [Schistosoma japonicum]
Y-Box binding protein
Ymf77 [Tetrahymena paravorax]

cp1013; 105; 112; 1206; 121; 1250; 1273; 1297; 1298; 1322; 1350; 1378; 1404; 1442; 1450; 1478; 1496; 1544; 1586; 1592; 1702; 1755; 1782; 1784; 1795; 1815; 1868; 1900; 1921; 194; 1954; 196; 1973; 200; 2047; 2071; 2114; 2117; 2153; 2159; 2161; 226; 2269; 2308; 2310; 2336; 2345; 2351; 2363; 2374; 2394; 241; 2418; 2501; 2533; 2545; 2552; 2588; 2642; 2701; 2713; 2776; 2840; 2868; 2901; 291; 2924; 297; 3205; 34; 365; 3775; 386; 387; 391; 392; 396; 440; 444; 447; 4694; 472; 473; 482; 483; 5140; 5564; 566; 59; 6157; 6205; 626; 630; 6309; 6493; 6504; 6517; 6554; 6648; 6652; 6693; 674; 677; 6816; 6859; 7102; 7344; 747; 7519; 7526; 7531; 7536; 7565; 761; 7652; 7720; 7722; 7767; 7773; 7788; 7866; 7871; 7905; 7957; 7974; 800; 841; 868

DD only

2',3'-cyclic nucleotide 3' phosphodiesterase [Gallus gallus]
AF110987_1 proline-rich protein 3 [Arabidopsis thaliana]
arylalkylamine N-acetyltransferase [Gallus gallus]
ATP6_10016 ATP synthase F0 subunit 6 [Gallus gallus]
BUD13 homolog [Gallus gallus]
capping protein (actin filament) muscle Z-line, alpha 2 [Gallus
CDC-like kinase 3 [Gallus gallus]
chromosome 3 open reading frame 9 [Gallus gallus]
CIC2_RABIT Dihydropyridine-sensitive L-type
claudin 3 [Gallus gallus]
coatomer protein complex, subunit gamma [Gallus gallus]
cognin/prolyl-4-hydroxylase/protein disulfide isomerase [Gallus
CSPG5_CHICK Chondroitin sulfate proteoglycan 5 precursor (Acidic leucine-rich
dCMP deaminase [Gallus gallus]
DEAD (Asp-Glu-Ala-Asp) box polypeptide 5 [Gallus gallus]
DnaJ (Hsp40) homolog, subfamily C, member 3 [Gallus gallus]
glutathione S-transferase A3 [Gallus gallus]
glycine dehydrogenase (decarboxylating) [Gallus gallus]
gtpase_rho [Aedes aegypti]
gustatory receptor candidate 19 [Tribolium castaneum]
hypothetical protein [Gallus gallus] cp539
hypothetical protein [Yarrowia lipolytica]
hypothetical protein BURPS1710b_A0534 [Burkholderia pseudomallei
hypothetical protein EhV364 [Emiliania huxleyi virus 86]
hypothetical protein Mflv_4674 [Mycobacterium gilvum PYR-GCK]
hypothetical protein Strop_1450 [Salinispora tropica CNB-440]
JC1348 hypothetical 18K protein - goldfish mitochondrion
karyopherin (importin) beta 1 [Danio rerio]

ND4_10016 NADH dehydrogenase subunit 4 [Gallus gallus]
platelet-derived growth factor beta polypeptide [Gallus gallus]
predicted adhesin [Escherichia coli K12]
PREDICTED: hypothetical protein [Gallus gallus] cp5554; 1261; 2027; 380; 567; 668
PREDICTED: hypothetical protein [Rattus norvegicus]
PREDICTED: hypothetical protein, partial [Strongylocentrotus
PREDICTED: similar to Centaurin, beta 5 [Gallus gallus]
PREDICTED: similar to CG13731-PA [Homo sapiens]
PREDICTED: similar to echinoderm microtubule associated protein
PREDICTED: similar to Eukaryotic translation initiation factor
PREDICTED: similar to glycine receptor alpha 3 subunit [Gallus
PREDICTED: similar to KIAA1576 protein [Gallus gallus]
PREDICTED: similar to LOC495018 protein [Gallus gallus]
PREDICTED: similar to Mrps34-prov protein [Gallus gallus]
PREDICTED: similar to natural killer cell enhancing factor isoform
PREDICTED: similar to nucleoside diphosphate kinase [Gallus gallus]
PREDICTED: similar to P2X7 receptor subunit [Gallus gallus]
PREDICTED: similar to Peroxisome proliferator-activated
PREDICTED: similar to Prostaglandin F2 receptor negative regulator
PREDICTED: similar to retinal fascin [Monodelphis domestica]
PREDICTED: similar to Ribosomal protein S6 [Pan troglodytes]
PREDICTED: similar to RNA polymerase-associated protein RTF1
PREDICTED: similar to Rps21-prov protein [Gallus gallus]
PREDICTED: similar to Strawberry notch homolog 1 (Drosophila)
PREDICTED: similar to tetratricopeptide repeat domain 19 [Gallus
PREDICTED: similar to TGF-beta inducible early protein [Gallus
PREDICTED: similar to WD repeat and FYVE domain containing 3
PREDICTED: similar to zinc finger protein 792 [Ornithorhynchus
rCG40478, isoform CRA_m [Rattus norvegicus]
rCG59085, isoform CRA_b [Rattus norvegicus]
multiple coagulation factor deficiency 2 [Gallus gallus]
RH71862p [Drosophila melanogaster]
RuvB-like 1 [Gallus gallus]
secreted frizzled-related protein 1 [Gallus gallus]
similar to 40S ribosomal protein S2 [Gallus gallus]
syndecan 3 [Gallus gallus]
twinfilin-like protein [Gallus gallus]
ubiquitin C [Homo sapiens]
unknown [Gallus gallus]
WAS/WASL interacting protein family, member 1 [Gallus gallus]

cp1034; 1458; 1466; 1537; 1686; 17; 1711; 1713; 1783; 1807; 1849; 1977; 1979; 1988; 2088; 2146; 2406; 2407; 25; 2504; 2513; 2540; 2558; 2621; 2683; 2969; 273; 2749; 2797; 2851; 2979; 2921; 2933; 3079; 3285; 348; 4230; 4243; 4298; 4379; 44; 4531; 458; 4688; 4699; 470; 5197; 532; 535; 5380; 553; 577; 583; 586; 6172; 6191; 6193; 6231; 6417; 6472; 6669; 679; 6858; 6863; 6889; 6903; 697; 6977; 7049; 7051; 7055; 7099; 7101; 7195; 7245; 729; 7329; 7367; 7375; 7437; 7503; 758; 7584; 7615; 7640; 7740; 7768; 7779; 7822; 7878; 7892; 7960; 7976; 8005; 8013; 816; 885; 960

Light only

40S ribosomal protein S27A [Pseudopleuronectes americanus]
cadherin 2, type 1, N-cadherin (neuronal) [Gallus gallus]
EURL [Gallus gallus]
hCG1820686 [Homo sapiens]
heat shock protein 90 [Gallus gallus]
hypothetical protein [Gallus gallus] cp5003
Mel1A
Pr112 gag-pol polyprotein precursor [Avian leukosis virus]
PREDICTED: hypothetical protein [Gallus gallus] cp669; 6938
PREDICTED: similar to Clathrin light chain B (Lcb) isoform 1 [Canis
PREDICTED: similar to notch 2 preproprotein [Gallus gallus]
PREDICTED: similar to poly(A)-binding protein [Equus caballus]
PREDICTED: similar to ribosomal protein L35 [Pan troglodytes]
PREDICTED: similar to RNA binding/signal transduction protein QkI-1
PREDICTED: similar to zinc finger and BTB domain containing 37
PREDICTED: SUMO1/sentrin specific peptidase 6 [Gallus
prohibitin 2 [Gallus gallus]
ribosomal protein S15a, isoform CRA_b [Mus musculus]

cp1733; 1876; 1883; 2587; 2751; 2764; 3341; 3358; 3729; 434; 530; 6094; 6384; 6393; 6618; 6822; 7316; 7473; 7648; 7674; 7717; 7776; 7797; 8002; 8061

NE only

PREDICTED: similar to iota-crystallin [Gallus gallus]
PREDICTED: similar to Ring finger protein 126 [Monodelphis
PREDICTED: similar to trans-Golgi protein GMx33 [Gallus gallus]
cp2094; 2729; 2772; 382; 5038; 531; 6169; 7763; 8051; 889; 904

VITA

Stephen Paul Karaganis
Department of Biology M.S. 3258
Texas A&M University
College Station, TX 77843

Education

Degree	*Institution*	*Years*	*Field of Study*
A.B.	Wabash College Crawfordsville, IN	1994-1998	Biology, Major Chemistry, Minor
Ph.D.	Texas A&M University College Station, TX	1998-2008	Circadian Biology

Professional Experience

Research

Undergraduate Research Assistant, Wabash College Biology Dept., to Dr. Eric Wetzel (Trematode Parasitology, 1997-1998)

Graduate Research Assistant, Texas A&M University Biology Dept., to Dr. Vincent Cassone (Avian Circadian Biology, 1998-2008)

Teaching Assistantships

Introductory Biology 1, 2 Labs (Biol 123; Biol 123H; Biol 124)
Human Anatomy and Physiology 1 Lab (Zool 319)
Animal Physiology Lab (Zool 388)
Regulatory and Behavioral Physiology Lab (Zool 434)

Publications

Cassone VM, Bailey MJ, Karaganis SP, Kumar V, Bartell PA (2005) Functional genomics of the avian pineal gland. In: Functional avian endocrinology (Dawson A, Sharp PJ, eds), pp 11-26. Dew Delhi, India: Narosa Publishing House.

Karaganis SP, Kumar V, Beremand PD, Bailey MJ, Thomas TL, Cassone VM (2008) Circadian genomics of the chick pineal gland *in vitro*. BMC Genomics (Re-submitted).

Karaganis SP, Bartell PA, Shende V, Moore AF. Modulation of circadian metabolic and clock gene mRNA rhythms by extra-SCN oscillators. Gen Comp Endocrinol (In preparation).

Paulose JK, Peters JL, Karaganis SP, Cassone VM. Pineal melatonin acts as circadian zeitgeber and growth factor in chick astrocytes. Glia (In preparation).